The generation and characterisation of DigLON-Fc (CO-Fc) recombinant protein and its interactions with the putative neuronal receptors

Thesis submitted with the requirements of the University of Liverpool for the degree of Doctor of Philosophy

By

Mohammed Abdulraheem M. Akeel

July 2010

DECLARATION

This thesis is the result of my own work. The material in the thesis has not been presented, nor is currently being presented either wholly or in part for any other qualification.

The research work was carried out in the Developmental Neurobiology Research group, led by Dr. Diana Moss, in the Human Anatomy and Cell Biology Division of the School of Biomedical Sciences, University of Liverpool.

ABSTRACT

IgLONs are cell adhesion molecules which belong to the Ig superfamily. They are thought to play a role in the development of the nervous system. There are four members in the group; CEPU-1, OBCAM, LAMP and Neurotractin; they are expressed inside and outside the nervous system and increase with the development. IgLONs are formed of three Ig domains that are attached to lipid rafts within the cell membrane by a GPI anchor.

Previous experiments suggested that single transfected IgLON-CHO cells fail to inhibit neurite outgrowth while double transfected cell lines do. It is proposed that IgLONs interact in the plane of the membrane as dimeric IgLONs (DigLONs).

To investigate the role of DigLONs, CEPU-OBCAM–Fc recombinant protein (CO-FC) was generated. CEPU- Fc was labelled with a V5 tag and OBCAM-Fc with a myc tag allowing characterisation by ELISA assays with both anti-V5 and anti-myc antibodies. Stable doubly transfected CHO cells secreted a mixture of CO-Fc heterodimeric, O-O-Fc and C-C-Fc homodimeric proteins. Therfore, anti-myc antibody will be used in detection of CO-Fc; however, OO-Fc will be detected.

CO-Fc inhibits the initiation of neurite outgrowth from E8 forebrain neurons when used as a substrate whereas no inhibition occurred with CEPU-Fc or OBCAM-Fc alone. Immunofluorescence studies show that CO-Fc recombinant protein binds to the surface of the E8 chick forebrain, E10 DRG and sympathetic neurons using anti myc antibody. Treatment of forebrain neurons with PI-PLC, to remove GPI anchored glycoproteins including IgLONs results in a loss of binding of CO-Fc to the neuronal cell surface. In addition, the inhibition of neurite outgrowth from E8 forebrain neurons reversed after PI-PLC treatment. All these evidences suggested that IgLON might be the putative receptor, or a part of complex with a transmembrane receptor.

Previously, E10 dorsal root ganglion neurons (DRG) and sympathetic neuronal growth was not inhibited by the CO doubly transfected cell line, while no inhibition occurred with the concentration that used with forebrain neurons. However, higher concentration of CO-Fc (4xfold) significantly inhibits the neurite outgrowth from both neurons. CO-Fc was tested on IgLON transfected CHO cell lines to elucidate the role of IgLONs in the CEPU-OBCAM putative receptor complex. It interacts with LAMP-CHO, CEPU-CHO, OBCAM-CHO and CL-CHO cells but, there was no interaction with CO-CHO cells. In E18 chick retina frozen section, CO-Fc binds to the outer plexiform layer of the retina.

A prelimanary fluorescence resonance energy transfer (FRET) experiment was carried out to distinguish between the CO-Fc heterodimer that is labelled with both myc and V5 tags from the mixture of OO-Fc which is only labelled with myc tag or CC-Fc which is labelled by V5 tag. A positive control was generated which is OO-myc recombinat protein detected with anti-myc Alexa fluor 555(acceptor) and AlexaFluor 488 (donor) antibodies on LAMP-CHO cells. The FRET ratio between the fluorphores was about 20 %.

This thesis is for my parents and my family

ACKNOWLEDGEMENTS

I would like to thanks Dr Diana Moss for giving me this opportunity to work in her group and for close supervision throughout my PhD and other members of the research group, Dr. Christine McNamee, Michael Lyons and the new member Rachel Carter for their support and friendship.

I would also like to acknowledge Human Anatomy and Cell Biology Department, University of Liverpool for the friendly scientific environment,

I am also very lucky to have great support and encouragement from my family and friends.

Finally, it is an opportunity to acknowledge my sponsor, Jazan University, Kingdom of Saudi Arabia.

ABBREVIATIONS

AU	arbitrary unit
BMP	Bone morphogenic proteins
Bp	base pair
BSA	bovine serum albumin
C	cerebellum purkinji membrane protein
C+O	CEPU-1+OBCAM IgLONs
CAM	cell adhesion molecule
CEPU-1	cerebellum purkinji membrane protein
CEPU-se	secreted CEPU-1
CGCs	cerebellar granule cells
CHO	Chinese Hamster Ovary
CL	CEPU-1: LAMP DigLON
CNS	central nervous system
CO	CEPU-1:OBCAM Diglon
CO-Fc	CEPU-1:OBCAM-Fc recombinant protein
DCC	Deleted in colorectal cancer
Diglon	Dimeric IgLON
DMEM	Dulbecco's modified Eagle's medium
DRG	dorsal root ganglion
E	embryonic day
EDTA	ethylene diamine tetra acetic acid
ELISA	Enzyme Linked Immuno Substrate Assay
F-actin	Filamentous actin
FC	fragment C from the Human IgG heavy chain
FCS	foetal calf serum
FGF	Fibroblast growth factor
FN III	Fibronectin type III repeat
GFP	green fluorescent protein
GPI	glycosyl phosphatidyl inositol
HBSS	Hanks balance salt solution
HIS6	6 histidine repeat tag

HNT	CEPU-1 gene name
HRP	horseradish peroxidase
Ig	immunoglobulin
IgG	immunoglobulin G
IgLON	Ig superfamily LAMP OBCAM NEUROTRACTIN/CEPU-1
IgSF	immunoglobulin superfamily
IPL	inner-plexiform layer of the retina
kb	kilo base pair
kD	dissociation constant
Kilon	Kindred IgLON
L	limbic associated membrane protein
LAMP	limbic associated membrane protein
LB	Luria broth
LDS	Lithium dodecyl sulphate
LMC	lateral motor column neuron
LO	LAMP: OBCAM
LSAMP	LAMP gene name
LTP	long-term potentiation
N-CAMs	neuronal cell adhesion molecules
NEGRI	Kilon gene name
np	Neuroplastin
Ntm	Neurotrimin
Ntr	Neurotractin
O	opiate binding cell adhesion molecule
OBCAM	opiate binding cell adhesion molecule
OD	optical density
OPCML	OBCAM gene name
OPL	outer-plexiform layer of the retina
p38MAPK	mitogen-activated protein kinase p38
PAGE	polyacrylamide gel electrophoresis
PBS	phosphate buffered saline
PCR	Polymerase chain reaction
PIC	Protease inhibitor cocktail
PI-PLC	phosphatidyl inositol-specific phospholipase C

PL	poly-L-Lysine
PNS	peripheral nervous system
PSD	postsynaptic density preparations
PTX	pertussis toxin
Robo	roundabout receptor
ROCK	Rho-associated coiled-coil-forming kinase
RT	room temperature
RTPCR	reverse transcriptase polymerase chain reaction
Sema3A	secreted semaphoring class 3
Smo	smoothened receptor
TA	Tris acetate buffer
TAE	Tris acetate EDTA buffer
TMB	3,3',5,5'-Titramethylbenzidine dihydrochloride
Tris	Trizma base
UV	ultra violet
WT	wild type
x-gal	x-galactosidase

Table of Contents

Chapter One

Introduction

Development of the nervous system:

Life starts as a single fertilised egg or a zygote which then initially divides into many undifferentiated cells. These cells will form eventually, a structure called a blastula which has an opening called a blastopore. Gastrulation is a movement of the primitive cells (gastrula) through an opening called a blastopore. The gastrula has three layers; the outer is ectoderm followed by mesoderm and the inner is the endoderm (Leptin, 2005; Solnica-Krezel, 2005).

In the dorsal ectoderm, a flat dish-shaped area invaginates at the centre to form the neural plate and then closes to form the neural tube, which is the origin of the central nervous system (Munoz-Sanjuan and Brivanlou, 2002). The floor plate is a transient structure that originates from the mesoderm. A structure lies below the neural tube called the notochord which derives from the mesoderm (Placzek et al., 1990; Stemple, 2005). Some of the cells above the neural tube migrate away to form the neural crest, whereas somites lie beside the neural tube (Wilson and Maden, 2005). At the bottom of the neural tube is an area called the floorplate while at the top is the roof plate (Lee et al., 2000). The anterior end of the neural tube forms the forebrain which develops into the telencephalon and the diencephalon, whereas the posterior part forms the midbrain, hindbrain and spinal cord. After the gastrulation stage, the neurulation stage starts with migration of neural crest cells to form sympathetic ganglia, sensory (dorsal root) ganglia and Schwann cells and other structures (figure 1.1).

There are four molecules that are particularly important for the development of the central nervous system, fibroblast growth factors (FGF), Sonic hedgehog (SHH), Bone morphogenic protein (BMP) and retinoic acid (Wilson and Maden, 2005). There is evidence of the importance of these molecules as destruction of the

notochord leads to malformation of floorplate. Whereas addition of another notochord by grafting result in induction of extra floor plates and motor neurons (Placzek et al., 1990; Yamada et al., 1991)

Important secreted molecules in development of CNS:

From Notochord and floor plate:

Sonic hedgehog (SHH):

Sonic hedgehog is a signaling molecule that is secreted by the notochord and floor plate. Sonic hedgehog is essential for the floor plate development (Placzek et al., 1990; Stemple, 2005). The inactivation of SHH either by antibody or blocking its gene led to failure of induction of floor plate. Furthermore, increased expression of SHH led to increased induction of skeletal muscle, skin and vertebrae (Wilson and Maden, 2005), floor plate and motor neurons (Marti et al., 1995). SHH plays an essential role in specification of the motor neurons and interneurons (Ericson et al., 1997; Ericson et al., 1996).

Other experiments demonstrated that the induction of floor plate cells and motor neurons depends on the precise concentration of the SHH (Roelink et al., 1995). High level expression of SHH induces the floor plate, whilst the ventral motor neurons are induced at lower concentrations by activation of specific homeodomain transcription factors which are components responsible for SHH gradient such as *Pax6 and Nkx2.2* (Ericson et al., 1997). SHH has an important role in the glial cell differentiation beside the floor plate differentiation (Lu et al., 2000). As described before, the role of SHH in induction of ventral motor interneuron precursor types (V0-V3). However, some classes of the ventral interneurons develop in SHH mutant, which suggests a role of other molecules.

From the Roof Plate:

There are secreted proteins from the roof plate which have a similar role as the floor plate as an organising centre for the dorsal neurons of the spinal cord (LaBonne and Bronner-Fraser, 1999).

Experiments were carried out to test the role of the roof plate in the differentiation of the dorsal interneurons in mouse embryo, namely ablation of the roof plate. The result of this experiment was loss of all interneuron classes in the dorsal region of the spinal cord (Lee et al., 2000).

BMPs:

BMPs (bone morphogenic proteins) are a subfamily of the TGF-β superfamily that is comprised of more than 30 proteins (Kingsley, 1994; Zhao, 2003). They have a role in dorsoventral and or anterior posterior patterning during embryogenesis (Mishina, 2003), in addition to their functions in the progression, differentiation and development of particular regions in the brain.

BMP2 has a role in migration of neural crest cells in developing embryo (Correia et al., 2007). It is expressed in the roof plate and has a role in the closure of the neural tube and is prominently in the surface ectoderm which implies a role in the cephalic region (Furuta et al., 1997). There is a relation between BMP2 and the glial or CNS fates and retinal patterning, astrogliogenesis and neurogenesis (Fukuda et al., 2007). In BMP2 null mouse embryos, the severity of defects in the development of the neural tube depend on the amount of signalling of BMP2, suggesting a role of BMP2 in development of neural tube particularly the cephalic region (Castranio and Mishina, 2009).

BMP4 is also expressed in the roof plate and involved in the induction of neurons with FGFs (Linker and Stern, 2004). Both BMP4 and BMP7 interact with

Tsg protein biochemically and genetically (Zakin and De Robertis, 2004). There is a co-expression of BMP7 and Tsg in ventral mesoderm and endoderm during embryogenesis (Zakin et al., 2005). In BMP7 compound mutants, Tsg is necessary for the formation of the posterior ventral structures (Zakin et al., 2005).

GDF7 is another protein that belongs to this family, and is expressed by cells in the roof plate of the mouse embryo. The differentiation of D1A and D1B subtypes of dorsal sensory interneurons requires GDF7 as demonstrated by creating GDF7 null mutants mouse embryo. The analysis of these mutants revealed loss of D1A dorsal sensory interneuron's production. This evidence suggested expression of GDF7 is essential for the neuronal cell types in the dorsal spinal cord (Lee et al., 1998).

There is a possibility that BMP 7 and GDF7 act as a heterodimer complex on the cells of roof plate to function as chemorepellent. This evidence suggested the heterodimer complex is essential for commissural axon trajectory (Butler and Dodd, 2003), also their repellent action on precommissural axon, which prevent it from passing to the dorsal region (Butler and Dodd, 2003; Lee et al., 1998).

In addition, experiments in Zebrafish revealed that BMPs are necessary for development of the sensory neurons and interneurons (Nguyen et al., 2000). BMP, dorslin and activin are members of the TGF-B family, which control the fate of dorsal region of the neural tube (Liem et al., 2000; Liem et al., 1997).

Noggin, chordin and follistatin are BMP antagonists that are expressed in the notochord, whereas BMPs are secreted from the roof plate (Chizhikov and Millen, 2005; Lupo et al., 2006; Wilson and Maden, 2005). There is a role for BMPs and their antagonists in specification of both ventral and dorsal cell types. The integration between BMP and SHH signalling, promotes the response of neural cells to SHH.

Incubation with BMP and SHH results in reduction of the ventral cell fate of spinal cord when compared with SHH only. However, incubation of SHH with a BMP antagonist such as follistatin on spinal cord explants results in increase in the ventral cell fate (Liem et al., 2000; Lupo et al., 2006). The loss of roof plate cells leads to abortive midline induction and holoprosencephaly which is the most common congenital malformation of the brain particularly, in the dorsal telencephalon (Cheng et al., 2006).

Axon guidance:

The nervous system is formed by network of neurons that innervates the whole body. Each Neuron consists of a cell body, with an extended long axon from one side and multiple dendrites from the other side. A synapse is a point of meeting between two neurons which is responsible for signal transmission, most commonly between an axon and dendrites. Axons travel for long distances to reach their targets; certain factors control this process. In particular, specific molecules act as cues to guide these axons by attracting or repulsing mechanisms toward the final destination. These molecules are called axon guidance cues and could be attractive or repulsive. Some of these cues work as both depending on which receptor subtype are expressed on the surface of growth cone. Axon guidance molecules can be contact-mediated or sereted gradient.

The growth cone is the highly sensitive region of the axon which explores the surrounding environment searching for guidance cues that allow the axon to either elongate or shorten depending on the type of these cues. In response to this process the growth cone sends projection like endings called lamellipodia and filopodia (figure1.2). Actin filaments form the cytoskeleton of lamellipodia, where the filopdia have F actin bundles, which are responsible for growth cone movement. The microtubules move to the proximal part of the growth cone when associated with actin filaments. This, according to the polymerisation or depolymerisation of the actin filaments is at the negative and positive ends (Huber et al., 2003).

Netrin:

Netrin-1 is the earliest secreted protein that was identified in chick brain that is considered an attractant guidance molecule in the nervous system of vertebrate animals (Serafini et al., 1994). In particular, commissural axons are attracted to the midline while trochlear axons are repelled (Serafini et al., 1996). Netrin may act as attractant or repellent according to the receptor expressed on the surface of the growth cone (Chisholm and Tessier-Lavigne, 1999; Mehlen, 2003).

Netrin-1 mRNA was expressed in the floor plate while Netrin-2 in the ventral two thirds of the spinal cord. Interestingly, both molecules act together to attract the commissural axons (Kennedy et al., 1994). Deleted in colorectal cancer (DCC) is an Ig superfamily transmembrane protein which has a role in commissural axons guidance by Netrin-1. Netrin-1 becomes an attractant when bound to DCC. However, formation of a complex of DCC and UNC-5 heterodimer receptor on the surface of the growth cone alters the Netrin-1 action. It becomes repulsive such that trochlear axons are repulsed from the midline (Huber et al., 2003). The level of cAMP is essential with DCC signalling, any decrease in the level of cAMP led to repulsion while any increase resulted in attraction (Huber et al., 2003).

The commissural axons were unable to recognise the floor plate in absence of DCC, while most axons are misdirected in both Netrin and DCC mutants. However, some axons are still attracted to the floor plate. This suggested the action of other cues that are able to attract the commissural axon to the floor plate in addition to Netrin (Fazeli et al., 1997; Serafini et al., 1996). There is evidence that SHH has a role in attraction of commissural axon to the floor plate when it binds to Smoothened (Smo), Smo or SHH receptor (Charron et al., 2003). In addition, SHH and Netrin together attract axons to the midline of the spinal cord (Salinas, 2003).

Loss of the growth cone response to guidance cues could be due to down regulation of surface receptors when stimulated by these cues, as occurred in the embryonic cortical neurons when stimulated by Netrin-1 that ended in a remarkable decrease of DCC expression on the cell surface. This evidence suggested that Netrin-1 encourages the proteolytic cleavage of DCC (Kim et al., 2005).

Slit:

Slit is a protein secreted by the notochord that contributes to the successful crossing of the midline by commissural axons. Expression of Slit was detected early in the notochord, then the floor plate and finally in roof plate and motor neurons. Some axons are attracted to the midline and once they cross the midline, they navigate away, while other axons are repelled from the midline. A harmony is required between these molecules and the receptors expressed on the surface of the axons guide them to their targets. For example, Netrin, which is produced by the ventral floor plate, guide the commissural axons to the midline (Kennedy et al., 1994). Robo (roundabout) receptor expressed on the surface of the commissural axons, which interacts with Slit that is secreted by the floor plate. This interaction results in repulsion of these axon from the floor plate (Brose et al., 1999; Hu, 1999; Kramer et al., 2001) Robo1 and DCC interacted to decrease the reaction of the axons to the Netrin allowing them to cross the midline (Dickson and Gilestro, 2006; Stein and Tessier-Lavigne, 2001). To avoid crossing back to midline, Robo receptor is re-expressed after leaving the midline (Keleman et al., 2002; Keleman et al., 2005).

Slit is expressed in different isoforms; slit1 and slit2, which are secreted by the floor plate and interact with Robo-2 expressed on inferior olivary nucleus cells. In forebrain, Robo-1 as well as Robo2 are expressed especially in the nuclei and axon tracts. Robo-1 is crucial for embryonic vertebrate forebrain axon guidance and neural

differentiation. Abnormal expression of Robo-1-resulted in disruption of forebrain axon development and ectopic differentiation of the neurons (Connor and Key, 2002).

Semaphorins:

Semaphorins are a large family of axon guidance molecules which have an important role in guiding axons in the nervous system in both invertebrates and vertebrates (Tamagnone and Comoglio, 2004; Yazdani and Terman, 2006). The role of Semaphorins is guiding axons through repulsion or attraction. For example, cortical axons guided by the repellent action of semaphorin D and attraction effect of semaphorin E. Interestingly, semaphorin 1 which is mainly repellent, becomes an attractant molecule when overexpressed in developing peripheral neuron (Wong et al., 1999).

There are secreted or membrane bound isoforms of semaphorins. They interact to form homodimers to initiate signalling pathway. Complexes of plexins and neuropilins are surface receptors that are expressed on axons are required for the signalling of semaphorins (Raper, 2000; Tamagnone and Comoglio, 2000).

Motor axon growth and guidance are interrupted due to absence of Sema3A-NP-1 signalling, which results in dorso-ventral guidance defect in both medial and lateral motor axons. The medial subset of lateral motor column (LMC) neurons are guided to the ventral limb by sema3F-NP-2 (Huber et al., 2005). There is a link between altered function of semaphorin molecules and certain degenerative diseases such as epilepsy, schizophrenia, Alzheimer, Parkinson's disease and retinal degeneration (Eastwood et al., 2003; Rice et al., 2004; Yazdani and Terman, 2006).

Ephrins:

Ephrins are membrane bound axon guidance molecules which function in contact with their receptors on the opposing cell, Ephrin (Eph) tyrosine kinases are surface receptors for Ephrins. Eph A receptors interact with class A Ephrins which have a GPI anchor, while Eph B binds to class B Ephrins that have a cytoplasmic domain. Initially, *cis* interactions between Ephrins and their Eph receptors on the cell surface result in dimer formation, followed by *trans* interaction between these dimers and dimers on the adjacent cell to form tetrameric complexes which initiate signalling pathway in both directions (Kullander and Klein, 2002; Murai et al., 2003).

During gastrulation, Ephrins and Eph B have an essential role in cell movement, furthermore, B-Ephrins were detected in Zebrafish particularly in the notochord and prechordal plate (Chan et al., 2001). In addition, they have a role during hindbrain rhombomere development, migration of neural crest and synaptogenesis (Klein, 2001).

During development of the retinal tectal system, Ephrins and Eph receptors are essential for the guidance of retinal ganglion cells axons, to form the retincollicular map (Erskine and Herrera, 2007; Huot, 2004; Knoll and Drescher, 2002).

In ephrin-A5 knockout mice, the commissural axons were temporarily changed at P5 in the hippocampus. In the dentate gyrus, they lost the direction during the development and the number of synapses and the commissural layers were changed. This evidence suggests that Ephrin-A5 plays a role in hippocampus synapse maturation, whereas mRNA of ephrin-A3 expressed in the cells of the hippocampal and the dentate gyrus during postnatal development (Otal et al., 2006).

Wnt:

Wnt plays a role in attraction and turning of commissural axons after crossing the midline. It is a secreted axon guidance molecule that interacts with surface receptor on the commissural axons called Frizzled3 (Zou, 2004). Wnt is essential for anterior projection, so, lack of Frizzled receptor in mutant embryos leads to a defect in anterior projection of commissural axons after crossing the midline. The attraction role of Wnt could be reversed by the effect of secreted frizzled-related protein which is considered as a Wnt antagonist (Lyuksyutova et al., 2003).

Lipid rafts and their role as location for GPI-anchored proteins:

Lipid rafts are unique microdomains in the cell membrane which are characterised by their high constitution of cholesterol and sphingolipids that provide a tight ordered state (Figure 1.6)(Brown and London, 2000). The size of these microdomains is open to debate, some people say it is less than 5nm which was determined by fluorescent energy transfer (FRET) assays (Anderson and Jacobson, 2002; Sharma et al., 2004), while others suggest is 200nm (Simons and Ikonen, 1997; Simons and Toomre, 2000). GPI- anchored proteins and cell adhesion molecules locate to lipid rafts giving these putative microdomains an importance in signal transduction for extracellular cues (figure1.5) (Nakai and Kamiguchi, 2002). Most cell surface GPI anchored proteins are using lipid rafts as platforms for their signalling pathways, in addition, many signalling pathways such as Rho and GTPase and Src-family of tyrosine kinases are associated with these microdomains to regulate the actin cytoskeleton, cell adhesion and motility (Guirland and Zheng, 2007). The clustering of individual rafts collectively by cross-linking and antibody patching suggested they may facilitate signal transduction (Friedrichson and Kurzchalia, 1998).

These microdomains play an essential role during the development of neuronal axons. For example, Netrin-1 axon guidance molecule leads to extension of commissural neurons outgrowth when they form a complex with DCC receptor that is located within the lipid rafts (Herincs et al., 2005). In addition, lipid rafts play a role in the development of normal brain and recovery after injury and diseases by acting as a platform for various signaling pathways (Guirland and Zheng, 2007).

Cell adhesion molecules Ig Superfamily:

Ig Superfamily is characterised by the presence of Ig domains and fibronectin III repeats, they are subdivided into subfamilies according to the number of Ig domains and FNIII repeats. Their GPI anchor locates them in lipid rafts of cell membrane or they may be transmembrane, with some cytoplasmic domains having tyrosine kinase or phosphatase activity.

N-CAMs:

N-CAMs are cell adhesion molecules that are expressed on the surface of neuronal cells, and have a role in development of the nervous system by promoting neurite outgrowth and axon guidance (Brummendorf and Rathjen, 1995; Marg et al., 1999; Stoeckli and Landmesser, 1998). They have homophilic or heterophilic interactions between the molecules within the Ig superfamily either in *cis* or *trans* on the plane of membrane.

They are composed of five Ig domains and two FNIII extracellular repeat domains. They are classified into different isoforms according to the molecular weight, N-CAM 180, N-CAM 140, N-CAM 120, in addition to a secreted form (Hubschmann et al., 2005; Kalus et al., 2006). They are expressed by different cells, for instance, N-CAMs 120 are GPI-anchored molecules expressed by both neural and glial cells, N-CAMs 140 and N-CAMs 180 are class 1 transmembrane proteins with cytoplasmic domains. They have an essential role in synaptogenesis and synaptic plasticity in adulthood (Doherty et al., 1995). The N-CAM subfamily is modified due to the insertion of optional alternative spliced exon (VASE) in the fourth Ig domain beside the posttranslational addition of poly-sialic acid (PSA) to the fifth Ig domain. The increase in expression of PSA in the embryo is only in sites with a high plasticity in adult, and expression of VASE exon during development led to a

hypothesis that any increase in VASE with a decrease in PSA expression changed N-CAM from a plasticity-promoting molecule to a stability-promoting molecule (Bonfanti, 2006; Gascon et al., 2007; Rutishauser, 2008). Furthermore, N-CAMs interact with the fibroblast growth factor receptor (FGFR). There is a more compact interaction between Ig domains 1&3 due to decrease expression of PSA while PSA-N-CAMs are less tightly packed (Ronn et al., 2000).

The FGFR has a crucial role in N-CAM mediated axonal elongation (Kiselyov et al., 2003; Neiiendam et al., 2004; Saffell et al., 1997). The hypothesis is that N-CAMs form dimers on the surface of the cell, a trans homophilic interaction of N-CAMs activate these dimers, which resulted in clusters formation by FGFR and N-CAM molecules that increase the local concentration of FGFR (Kiselyov et al., 2005). However, the real mechanism of N-CAM activation of FGFR is not fully understood.

Both N-CAM 140 and N-CAM 180 depend on the intracellular and extracellular interaction partners to trigger the downstream signal complexes. These isoforms are located either within or outside lipid rafts of the cell membrane. N-CAM 140 within the lipid raft is able to signal alone possibly through the FYN/FAK complex. Whereas, N-CAM 140 outside the lipid rafts signals mainly through the FGFR (Niethammer et al., 2002). N-CAM 120 is GPI anchored, while N-CAM 140 and N-CAM 180 are targeted by the lipid rafts due to palmitoylation of four residues in the intracellular juxtamembrane region (Neiiendam et al., 2004).

L1:

L1 is essential for axon elongation in addition to its role in pyramidal tract formation, cerebral cortical motor neurons connection and interneurons to the spinal cord. L1 is another neural transmembrane glycoprotein subfamily belonging to the Ig superfamily. It consists of six Ig domains and five FNIII repeats (Brummendorf and Rathjen, 1996). L1 interacts in *trans* either homophilically or heterophilically with other cell adhesion molecules such as Axonin/TAG-1, F3/F11/Contactin (Brummendorf and Lemmon, 2001).

There is a link between L1 and Sema3A signalling pathway during corticospinal tract axon guidance. This was suggested because the repulsive signal of Sema3A in the ventral spinal cord was lost in L1 deficient mice. The extra cellular domains of the L1 interact in cis with NP-1 forming the NP-plexin-Sema3A receptor complex (Castellani et al., 2000).

There are cell adhesion molecules with three Ig domains that belong to Ig superfamily; that are thought to play a role in development of the nervous system namely Synaptic cell adhesion molecules (SynCAMs), nectin, neuroplastins and IgLONs.

SynCAMs:

SynCAMs play a role in neuronal differentiation of the central and peripheral nervous system during development and in the adult brain. There are four proteins 1-4, with their corresponding CADM1-4 genes (Biederer, 2006). They are formed of three extracellular Ig domains with a transmembrane domain and cytoplasmic domain (Biederer, 2006). All SynCAMs are expressed in the nervous system whereas synCAM1 is mainly expressed in the brain with expression pattern outside the nervous system in lung and testis (Fogel et al., 2007). These molecules are expressed

in synapses of the developing hippocampal neurons in vitro (Fogel et al., 2007), especially SynCAM1-3 which are expressed at both pre and post synaptic membrane (Biederer et al., 2002). SynCAM4 is expressed by cerebellar Purkinje cells, whereas synCAM3 is expressed by cerebellar granule cells. This suggests to a role for synCAM3-4 interaction between these cells during cerebellar differentiation including synaptogenesis (Thomas et al., 2008).

SynCAMs have homophilic and heterophilic interactions inside the family, the heterophilic interaction between synCAMs1 and 2 promotes synaptic transmission (Biederer et al., 2002; Fogel et al., 2007; Sara et al., 2005). SynCAMs 3 and 4 interact (Biederer et al., 2002; Fogel et al., 2007; Kakunaga et al., 2005; Maurel et al., 2007; Shingai et al., 2003) as do synCAMs 2 and 4 (Thomas et al., 2008). SynCAMs 1, 2 and 3 also have homophilic interactions.

Nectins:

Nectins are a family of cell adhesion molecules that is similar to the SynCAM family in the structure (3Ig) and the number of members within the family (1-4) with variant splicing forms (Cocchi et al., 1998; Lopez et al., 2001; Reymond et al., 2001; Satoh-Horikawa et al., 2000; Takahashi et al., 1999). They have extracellular or intracellular interactions which lead them to have essential roles in cell adhesion, proliferation, polarisation, in addition to their role in formation of intracellular junctions. Nectins 1, 2 and 3 are expressed in embryo and adult tissues while nectin4 is expressed mainly in human placenta (Reymond et al., 2001).

There are *cis* and *trans* homophilic and heterophilic interactions between Nectins as well as other molecules. Initially, Nectins form *cis* dimers on the surface of the cell through the second Ig domain then these dimers interact in *trans* with Nectins or other molecules on the adjacent cells through the first Ig domains. In

trans, nectin1 interacts with nectins3 and 4, while nectin2 interacts only with nectin3. In addition, nectin-3 interacts with nectin-like molecule-5 (Necl-5) that helps in the organisation of cell movement and proliferation. On the other hand, *cis* interactions occur between nectins1-3 with integrin α-β which results in signal transduction to the cytoplasm to rearrange the actin cytoskeleton (Ogita and Takai, 2006), while nectin-3 interacts in *cis* with platelet derived growth factor receptor (PDGFR) that promotes the signalling of cell survival (Rikitake and Takai, 2008).

The ectopic overexpression of nectin-1 in dendrites of cultured rat hippocampal neurons, (which normally express nectin-3 on dendrites and nectin-1 on axons) led to abnormal dendro-dendritic and excessive axodendritic interactions. This suggests the essential role of expression of nectin-1 is on axons and nectin-3 is on dendrites (Martinez-Rico et al., 2005; Togashi et al., 2006).

Neuroplastins:

Neuroplastins are cell adhesion molecules of Ig superfamily that are thought to have a role in the development and plasticity of synapses in human and vertebrates (Bernstein et al., 2007; Smalla et al., 2000). There are two isoforms of neuroplastin (np); np -65 which is comprised of three Ig domain whereas np-55 that has two Ig domains (2-3) (Owczarek et al., 2009). They were called previously, gp65 and gp55. Np-65 is expressed mainly in brain while np-55 is more widely broadly expressed (95% of neuroplastins) (Smalla et al., 2000). Both isoforms are expressed in cell bodies and neurites of forebrain, cerebellar neurons, developing and adult retina and optic nerve (presynaptic). Interestingly, there are variations in expression patterns of neuroplastins between different species in vivo and in vitro, where np-55 is expressed mainly in rat and mouse cerebellum while np-65 is common in human cerebellum and hippocampus (Bernstein et al., 2007; Buckby et al., 2004).

Immunocytochemistry studies, revealed that both isoforms are expressed in both innerpexiform (IPL) and outerplexiform (OPL) layers of retina (presynaptic), while *in situ* hybridization studies suggest pre &post synaptic expression of np-65 in the outer plexiform layer which increased postnatally (OPL) (Kreutz et al., 2001).

Np-65 has a role in initiation of the long-term potentiation (LTP) of hippocampal neurons, through mitogen-activated protein kinas p38 (p38MAPK) activation. The mechanism of np-65 in p38MAPK modifies the expression of surface glutamate receptor (Empson et al., 2006). The mechanism of np-55 was not clear. Furthermore, np-55 induced signalling is suggested to have a role in synaptic plasticity (Owczarek et al., 2009), there is evidence that suggests a genetic relation between neuroplastin and schizophrenia (Saito et al., 2007).

IgLONs Family:

IgLONs are cell adhesion molecules that are members of the Ig superfamily. They are thought to have a role for the development of the nervous system by acting as axon guidance molecules. IgLONs are comprised of four members, opiate-binding cell adhesion molecule (OBCAM) (Schofield et al., 1989), limbic system-associated membrane protein (LAMP) (Brummendorf et al., 1997; Hancox et al., 1997; Pimenta et al., 1995; Wilson et al., 1996), Neurotrimin (Ntm) (Struyk et al., 1995) and the last discovered member is Kilon (kindred-IgLON) (Funatsu et al., 1999). GP55 glycoprotein has a mixture of all members of the group in chick (Wilson et al., 1996). Cerebellum-Purkinji-1 (CEPU-1) is a chick homologue for Neurotrimin (Brummendorf and Rathjen, 1996) whereas Neurotractin (Marg et al., 1999) is the homologue for Kilon in chick (figure1.3).

Structure of IgLONs:

IgLONs are highly glycosylated GPI-anchored proteins which are formed of three Ig domains, and are located in lipid rafts on the cell surface. IgLONs have six or seven N-glycosylation sites which comprised more than 20% of their molecular mass. In rat brain, IgLONs were analysed for glycosylation sites, the peptide and carbohydrate section. The glycosylation is important for cell-cell interactions (Kleene and Schachner, 2004). The first Ig domain is highly glycosylated with high mannose oligosaccharides in all IgLON proteins. The high heterogenousity of the third Ig domains due to the linkage of diverse oligosaccharides which include BA-2, a brain specific glycan, is more abundant in mammalian brains than other tissues (Chen et al., 1998; Itoh et al., 2008; Nakakita et al., 1998)(figure1.4).

IgLONs have different isoforms in chick; there are α1 and α2 isoforms for OBCAM, CEPU-1 (Ntm) and LAMP which differ in long signal peptide of N-

terminal, there is also a β isoform for CEPU-1 and LAMP with additional 11 or 12 amino acids (Brummendorf and Rathjen, 1996; Lodge et al., 2000). In addition, there are two isoform for Neurotractin (Kilon), Ntr-L is the long isoform and Ntr-S is the short which has only two Ig domains (Funatsu et al., 1999; Marg et al., 1999). Exceptionally, CEPU-1 exists in a secreted isoform CEPU-1-Se, where no GPI anchor is attached to the molecule (Lodge et al., 2000).OBCAM also has a putative secreted isoform which was isolated by our research group (unpublished data). IgLONs show a high sequence homology between their members (Brummendorf and Rathjen, 1996).

IgLONs activity:

GP55 is chick glycoprotein which has a mixture of IgLONs molecules; CEPU-1, OBCAM, LAMP and Neurotractin (Wilson et al., 1996). Forebrain and dorsal root ganglion (DRG) neurons were unable to initiate their neurite when cultured on GP55. This is supported by another experiment in which the forebrain and DRG neuronal cell bodies were unable to send their neurites across an island of GP55 (Clarke and Moss, 1994, 1997). However, the inhibition that was caused by GP55 was reversed by using pertusis toxin (PTX) (Clarke and Moss, 1997). This evidence suggested the role of IgLONs as negative guidance molecules during development was possibly through a trimeric G protein complex.

Neurite outgrowth assays were used to investigate the activity of single IgLONs on the ability of the neurons in extension of their neurites. Surprisingly, DRG neurons were able to extend their neurites on single IgLON-transfected CHO cells and when single IgLON-Fc recombinant proteins were used as substrate,

furthermore, no inhibition occurred with a mixture of IgLON-Fc recombinant proteins (McNamee et al., 2002).

The neurite outgrowth from DRG and hippocampal neurons was encouraged by Ntm-Fc recombinant protein, whereas neurite extension by sympathetic neurons was inhibited (Gil et al., 1998). This suggested a dual effect of neurotrimin on the neuronal outgrowth. DRG neurons that express Ntm and LAMP or OBCAM at low level were cultured on LAMP-CHO cells as substrate resulted in reduction of the length of neurite outgrowth. This evidence suggested the inhibition of neurite extension due to a heterophilic *trans* interaction between Ntm and LAMP (Gil et al., 2002).

CEPU-Se is a secreted isoform of CEPU-1, mRNA of both CEPU-Se and CEPU-1 are co-expressed in retina and developing and adult cerebellum. CEPU-Se needs to be in dimeric form to interact in *trans* with CEPU-1, OBCAM and LAMP-CHO cell lines, whereas it showed no homophilic or heterophilic interaction with IgLON-transfected cell lines when provided as a monomer. CEPU-Se/laminin substrate allows dissociated DRG neurons to grow and extend their neuritis. However, DRG explants were unable to extend their neurites to areas coated with CEPU-Se, so, it may have a role in modulation of IgLONs interactions (Lodge et al., 2001).

Previously, cell adhesion assays revealed that CEPU-1-Fc bound to chick sympathetic neurons that express LAMP, CEPU-1 and OBCAM (Lodge et al., 2000; McNamee et al., 2002). These assays carried out on cerebellar granule cells also showed strong binding to CEPU-1-Fc and OBCAM-Fc while LAMP-Fc bound weakly, even though reverse-transcription PCR and immunofluorescence staining revealed that cerebellar granule cells express CEPU-1, OBCAM and LAMP (Reed et

al., 2004). Investigation on the ability of binding the chimeric proteins to the surface of the cerebellar granule cells, and relative affinity of protein-protein interaction between IgLON molecules were carried out to clarify the previous results. LAMP-Fc did not bind to the cerebellar granule cells while both CEPU-Fc and OBCAM-Fc binding was detected. There was no explaination of the fact that LAMP-Fc was unable to bind since it should bind to CEPU-1 or OBCAM (Reed et al., 2004). Although, LAMP-Fc bound to transient transfected OBCAM-CHO cell line, this binding can be reduced or abolished by co-expression of LAMP. This suggests that IgLONs act as heterodimeric proteins on the plane of the membrane (DigLONs).

Recent result show inhibition of initiation of neurite outgrowth from forebrain neurons by CEPU-1-OBCAM or CEPU-1-LAMP transfected CHO cell lines, while single CEPU-1 or OBCAM transfected CHO cell lines failed to inhibit neurite outgrowth (Christine McNamee PhD thesis, University of Liverpool 2008) (figure1.5). CEPU-1-OBCAM transfected CHO cell lines also inhibit cerebellar granule cell neurite outgrowth whereas no inhibition occurred with single transfected CEPU-1 or OBCAM CHO cell lines. This evidence suggests that the pairs of IgLONs on the CHO cell surface may form dimers and explains the inhibition of neurite outgrowth caused by GP55 which may contain a combination of different IgLON molecules in heterodimeric forms (DigLONs) (Reed et al., 2004) (figure1.6).

Co-expression of IgLONs:

IgLONs are co-expressed in certain area of the nervous system during particular stages of development. Neurotrimin (CEPU-1) and OBCAM are usually co-expressed in the hippocampus (Struyk et al., 1995) whereas Kilon (Ntr) and OBCAM co-expressed in the cerebral cortex and hippocampus with an increase post natally (Miyata et al., 2003a). In addition, co-expression of both neurotrimin and LAMP using neurotrimin and LAMP antibodies revealed expression on a subpopulation of CNS neurons from E16 dorsal root ganglion (DRG), E18 thalamus, olfactory bulb and hippocampus. Double staining with specific antiserum showed co-localisation of both LAMP and Neurotrimin (CEPU-1) on surface of the most hippocampal neurons and 80-90% of olfactory neurons, whereas 10% express LAMP only (Gil et al., 2002).

IgLONs interactions:

IgLONs have homophilic and heterophilic interactions between the members of the group, and different studies were used to inspect these interactions using IgLON-Fc recombinant proteins and IgLON-transfected cell lines. CEPU-1, OBCAM and LAMP *trans* homophilic and heterophilic interactions were confirmed by the immuno-affinity studies of IgLON-Fc recombinant proteins and IgLON-transfected cell lines (figure1.7) (Brummendorf et al., 1997; Lodge et al., 2000; Reed et al., 2004). Some IgLONs are not known to have interactions with other molecules from outside the group. This was suggested when OBCAM-Fc and Ntm-Fc (CEPU-1) recombinant proteins bound to LAMP-transfected CHO cells, whereas other Ig superfamily molecules such as L1, contactin or NCAM recombinant proteins failed to bind to LAMP-CHO cells (Gil et al., 2002). The situation is different for Kilon

(Ntr) due to its two isoforms; Ntr (L) and Ntr(S), Ntr-Fc recombinant protein was used in binding studies with IgLON-transfected cell lines. The intensity of interaction varies according the cell line and the isoform of Kilon, on CEPU-1-transfected CHO cell line, both Ntr (L) and Ntr (S) interact strongly, whereas with LAMP-transfected CHO, Ntr (L) has weak interaction and Ntr(S) has much weaker interaction (Marg et al., 1999). Kilon interacts heterophilically with OBCAM in *trans (Miyata et al., 2003b).*

Expression of IgLONs:

IgLONs are expressed within the nervous system and specific regions in the body. They have roles during all stages of development and in the adult. They are thought to have a role in early development including migration and differentiation of the neuronal precursors in the central nervous system. Afterwards, with development the expression of IgLONs increases which suggested another role in axon outgrowth alteration. In addition, they might be regulating synapse formation. In adult, the level of expression becomes higher than in development which implies a role in synapse plasticity and nervous regeneration.

During migration and differentiation:

CEPU-1 and LAMP are suggested to be implicated in differentiation and migration of certain brain regions during early stages of development. In the neural tube, LAMP mRNA was expressed by the anterior region of the neural tube beside the migrating neural crest cells and the notochord. Their presence at this time suggested that IgLONs might be implicated in the neuro-epithelium and neural crest cells interaction (Kimura et al., 2001). CEPU-1 expression was faint in the anterior ectoderm, migrating mesenchyme and increases in intensity in the neural plate. Later on, mRNA of CEPU-1 is situated in the forebrain, midbrain and anterior region of

the hindbrain as broad band. As the embryo develops around the second embryonic day, it becomes more localised as distinct band to the midbrain-hindbrain boundary or at isthmus. At this stage, CEPU-1 and particular molecules such as Wnt1, EphB3 and FGF8 were colocalised, suggesting IgLONs may act alongside these molecules (Jungbluth et al., 2001; Kimura et al., 2001). By E3, CEPU-1, OBCAM and LAMP are expressed in the notochord, whereas the floor plate expresses CEPU-1 and OBCAM. This evidence suggested the role of IgLONs in induction of differentiation of the neural plate midline cells into floor plate. No expression of Neurotractin in this stage was detected (Sahar Youssef PhD thesis University of Liverpool 2007).

During axons outgrowth:

During development of the embryo, in rat brain, Neurotrimin (CEPU-1) has limited expression to postmitotic neurons, and then increased in forebrain at the age of 15 embryonic days, so it is considered the highest in primary sensory and motor regions of the brain (Gil et al., 2002; Struyk et al., 1995). Initially, LAMP is expressed by limbic system neurons, cortical and subcortical neurons, medial nucleus of the thalamus and eventually in regions of the brain that are related to learning, memory, cognitive behaviour and autonomic function (Horton and Levitt, 1988; Levitt, 1984; Pimenta et al., 1996; Reinoso et al., 1996). LAMP was suggested to be responsible for selective axon guidance to certain regions in the cerebral cortex due to its limited expression in non limbic thalamo-cortical regions; limbic thalamic axons that express LAMP were attracted to LAMP, while the non limbic thalamic axons were repelled (Mann et al., 1998). In LAMP knockout mice, there were no differences in axonal projection (Catania et al., 2008). Mainly, OBCAM is expressed in the cerebral cortical plate and hippocampus regions of the brain (Miyata et al., 2003b; Struyk et al., 1995). Kilon (Ntr) the last discovered member of the group; it is

expressed by embryonic age (E16) in rat brain and then shows gradual increase with development. In early postnatal rat, cortex and hippocampus are the sites for expression of kilon, while in adult, expression decreases in the cortex and remains high in dentate gyrus of hippocampus and cerebellum (Brauer et al., 2000; Funatsu et al., 1999). In chick, Neurotractin was expressed by a subset of commissural and longitudinal axon tracts in central nervous system with an increase during development which continues in the adult (Marg et al., 1999). LAMP may play a role in development of the visual system outside the nervous system, as it is expressed in the optic fibre layer of chick retina and the tectum at E7 age (Brummendorf et al., 1997). IgLONs are expressed in different layers of retina as revealed in previous immuno-localisation studies on E18 chick retina frozen sections. LAMP and CEPU-1 co-expressed in the outer plexiform layer which is the site for synapse between bipolar cells and photoreceptors. The inner plexiform layer is the region for retinal ganglion cells and bipolar cells to form the synapse, where LAMP and OBCAM colocalised. While Neurotractin expressed in the outer plexiform layer of the retina (Lodge et al., 2000).

During synaptogenesis:

The expression of IgLONs might be related to synapse formation particularly on dendrites. Firstly, expression patterns of Neurotrimin (CEPU-1) imply a role in formation of excitatory synapses in the cerebellum during development and maintenance to the adult stage (Chen et al., 2001). Initially, LAMP is expressed on both axons and dendrites in limbic brain tissue, and then postnatally remains at postsynaptic sites on dendrites (Horton and Levitt, 1988; Zacco et al., 1990). Specific antibody and antisense oligonucleotides were used to inhibit the expression of OBCAM on dendrites of hippocampal neurons. This resulted in a remarkable reduction in the number of synapses, while when OBCAM was over-expressed; an increase in synapse formation is observed. This evidence suggests OBCAM has a role in synaptogenesis (Miyata et al., 2003a; Yamada et al., 2007). Dendrites of the cerebral cortex and hippocampus and cell bodies of pyramidal neurons express kilon (Ntr) (Funatsu et al., 1999), kilon (Ntr) was identified on dendrites with double staining with post-synaptic vesicles protein synaptophysin (Schafer et al., 2005). In addition, kilon and OBCAM are co-localised mainly pre-synaptic

sites on dendrites and in synapses of developing and adult brains. This was confirmed with confocal imaging studies using the vesicle-associated membrane protein 2 (Miyata et al., 2003a).

During adulthood:

There is a link between synaptic plasticity and high level of expression of IgLONs in the limbic system and cerebral cortex during learning and development of new memories processes (Funatsu et al., 1999; Levitt, 1984; Pimenta et al., 1996; Struyk et al., 1995). Higher levels of LSAMP expression in rats correlates with anxiety and the rats become less liable to explore an elevated plus–maze (Nelovkov et al., 2003). LSAMP deficient mice become less alert and increase in their exploration activities of a novel maze (Catania et al., 2008).

A comparative study for IgLONs expression in epithelial ovarian tumours to normal ovarian tissue showed loss of gene expression of OPCML (OBCAM), LSAMP (LAMP) and NEGR1(Kilon) whereas HNT (Ntm) was increased (Ntougkos et al., 2005). While the loss of OPCML gene expression is related with epithelial ovarian cancer (Sellar et al., 2003) as well as with gliomas (Reed et al., 2007). This suggests a role for IgLONs in the suppression of tumours. In tumours, the patients have a bad prognosis due to low expression of LSAMP gene (Ntougkos et al., 2005). There is a relation between LSAMP translocation with familial clear renal cell carcinoma (Chen et al., 2007).

In this thesis, the aim is to generate CEPU: OBCAM-Fc (CO-Fc) heterodimeric recombinant chimeric protein and use it as tool to further characterise the previous results of the CO double transfected CHO cell line which inhibit the initiation of the neurite outgrowth of E8 forebrain neuron.

The first step is the generation of myc epitope tagged OBCAM-Fc by cloning this construct into pBudCE4.1 plasmid, followed by single or double transient transfections in order to test pBudCE4.1-OBCAM-Fc-myc and/or pcDNA6-CEPU-Fc-V5 constructs. The next step is generation of stable CHO cell line and using ELISA assay, dot blot and Western blotting for characterisation of CO-Fc heterodimeric recombinant protein (figure 1.12).

Finally, the activity of CO-Fc recombinant protein will be tested on neurite outgrowth assay and compare it with the previous results of CO-CHO double transfected cell line. In addition, immunofluorescence studies will be carried out to investigate its interaction with the putative receptors on the cell surface of the neurons, chick retina frozen sections and IgLON-transfected cell lines to identify the role of IgLONs in formation of the putative receptors complex (figure1.13).

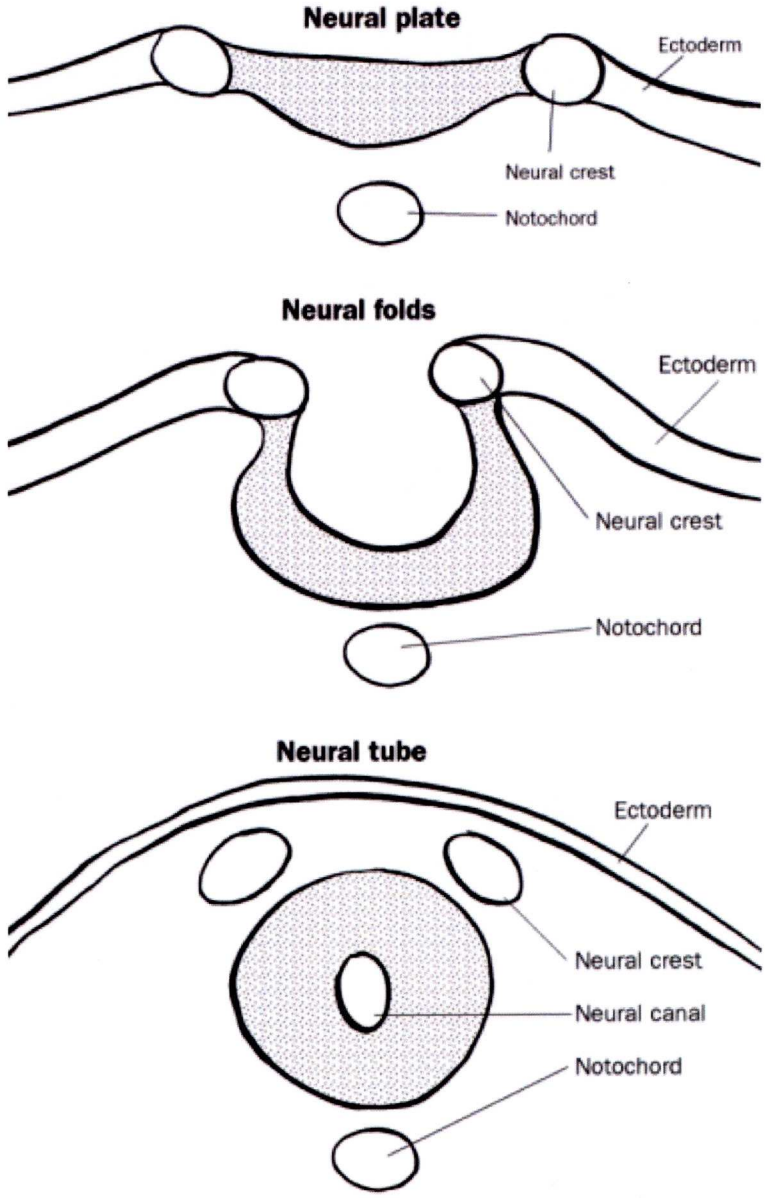

Figure 1.1: The structure of the neural tube

An illustration describes the formation of the neural tube from folding of the neural plate to form the neural groove which then ends with formation of the neural tube. Neural tube is formed by important structures; which have roles in the development of the nervous system such as roof plate and floor plate and the neural canal in the middle. Notochord lies below the neural tube while the neural crest above it.

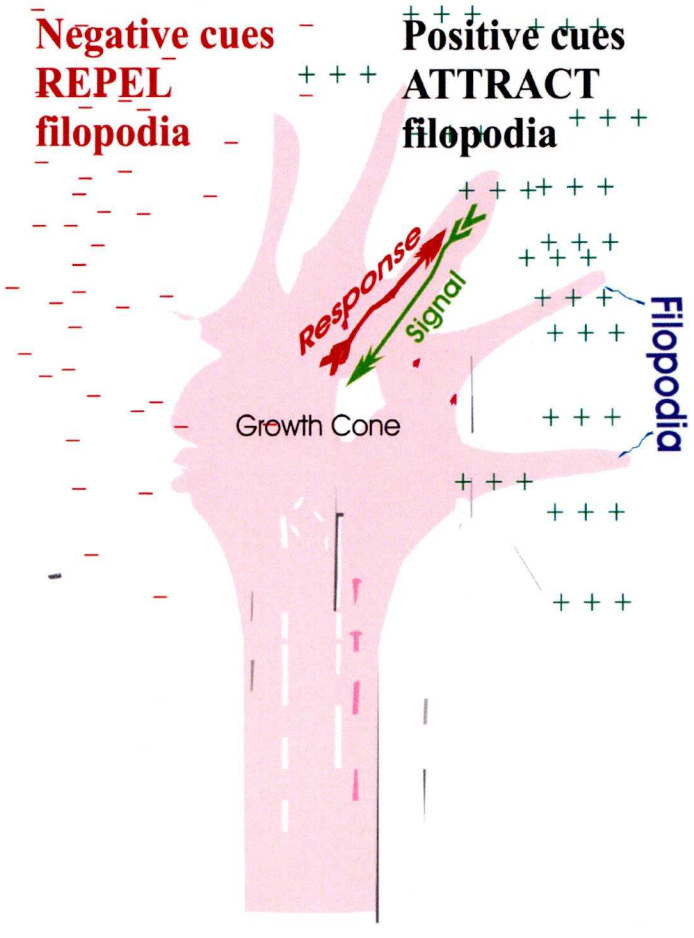

Figure 1.2: Axon growth cone that attracted to its target by the action of positive and negative cues

A diagram describes the structure of a growth cone which is formed of lamellipodia and filopodia surrounded by different guidance cues; positive and negative. The growth cone is guided to its target by the action of both cues. The cytoskeleton of the growth cone is rearranged in response to the signal of the surrounding guidance cues. Adapted from (Huber et al., 2003)

Attractive Cues (positive)		Repulsive Cues (negative)	
Receptor	**molecule**	**Receptor**	**molecule**
DCC	**Netrin**	**DCC+UNC**	**Netrin**
		Plexin+NP(L1)	**Sema3**
		Eph	**Ephrins**
Frazzled	**Wnt**	**Derailed**	**Wnt**
		Robo	**Slit**
Plexin B	**Sema4**	**Plexin A**	**Sema1**

Table1.3: List of attractive and repellent axon guidance molecules and their receptors

A table listed the different axon guidance molecules and their receptors, whether attractive or repulsive.

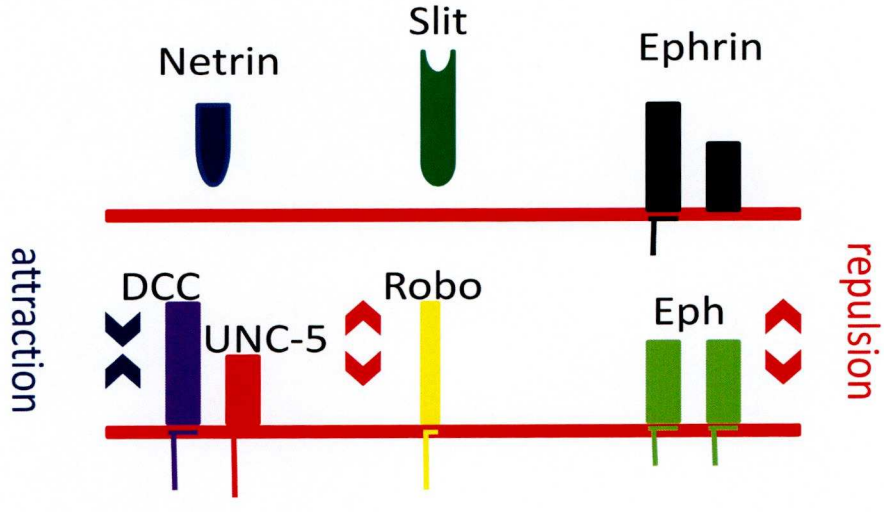

Figure 1.4: Attractive and repellent axon guidance molecules and their receptors

An illustration describes the interaction between the cell adhesion molecules with their receptors on the adjacent cell. These molecules became attractive or repellent according to the type of the receptor that expressed. Netrin and DCC (positive), while netrin, DCC and UNC5 (negative). Slit and Robo (negative), Ephrin and Eph receptor (negative).Semaphorin and NP (L1) (negative) (Dickson, 2002).

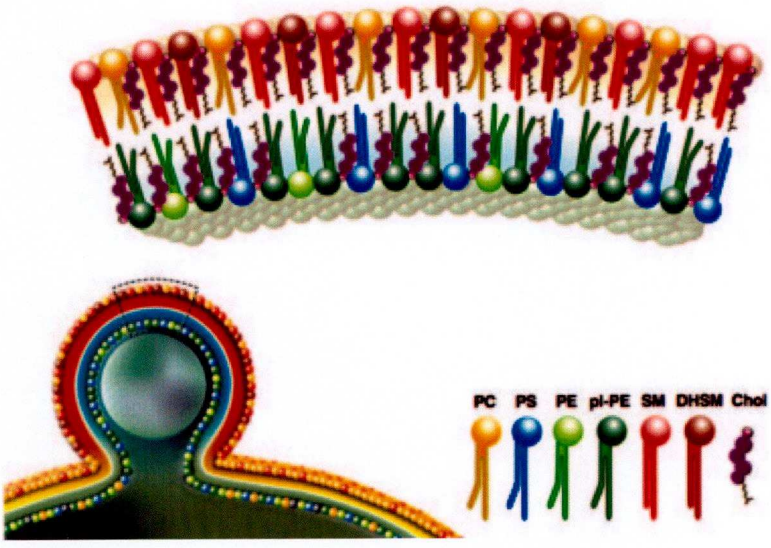

Figure 1.5: Structure of Lipid rafts microdomains in the cell membrane

A diagram describes the structure of lipid rafts which consist of sphingolipids and cholesterol. Sphingolipids are arranged tightly to be detergent insoluble low-density regions. They act as platform for GPI anchored proteins. Adapted from (Munro, 2003).

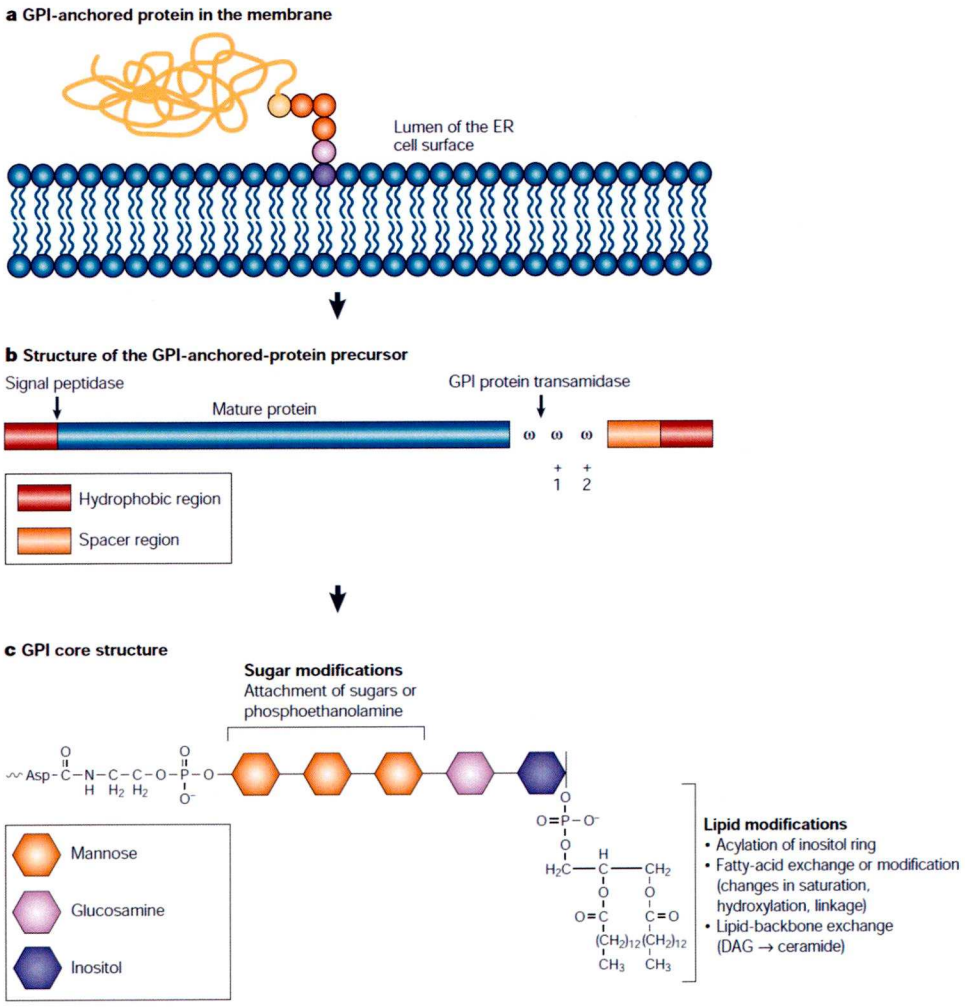

Figure 1.6: Structure of GPI anchored protein that attached to lipid rafts

A) The GPI anchored protein that located on the extracellular leaflet of the plasma membrane by their GPI anchor

B) These proteins are synthesised in the lumen of endoplasmic reticulum with its hydrophobic amino terminal region signal sequence and carboxyl terminal region that attached the protein to GPI anchor.

C) The anchor is joined to the C-terminal amino acid by an ethanolamine, which is linked to an oligosaccharide that consists of three mannose, N-acetylgalactosamine, and glucosamine. The oligosaccharide is in turn joined to the inositol head group of phosphatidyl inositol. The two fatty acid chains of the lipid are embedded in the plasma membrane(Mayor and Riezman, 2004).

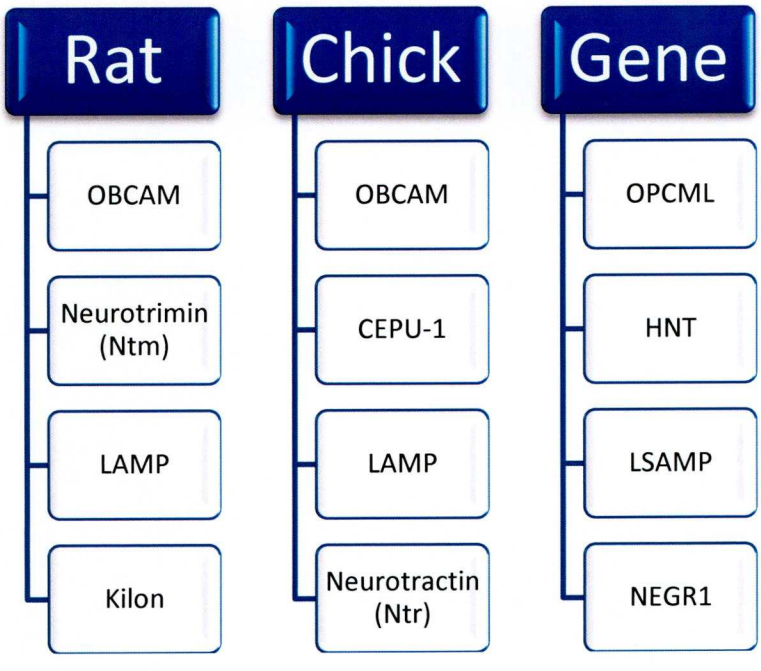

Figure 1.7: IgLON molecules in Rat and Chick and their related Genes

An illustration listing the different IgLON molecules in rat; and their chick homologues plus the name of their genes

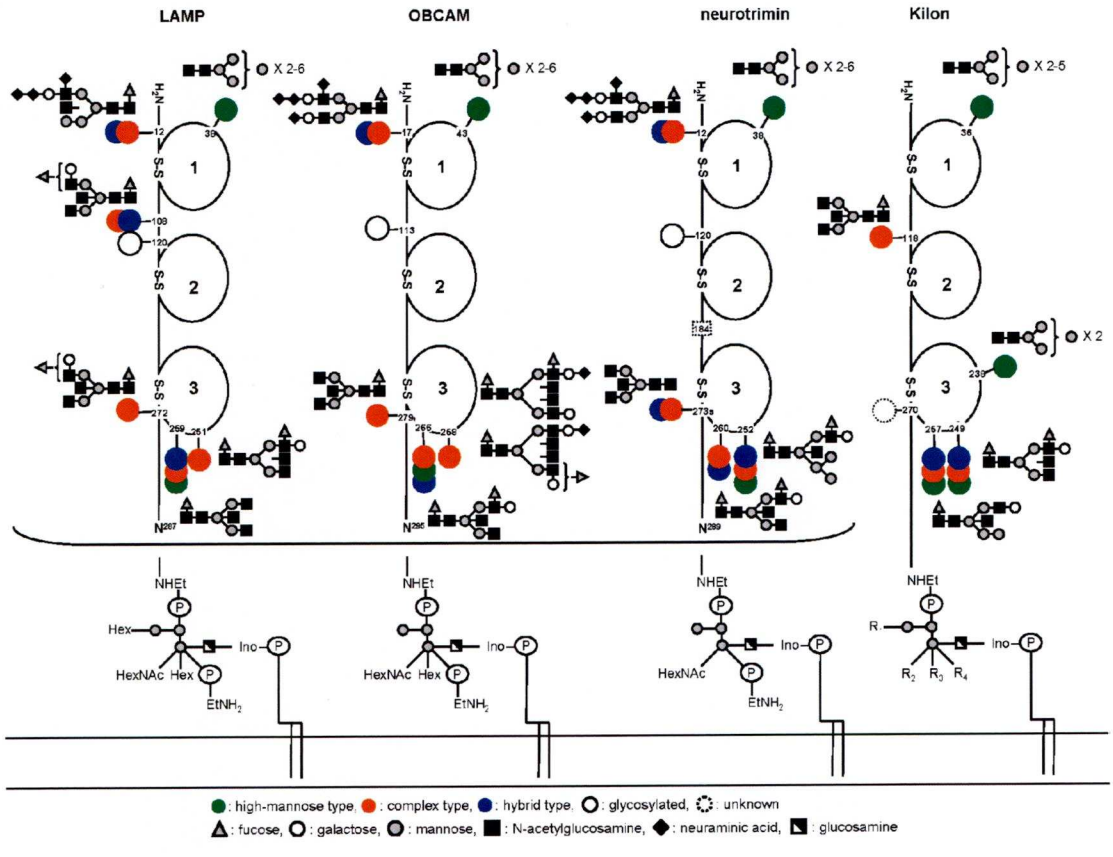

Figure 1.8: Structure of IgLONs cell adhesion molecules

A schematic diagram describes the structure of different IgLON molecules; LAMP, OBCAM, Neurotrimin (CEPU-1) and Kilon. There are multiple glycosylation sites. IgLONs formed by three Ig domains and attached to the lipid rafts of cell membrane by GPI-anchor (Itoh et al., 2008).

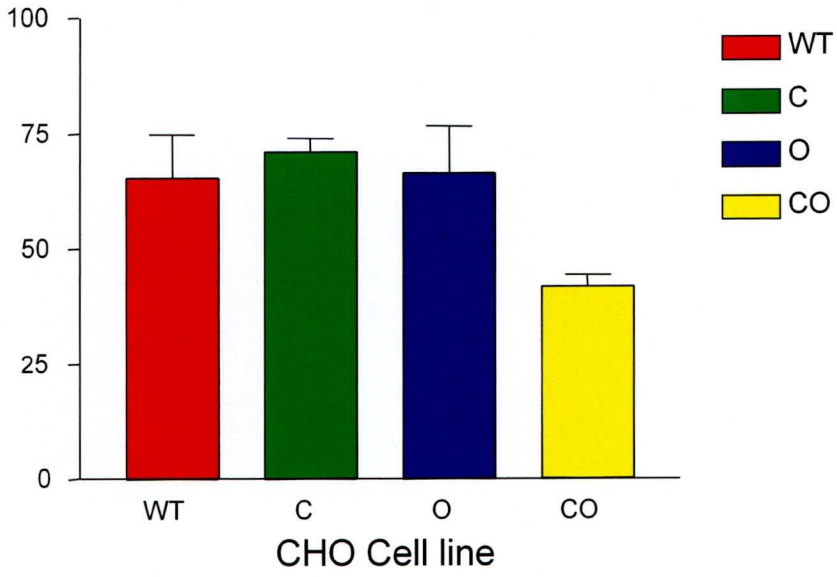

Figure 1.9: CEPU-1 and OBCAM double transfected CHO cell line inhibit the neurite outgrowth from E8 forebrain neurons

CO-CHO cells inhibit the neurite outgrowth from E8 forebrain neurons, where the outgrowth was about 40% (yellow bar), while WT (red bar), CEPU-1(green bar) and OBCAM (Blue) CHO cell line failed to inhibit their outgrowth, The percentage of the outgrowth was about74%, 68% and 77% respectively (p value <0.01)(Christine McNamee PhD Thesis University of Liverpool 2008).

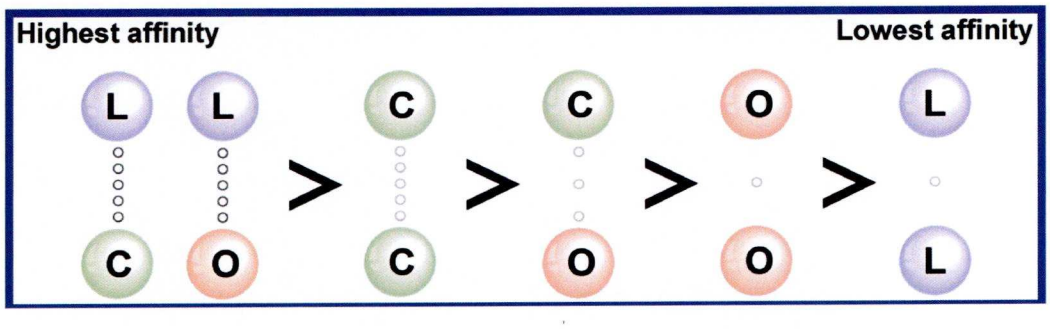

Figure 1.10: Homophilic and heterophilic *trans* interactions between IgLON molecules

A diagram describes the affinity of trans interactions between CEPU, OBCAM and LAMP molecules. The highest interaction is between LAMP and CEPU-1 then LAMP and OBCAM followed by the homophilic trans interaction of CEPU-1, the next is CEPU-1 and OBCAM and finally the lowest interactions are the homophilic interactions of OBCAM and LAMP based on ELISA assays (Reed et al., 2004).

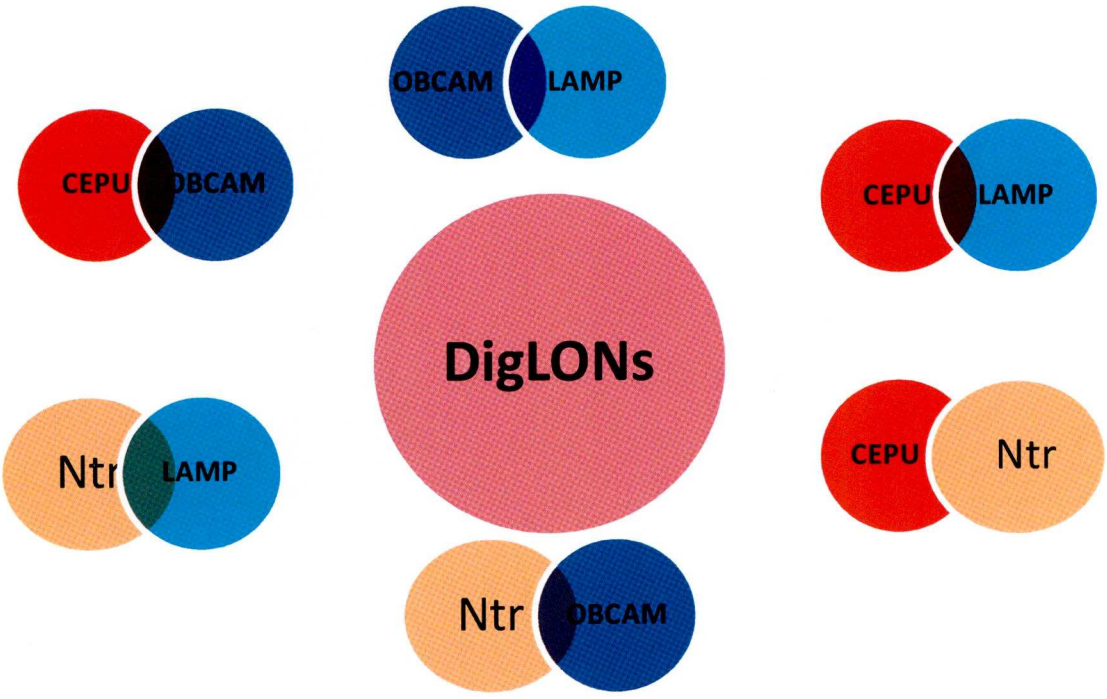

Figure 1.11: the proposed DigLONs that can be formed by IgLONs

A diagram describes the possibility of six DigLONs formation of four IgLON molecules; CEPU-1, OBCAM, LAMP and finally Neurotractin. There is evidence for CEPU-1: OBCAM CEPU-1: LAMP and OBCAM:LAMP existing as DigLONs (Reed et al., 2004).

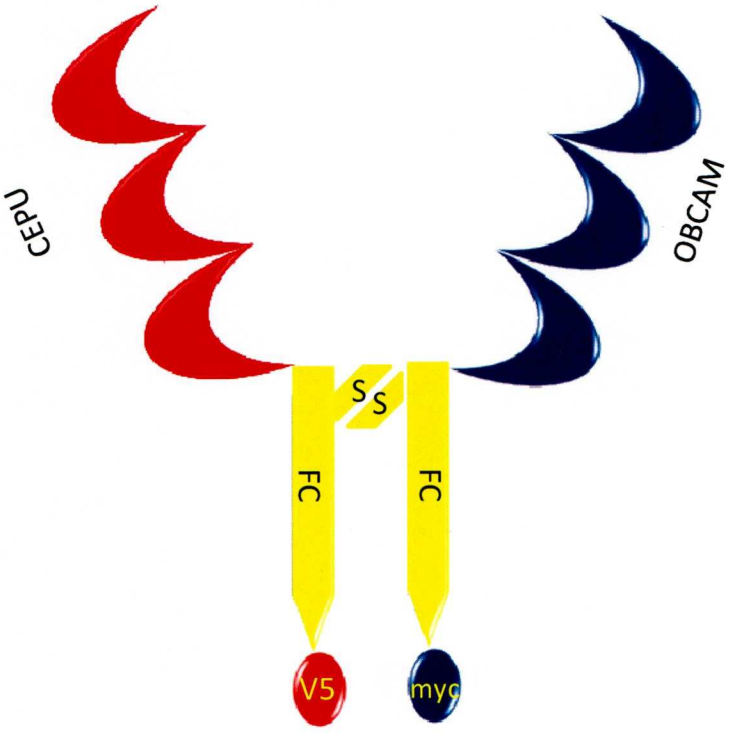

Figure 1.12: proposed structure of CO-Fc IgLON Heterodimer complex

A schematic diagram describes the structure of CEPU-1: OBCAM-Fc heterodimer complex which is formed of V5 tagged CEPU-1 chain and myc tagged OBCAM chain, both chains are attached at Disulfide Bridge of the human Fc tails.

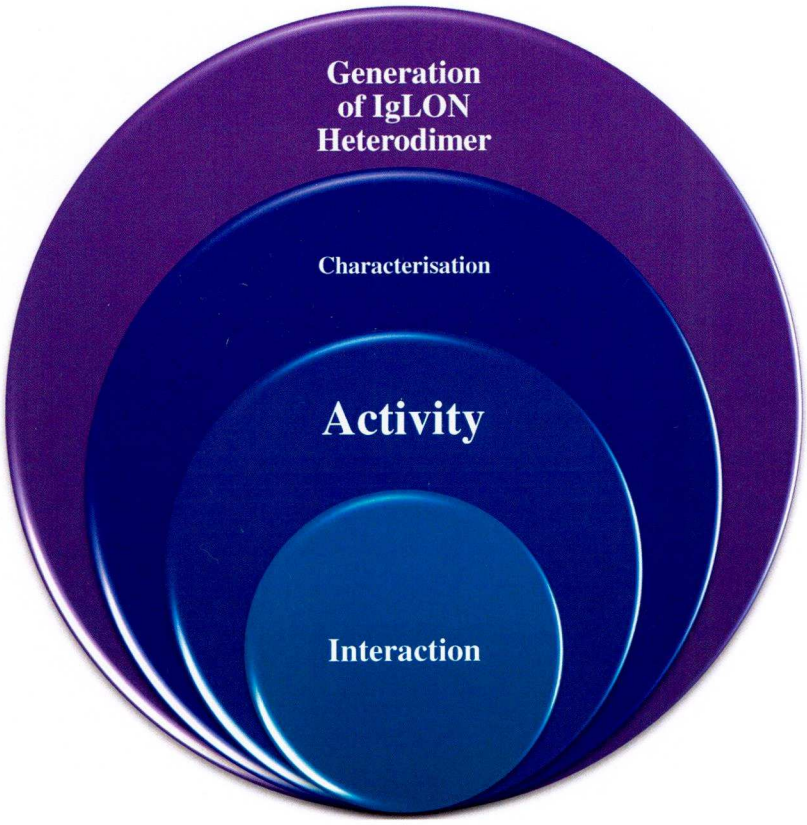

Figure 1.13: Aim of the thesis

This illustration describes the aim of this thesis starting from the molecular section of the project which is cloning of OBCAM-Fc into pBudCE4.1 to form pBudCE4.1-OBCAM-Fc-myc construct, then testing of this construct by transfection of CHO cells, followed by stable double transfection with pcDNA6-CEPU-Fc-V5 to produce CO-Fc recombinant heterodimeric protein. The recombinant protein was then analysed by ELISA assay for characterisation of this protein as well as dot blot and Western blotting. Finally, the activity of this protein was tested on neurite outgrowth assay and its interaction with the putative neuronal receptors.

Chapter Two

Materials and Methods

Molecular Biology:

OBCAM-Fc sequence was cloned into pBudCE4.1 vector (Invitrogen) to add myc-His6 tags to the 3 prime end of the OBCAM-Fc sequence prior to stop codon. Primers were designed to add HINDIII and xba1 restriction sites in frame either end of the OBCAM-FC sequence to enable cloning into the pBudCE 4.1 vector. PCR was used to amplify OBCAM-Fc construct which had previously been cloned into pcDNA3 plasmid using proof reading Taq (Invitrogen).

PCR reaction for OBCAM-Fc construct in pcDNA3:

Forward Primer:_5'-CCACTGCTTACTGGCTTATC-3'
Reverse Primer:_5'-GTCGCACTCATTTACCTCTAGACAG-3'

0.1µg-0.001µg Plasmid DNA		1µl
10mM d NTP mix		1.5µl
10µM of both forward and reverse primers		1.5µl
50mM $MgSO_4$ (pfx Taq polymerase) or		
50mM $MgCL_2$ (ordinary Taq polymerase)		1µl
10XTaq polymerase amplification buffer		5µl
Taq polymerase or proof reading Taq		1µl
PCR grade water	total volume	50µl

A negative control was used with no DNA.

Temperature	Time	Cycles	Function
94	10 minutes	1	Taq activation
94	1 minute	30	DNA denaturating
56	1 minute		Primer annealing
68 or 72	2minutes		Strand extension
68 or 72	10 minutes	1	Strand completion

Table: PCR reaction.

Agarose gel electrophoresis DNA analysis:

Products of PCR were mixed with 2µl of x5 Blue juice ™ loading buffer (Invitrogen) plus 1.5µl/sample SYBER™ green DNA dye (Sigma). They were then loaded onto a 1% Agarose gel, in TAE buffer containing 40 mM Tris-acetate 1m M EDTA (50x stock 242g Tris base 571ml glacial acetic acid, 100 ml 0.5M EDTA pH8.0 per litre). UV excitation of SYBER ™ green was used to visualise the PCR product at a wavelength of 586nm and emission of 605nm. A molecular weight marker 1Kb was used to identify the size of the PCR product.

TA Cloning of PCR product into PCRII TOPO™ vector:

TOPO TA™ (Invitrogen) cloning kit was used to clone the PCR product into pCRII TOPO™ vector (Invitrogen). Three µl of PCR product was incubated with 1 µl pCRII TOPO ™ vector, 1µl TOPO™ salt buffer and 1 µl of sterile water at room temperature for 5 minutes, finally placed on ice for 20 minutes. The TA cloning product was used to transform DH5α-T1® competent bacteria. Because proof reading Taq was used for PCR reaction, 0.7-1unit of ordinary Taq was added to the reaction to add the 3'A-overhangs

Competent bacteria transformation:

DH5α-T1® Competent bacteria were thawed on ice and 2 µl of TA cloning product was mixed gently into the bacteria cells then incubated on ice for 15 minutes. Immediately, the bacterial cells were given a heat shock in a water bath at 42°C for 30 seconds. Two hundred and fifty microlitres µl of room temperature SOC medium was added to the mixture and shaken at 250 rpm at 37°C for 1hour. 10, 50 and 100 µl of the transformed competent bacteria were cultured on pre-warmed Luria Broth (LB) or low salt LB agar plates with Kanamycin (50mg/ml) antibiotic for pcRII vector or Zeocin (50mg/ml) for pBudCE4.1vector. These plates were incubated for 24 hours at 37°C to allow the transformed bacteria to grow in colonies.

Miniplasmid prep:

Sigma Miniplasmid kit was used to isolate the plasmid DNA. The maximum yield of DNA out of the kit was about 20μg. The transformed competent bacteria were cultured overnight in 5ml of LB broth (or low salt LB broth) with 50 mg/ml Kanamycin antibiotic (or Zeocin). The cultured mixture was spun at 3000 rpm for 10 minutes, and then the pellet was resuspended in RNAase buffer of the kit. Under alkaline condition, these bacteria were lysed and neutralised, followed by steps of binding of DNA to column provided with the kit. The column was spun with the washing buffer, finally the DNA was eluted in 50 μl DEPC treated water and stored at-20°C. 1μl of a Miniplasmid prep DNA product was loaded and run on 1% Agarose gel, 1KB marker (Invitrogen) to identify the size of the miniplasmid product.

Double digestion with restriction enzymes:

Hind III and Xba1Restriction enzymes (Invitrogen) were used to digest the OBCAM-Fc insert out of the pCRII II TOPO intermediate vector and pBudCE4.1 final vector (Invitrogen). Sixteen microlitres μl of DNA were digested with 2μl of reactive buffer and 1μl of each restriction enzyme, followed by incubation of the mixture for 1 hour at 37°C. The products were loaded onto a 1% Agarose gel, and a 1KB marker was used to measure the size of the OBCAM-Fc insert and the opened pBudCE4.1 vector. Both digested OBCAM-Fc insert and pBudCE4.1 vector were loaded on run on Agarose gel. The bands at the right size were cut with a razor blade and centrifuged at the maximum speed through a glass wool column to purify the DNA from the agarose gel. The flow through of the column was precipitated in 2 volumes of molecular grade ethanol and 1/10 of 3M sodium acetate and incubated for at least one hour in - 80 °C. Centrifuge the solution at 15,000xg for 30 minutes to

pellet the DNA. The pellet was dried and resuspended in 50 µl sterile de-ionised water.

Ligation of insert into digested final vector:

Invitrogen Qubit assay kit was used to measure the concentration of the vector and the insert. The following equation was used to calculate the amount of DNA required for the ligation reaction:

$$\frac{\mu g \text{ of vector x Kb size of insert}}{\text{Kb size of vector}} \times \frac{\text{molar ratio of insert}}{\text{vector}} = \mu g \text{ of insert}$$

$$\frac{100 \times 2.2}{4.2} \times \frac{3}{1} = 157\ \mu g$$

Ligation	Quantity
pBudCE4.1 vector	3 µl
OBCAM-Fc insert	4 µl
Ligation Buffer	2 µl
T4 ligase enzyme	1 µl

Table: ligation of the insert to the final vector

Overnight incubation of the ligated OBCAM-Fc insert with pBudCE4.1 final vector at the ratio of 3:1 the insert to the vector at 14°C with 1µl T4 Ligase enzyme and 4µl buffer follow the manufacturer's instructions (Invitrogen). Competent bacteria were transformed with the ligation product and spread on low salt LB agar plates, and then these plates incubated overnight at 37°C.10 well formed colonies were grown and screened for OBCAM-Fc-pBudCE4.1 by PCR using Taq polymerase (Invitrogen) with same forward and reverse primers and in addition to negative control.

Plasmid Sequencing:

OBCAM-Fc construct was sent to be sequenced to (Lark) (Cogenics) to confirm the cloning of OBCAM-Fc insert into pBudCE4.1 vector (Invitrogen) vector plasmid using forward T7P primer.

Endotoxin free midi plasmid prep:

The isolation of the endotoxin free plasmid DNA was performed by using Sigma Gen Elute endotoxin free plasmid midi prep. Up to 250µg was expected according to the manufacture's protocol. The transformed competent bacteria were enucleated into 40 ml LB broth (or low salt LB broth) containing antibiotic and incubated and shaken at 37°C and 250 rpm. Then, the overnight bacteria culture was pelleted by spinning at 3000xg for 5 minutes and lysed in a modified alkaline-SDS procedure. The endotoxins were removed from the clear lysate. Plasmid DNA was purified through a column in the presence of high salt. After binding and spin washing steps, the pure plasmid DNA was eluted in endotoxin free water.

Ethanol precipitation:

Two volumes of molecular grade (Sigma) and $1/10^{th}$ volume of 3M sodium acetate were added to the total volume of endotoxin free plasmid to purify and concentrate the plasmid. The solution kept in -80°C for 2-24 hours, and then spun for 30 minutes at 15000xg. The dried and precipitated pellet was resuspended in 50 µl of DEPC water.

CHO-cell lines Tissue culture:

Production of recombinant chimeric heterodimeric protein:

Transfection of CHO cells:

For transient transfection, CHO cells were cultured in 6 well-plate tissue plate at cell density of 0.8-1x10^5 with 13mm glass cover slips in DMEM/F12 plus 10%FCS growth medium for 24 hours incubation at 37°C, 5% CO2 level. Firstly, ethanol precipitated endotoxin free pBudCE4.1-OBCAM-Fc-myc-His6 (1μg/μl) and/or pcDNA6-CEPU-V5-His6 (1 μg/μl) plasmid were diluted into 150m M NaCl buffer, briefly, the solution were mixed using vortex and microfuge. ExGEN500 (Fermentas) transfection reagent was added to the solution at a ratio of 3:1 according to the manufacturer's instructions, immediately, the solution of transfection were vortexed for 10 seconds and incubated for 10 minutes at room temperature then added to CHO cells drop wise and the plate was rocked vertically and horizontally and centrifuged for 5 minutes at 90xg. The cells were incubated for 24 hours at 37°C, 5% CO2 level. The GFP was cloned into pBudCE4.1 vector already under EFα1 promoter. The transfection efficiency was assessed by counting the number of cells that expressing GFP (fluorescent) to the total number of cells (phase) in three microscopic fields in each cover slip using fluorescence microscope.

For Stable transfection, CHO cells were cultured and transfected as before for transient transfection. Killing curves were carried out for Blasticidin and Zeocin antibiotics. The selective antibiotics were added to the growth medium after 48 hours incubation from the transfection. The cell count should be less than 50% confluency to increase the efficiency of the antibiotic. Once the transfected cells started to establish small colonies, these cells were subcloned into a 96 well plate by detaching

them from the plate using 1% trypsin EDTA. 100 cells were resuspended in 10 ml of culture medium using haemocytometer in order to grow only single cell in each well of the 96 well plate.

Transfection of J558L myeloma cells using nucleofector electroporation (Amaxa):

0.5 ml of supplement that supplied with the kit was mixed gently to nucleofection solution before nucleofection. J558L myeloma cells were cultured in 5% FCS DMEM growth medium at 37°C and 10% CO2 incubator. $2x10^6$ cell/ml were centrifuged at 90xg for 10 minutes at room temperature and the supernatant was discarded. 100µl of nucleofection solution was added to the pellet of the cells. Immediately, 2µg/µl of endotoxin free plasmid was added to the suspension which was transferred carefully (no air bubbles) into nucleofector cuvette using special micropipette supplied with the kit. T-16 nucleofector programme was selected for electroporation of J558L myeloma cells. 500µl of pre-warmed medium was added to the cells immediately after electroporation in the cuvette and then transferred into 24 well plate for incubation at 37°C and 5-10% CO2. The transfection efficiency was analysed after 24 hours by counting the cells expressing GFP to the total number of the cells in three different microscopic fields using the inverted fluorescent microscope (Leica DM IRS).

Protein A agarose beads purification of recombinant chimeric protein:

The culture supernatant of the stably transfected cells were collected after 7-10 days of incubation at 37°C and 5% CO2 to purify the recombinant protein. The total volume culture supernatant was centrifuged for 5 minutes at 3000 RPM in 10 (50ml universal tube) to get rid of cell debris, then the pH adjusted to pH 8 by adding 100µl of 2M Tris pH 8 to each tube. 50µl of protein A Agarose beads (Sigma) (100µg/ml) were added to each tube, then all tubes were incubated rotating for 2 hours to overnight at 4°C to allow the beads to interact with the Fc portions of the recombinant protein. The total volume of culture supernatant was run through a column, a flow through of the column was collected to check the efficiency of the process. The collected beads at the bottom of the column were washed with 100 mM Tris pH 8, followed by two washes with 10mM Tris pH 8. The protein was eluted in 0.2M Glycine pH 2.5 (Sigma) in fractions, immediately, pH of protein solution was adjusted by adding 2M Tris pH 8 and checked by pH paper. 2µl of each fraction of protein was dotted and dried on filter paper, then Comassie stain was used to visualise the concentration of protein in different fractions. 5ml of protein fractions were collected and concentrated to 1ml of high concentrated recombinant protein by using spin column, and then ELISA estimated the concentration of protein.

Preparation of Antibody coupled beads Column:

(1mg) of antibody (ant-myc or anti-V5) (Invitrogen) was coupled with AminoLink Plus immobilisation kit (PIERCE) using the pH 7.2 Coupling buffer (by dissolving BupH Pack contents in 500 ml of ultrapure water). The AminoLink Plus Resin was Suspended by end -over-end mixing, to avoid drawing air into the column, sequentially the top cap and then the bottom tab were removed, then the column was centrifuged to remove the storage buffer. The column was washed twice by adding 2ml of coupling buffer pH 7.2. 1ml of either anti-myc or anti-V5 antibodies was added to the column while the bottom cap was replaced, immediately, 2µl sample of the solution was saved to compare it with a sample of the supernatant. In the fume hood, 20 µl of Sodium cyanoborohydride solution (5M) was added to the reaction slurry, and then the column was incubated for 4 hours at room temperature with rocking. The column was centrifuged into a new collection tube with the top cap and the bottom tab was removed. The flow through of the column and a sample taken immediately prior to coupling were dotted on filter paper to check that the entire antibody was coupled with the AminoLink Plus Resin. The column was centrifuged to remove the coupling buffer and washed with 2ml of Quenching buffer (1M Tris HCl, 0.05%NaN_3, pH 7.4). In the fume hood, 20µl of Sodium cyanoborohydride solution (5M) was added to 1ml of Quenching buffer, this solution was added to the column, which was incubated for 30 minutes with rocking at room temperature. Carefully, the top cab and the bottom tab were removed and the column was centrifuged to remove the quenching buffer. The non-coupled antibody was washed away with 2ml of washing buffer (1M NaCl, 0.05% Na N_3) 4 times. The column was equilibrated with 2ml of storage buffer (washing buffer) twice.

Anti-myc or anti-V5 column Purification of CO-Fc:

Use either anti-V5 or anti-myc coupled column to purify CO-Fc from CC-Fc or OO-myc recombinant proteins. Incubation of 5ml of concentrated CO-Fc (result from protein A column) within the column 2 hours to overnight at 4°C while rocking. The column was centrifuged at 3000 RPM for 5 minutes, and then the flow through was collected to check the efficiency of the column. Then the column was washed 4-6 times with PBS and finally eluted with 0.2M Glycine pH 2.5 in 1ml fractions. ELISA assay was used to check the efficiency of the column with the flow through and the elution of the column.

Characterisation of heterodimeric recombinant chimeric proteins:

Enzyme linked immunosorbant assay (ELISA):

ELISA assay was used to estimate the concentration of IgLONs recombinant chimeric proteins secreted by transfected cell lines and to identify the ratio between the homdomeric and heterodimeric proteins. ELISA assay used 96 well plastic micro plate (Costar). The first coat was with 50 µl primary antibody either anti-myc or anti-V5 antibody (Invitrogen) (1mg/ml) (1:300) diluted in 100 mM in $NaHCO_3$ buffer pH 9.6 for 2-3 hours incubation at room temperature. 200 µl of 1%BSA in PBS was used to block the first layer for 1 hour, followed by three washes with 0.05%Tween20 (Sigma) in PBS. The second layer was 50µl chimeric IgLONs protein for 24 hours at 4°C. The protein was removed and the plate was washed carefully three times with washing buffer (0.05% Tween20 in PBS). The third layer was 50µl anti-V5 or anti-myc HRP-labelled antibody (Invitrogen) (1:500) diluted in blocking buffer for 2-3 hours at room temperature. 3-5 washes with the washing buffer was followed by incubation with 50-100µl freshly prepared 0.1mg/ml 3, 3', 5, 5'-titramethylbenzidine dihydrochloride (TMB) substrate (Sigma), followed by 1mg/ml TMB substrate tablet dissolved in 10 ml phosphate-citrate buffer) per well for 30-60 minutes. The reaction was stopped with 20 µl of 1M H_2SO_4 (Merck).The micro plate of ELISA assay was analysed by a JBIOLP400 ELISA microplate reader at an absorbance wavelength of 450nm. HRP enzymatic activity was responsible for the colour change in the TMB substrate; there was a relation between the amount of recombinant protein and the absorbance wavelength of 450 nm.

An arbitrary unit (AU/ml) was generated to deal with the quantification using the ELISA at the linear range of the curve, to measure the concentration of the recombinant chimeric proteins due to the difficulty in isolation of the heterodimeric

protein from the CC-Fc and OO-Fc homodimeric recombinant protein that secreted by CHO stable transfected cell line.

Western blotting:

NuPAGE™ (PAGE polyacrylamide gel electrophoresis) from Invitrogen was used for Western blotting analysis using Novex gel system. Lithium dodecyl sulphate (LDS) sample buffer was added to IgLONs recombinant chimeric protein which was loaded onto Novex ™ 3-8%Tris Acetate polyacrylamide gel and run in NuPAGE™ Tris Acetate buffer (Invitrogen) at 20-30 volts. The loaded proteins were transferred onto the BioTrace ™ (Pall Gelman laboratory) nitrocellulose transfer membrane, and then the membrane was sandwiched between 3M chromatography paper soaked in 0.3 M Tris pH 10.4-bottom buffer and 25mM Tris pH 9.4 top buffer containing 20% methanol was used to transfer sample proteins using a Biorad Trans-Blot ™ semi-dry cell. The nitrocellulose membrane was incubated overnight in 150mM NaCl, 10mM Tris pH8.4, 0.2%Tween 20 blocking buffer and stained with primary antibodies diluted 1:2000 to 1:5000 in blocking buffer plus 1% BSA, the secondary anti- HRP-labelled antibodies (DAKO) were used to stain the membrane to detect the primary antibody. The magic marker (Invitrogen) was used to measure the size of protein. Peco™ and Femto™ chemi-illuminescence substrates were used to visualise the protein bands onto Hyper Film ™ ECL (Amersham) chemiluminescent film using Kodak photo chemicals (Sigma).

Image J software was used to scan the bands of the western blot and then generate peak for each band. The peaks were cut then the weight of each peak was measured using the analytical balance to compare the density of the bands

Dot blotting:

2µl of protein sample was dotted and dried on a nitrocellulose membrane. The membrane was incubated overnight in 150 mM NaCl, 10mM Tris pH8.4, 2%Tween blocking buffer. The primary antibody was diluted 1:2000 or 1:5000 in blocking buffer plus 1%BSA and incubated for 1 hour at room temperature with gentle rocking. The blot was washed for 30 minutes with 3 changes of blocking buffer. The secondary anti-HRP labelled antibodies (DAKO) were incubated for 1 hour and washed for 30 minutes at room temperature. Peco ^{TM} or Femto chemi-illuminescence substrates were used to determine the concentration of the protein. The blot was developed on Hyper Film ^{TM} ECL (Amersham) chemiluminescent film using Kodak photo chemicals(Sigma).

Coomassie staining:

Coomassiecheck spelling blue staining solution was used to stain dot blot for fractions of protein on filter paper for 5 minutes to 1 hour at room temperature with gentle rocking. Once the dots stained, and then incubated in destaining solution with several changes.

Primary neurons culture:

The dissected chick E8 Forebrain tissues were torn into pieces and incubated in 1ml x 0.05% trypsin in HANKS Balanced salt solution (-) (HBSS) (Sigma) plus 100μg/ml DNAse (Sigma) for 30 minutes at 37°C, 5% CO_2. These forebrain tissues were washed in HBSS and followed by a wash with HBSS plus 1mg/ml soybean trypsin inhibitor (Sigma) for 2 minutes, and resuspended in DMEM/F12 growth medium plus Glutamax (Sigma) that contains 1.5%glucose, 100μg/ml transferrin (Sigma), 100μg/ml insulin (Invitrogen) and 50 units of penicillin/streptomycin (Invitrogen). Aclar cover slips were coated with 10 mg/ml Poly-L-Lysine in 100mM sodium borate buffer pH 8.4 for 1 hour and then washed into 24 well plate with HBSS. The forebrain cells were dissociated with a polished glass Pasteur pipette into a single cell suspension. A haemocytometer was used to count the cells that were distributed into 24 well plate in 0.5 ml per well. Forebrain neurons were cultured in 24 well tissue culture plates at a density of $2x10^5$ cell/ml.

Dissected chick E10 chick sympathetic or dorsal root ganglion tissues were incubated in 1ml of x 0.25% trypsin in HBSS (no EDTA) (Gibco) for 30 minutes at 37°C, 5% CO_2. Glass cover slips were coated with 10mg/ml laminin for 1 hour. A polished glass Pasteur pipette was used to dissociate the cells into a single cell suspension. A haemocytometer was used to count the cells that were distributed into 24 well plate in 0.5 ml per well These cells were washed and resuspended HBSS and then cultured in L15 glutamax growth medium (Gibco), 50 units of penicillin/streptomycin (Invitrogen) plus 0.5g methocel that contain 2ml of 30% glucose, 10% FCS and 5μl of NGF. Dorsal root ganglion or sympathetic neurons were cultured in 24 well plate at density $1x10^5$ cell/ml.

Live staining of neurons and cell lines with antibodies:

The cultured neurons were incubated for 2 days at 37°C, 5% CO_2 level at density of $2x10^5$ cell/ml in 24 well plate. These neurons grown on pre-coated aclar or glass cover slips with Poly-L-Lysine or laminin (Sigma) (10µg/ml), whereas IgLON-transfected cell lines; CEPU, OBCAM, LAMP, CO and CL CHO cell lines were cultured at $5x10^4$ in 24 well plate on glass cover slips. These cover slips were extracted carefully from each well, 30µl of rat antiCEPU-1, anti-OBCAM or anti-LAMP antibodies diluted 1:50 in 0.12 M phosphate pH 7.4 buffer 1%BSA were incubated at room temperature for 20 minutes. The cover slips were washed three times in HBSS. 30 µl of anti-rat Alexa Fluor 488 was used as secondary antibody (Invitrogen) diluted 1:200 in the same buffer and incubated for 30 minutes. The cover slips were dip washed again three times in HBSS. 4% paraformaldehyde (Sigma) was used to fix the live stained neurons or cells. These cover slips were dip washed three times in HBSS and one final wash in water, and then dried at room temperature.

In the case of IgLON-Fc chimeric recombinant protein, CEPU-1-Fc, OBCAM-Fc or CO-Fc, 30µl of 1: 100 diluted anti-human Fc fluorescent-labelled antibody (Jackson), mouse anti-myc antibody or anti-V5 antibodies (Invitrogen) diluted 1:50 in the same buffer. 30 µl 1:250 anti-mouse 488 Alexa Fluor (Invitrogen) was used as secondary antibody.

The lived stained cells were fixed with 4% Paraformaldehyde (Sigma) in PBS for 5 minutes, followed by three washes in HBSS and final wash in water to remove in residual paraformaldehyde. These cover slips were dried and mounted in Dako™ mounting medium on glass slides.

Neurite outgrowth assay:

Nitrocellulose membrane solution was prepared by resuspending 2cm x 3cm square of Protran BA 85-nitrocellulose membrane (Schleicher & Schuell) in 2ml tissue grade methanol (Merk). This solution was used to coat 13mm glass cover slips with 20 µl per each cover slip for 1 hour at room temperature. These cover slips were coated with 20µl of (100µg/ml) protein A (Sigma) for an hour. Followed by, spreading of 30µl of (10mg/ml) Poly- L-Lysine for fore brain neurons or laminin for dorsal root ganglion and sympathetic neurons diluted in100mM sodium borate buffer pH 8.4 (FB) or PBS (DRG or sympathetic) per cover slip and then incubated for 1 hour at room temperature. 1% tissue culture grade BSA (Sigma) in PBS was used to block the cover slips for 1 hour. Three cover slips were coated with 30µl (700AU/ml) of CO-Fc chimeric protein per cover slips for 1 hour. In parallel, three cover slips were coated either with CEPU-Fc or OBCAM-Fc chimeric proteins (100µg/ml) as control. All cover slips were washed with HBSS in 24 well plate before adding dissociated neurons at density of 2 $x10^5$ cell /well and incubated at 37°C, 5% CO_2 for 24 hour in the medium. The neurons with their neurites were fixed with 4% Paraformaldehyde in 0.12 M phosphate buffer pH 7.4. The neurons were stained with 1% weight: volume Cresyl violet crystals (Sigma) in PBS for 5 minutes to visualise the neurites. These cover slips were washed with HBSS, and mounted with DAKO medium. The percentage of the neurite outgrowth was measured by counting the number of the neurons with extended neurite to the total number of the neurons. There were certain criteria for counting the neurons, only the single neurons were counted. Leica's camera and software were used to take photographs. These experiments were repeated three times and then PRISM software was used to analyse these data.

Removal of GPI-anchored proteins by Phosphoinositol specific phospholipase C (PI-PLC) treatment:

For immunofluorescence, IgLONs were removed from the surface of forebrain neurons by treatment with 100m U /ml Phosphoinositol specific phospholipase C (PI-PLC) (Invitrogen) in forebrain medium for 1 hr. Cells were then stained as described previously.

For neurite outgrowth assay, they were pre-treated in suspension prior to plating for 1 hour at 37C and 5%CO2 level in FB medium with 100m U /ml PIPLC. Neurons were cultured onto 24 well plate with 13mm cover slips coated with various substrates as described previously in medium that contain 50 m U /ml PI-PLC (Invitrogen).

Tissue frozen section:

E 18 chick retina was dissected and fixed with 4% Paraformaldehyde for 2 hours at room temperature. The fixed tissues were incubated consecutively in 6%, 12%, and 18% sucrose in 0.12M Na phosphate buffer pH 7.4, with gentle mixing until the tissue sank to the bottom of the tube. These tissues were cut and mounted in Cryo-M-Bed (Bright instruments, UK) on cork discs. Isopentane suspension over liquid nitrogen was used to freeze the tissues. The frozen tissues were stored at -80°C for further use. Cryostat (Bright) was used to cut 12-15μm sections; they were adhered to subbed glass slides. These slides were precoated with subbing solution which was prepared by stirring water with gelatin (1.5%) at 60°C. Chromic potassium (0.1%) sulphate was added to gelatin once dissolved and cooled. Then add ethanol (30%) and acetic acid (7%).The slides were dipped into subbing solution and drained on paper and then air dried.

Fluorescent microscopy and photography:

Both fluorescent (Leitz DMIRB) and inverted fluorescent Leica microscopes (DM IRB) models were used to visualise the stained tissue and cells. Oil immersion lenses with different objectives were used to examine the samples. Photographs were captured with a Leica's digital camera and analysed with Leica's package software.

Chapter Three

Generation of OBCAM-Fc-myc-His6 construct in pBudCE4.1 Vector

INTRODUCTION:

In this chapter, the aim was to generate a pBudCE4.1-OBCAM-Fc-myc construct and test it by transient transfection of CHO cells followed by Western blotting to characterise the secreted proteins to ensure that each chain is formed. A previously generated pcDNA6-CEPU-Fc-V5 construct would also be tested. Following double transfection of CHO cells with each construct ELISA assays will also be used to show CO-Fc exists as a complex and to determine the ratio between CO-Fc heterodimer and OO-Fc and CC-Fc homodimeric recombinant protein.

A doubly transfected CHO cell line expressing both CEPU-1 and OBCAM inhibited the initiation of neurite outgrowth of E8 Forebrain neurons, while no inhibition occurred with the singly transfected CHO cell lines (figure 1.9). This evidence suggested that IgLONs could have different activities when they exist in the dimeric form of IgLON (DigLON). DigLONs are formed by a combination of the two different members of the group. This provided the basis for the preparation of a cell line that secrets both proteins CEPU-Fc and OBCAM-Fc together. Both proteins will be secreted into the medium instead of being attached to the surface of the CHO cells by a GPI anchor. Loss of the attachment to the cell membrane will result in secreted proteins. The secreted proteins can be isolated, concentrated and manipulated and hence will allow experiments not possible with the proteins expressed on the surface of CHO cells. In addition, assembly of CEPU-1 and OBCAM as complex will ensure that they are at close proximity. Their detection in the medium will be difficult without something that can be used as a label for the heterodimer.

There are many routes to label the CEPU-OBCAM heterodimer; direct labelling with antibodies is one of the choices. However, anti-CEPU-1 and anti-OBCAM rat

antiserum cannot be used due to cross reactivity. Another option is cloning of CEPU-1 and OBCAM into a vector that has two epitope tags under different promotors, such as the pBudCE4.1 vector that has a V5 epitope tag under EF-α1 promoter and myc epitope tag under CMV promoter. However, the expression of each chain might be unbalanced due to differing strengths of the two promoters. Therefore, cloning of each one alongside an epitope tag into two separate plasmids with specific antibiotic resistance will label OBCAM and CEPU-1 with different tags. Cloning of CEPU-Fc into pcDNA6 that has V5 epitope tag and is resistant to both Ampicillin and Blasticidin antibiotics was carried out previously (kind gift from M. Lyons & D.Moss). OBCAM-Fc will be cloned into pBudCE4.1 that has a myc epitope tag under CMV promotor. pBudCE4.1 is resistant to Zeocin antibiotic. This plasmid also has the advantage of having GFP cloned into the second polylinker under the EF1 promoter.

These epitope tags will be used in characterisation of the heterodimer by different methods such as ELISA, dot blot and Western blotting. They can be used also in the detection and interaction of the heterodimer. Each protein can be identified separately because there is no cross reactivity between these tags. Furthermore, Protein A agarose beads will be used in purification of the recombinant chimeric protein using the human Fc of each protein. CO-Fc IgLON heterodimer will be used as a tool to identify the putative receptor complex on the surface of the neuron.

RESULTS:

The first step in the preparation of the epitope-tagged OBCAM-Fc was to clone OBCAM-Fc into pBudCE4.1 (figure3.1) such that the myc-His6 was in frame with the terminal exon of the human Fc. Primers were designed to achieve this as described in figure (3.2). OBCAM-Fc was amplified from pcDNA3 using proof reading Taq polymerase in three dilutions, 1:10, 1:100, and 1:1000 as shown in figure3.3. The use of proof reading Taq polymerase was used to avoid any mismatches that happened with the ordinary Taq polymerase. The PCR product obtained from the most diluted sample (1:1000) was cloned into pCRII TOPO as an intermediate vector using the T/A cloning kit (figure 3.4). Both pCRII TOPO and pcDNA3 are resistant to Ampicillin while pcRII TOPO is also resistant to Kanamycin. DH5α-T1 competent bacteria were transformed with T/A cloned product and colonies selected with Kanamycin. Ten colonies were screened and five colonies have the insert when screened by PCR with the forward and reverse primers but using Taq polymerase (figure3.5). The best colony that contains OBCAM-Fc insert was grown in overnight culture of LB broth with kanamycin antibiotic, and then a Miniplasmid prep was carried out. This insert was double digested out of the pCRII vector with HINDIII and Xba1 restriction enzymes (figure 3.6). These restriction sites were incorporated into the primers for this purpose. The insert was cut and isolated from the Agarose gel using glass wool tubes to get high and pure yield of OBCAM-Fc that is needed for the ligation with digested pBudCE4.1vector. pBudCE4.1 plasmid was ligated with the insert and used to transform DH5α1T competent bacteria; colonies selected in the presence of Zeocin. These were screened by PCR to confirm the cloning of the insert into the final vector (figure3.7) and figure 3.8 shows the plasmid preparation from one colony.

In figure 3.8, plasmid from a miniplasmid preparation was run on a 1% Agarose gel and a band for OBCAM-Fc in pBudCE4.1 plasmid was observed. pBudCE4.1 was double digested with the same restriction enzymes as before to confirm the cloning of the insert into pBudCE4.1 final vector (figure3.9).

The plasmid was sequenced and the sequence of the OBCAM-Fc construct (figure3.10) was blasted at www.ncbi.com and the results confirmed that the sequence had more than 98% identity with chick OBCAM hence confirming the insertion of the correct sequence.

The next step is to test whether the two constructs code for OBCAM-Fc and CEPU-Fc respectively including the appropriate epitope tag by single transient transfection of CHO cells. Single transfection of CHO cells with either pcDNA6-CEPU-Fc-V5 construct or pBudCE4.1-OBCAM-Fc-myc construct was carried out using ExGene500 (Fermentas). Firstly, the transfection efficiency of OBCAM-Fc construct in pBudCE4.1 was confirmed by the expression of GFP because GFP was also expressed by the same plasmid. Figure 3.11 shows a phase photomicrograph of for a group of cells and the corresponding fluorescent photomicrograph shows a subset of the cells are green due to GFP expression of pBudCE4.1 (figure 3.11). The efficiency of the transfection was about 30%. After 7 days, the medium off the CHO cells transiently transfected with CEPU-1-Fc or OBCAM-Fc constructs was collected and spun to remove cell debris and then the chimeric proteins were concentrated with protein A Agarose beads. Western blotting and ELISA assay were used to test the presence of both CEPU-1-Fc-V5-His6 and OBCAM-Fc-myc-His6 chimeric recombinant proteins. Figure 3.12 shows a western blot of the medium from the transient transfected CHO cells. The first blot was stained with rat anti-CEPU-1 antisera, anti-rat HRP labelled, and the second one was stained with mouse anti-V5

antibody and anti-mouse HRP labelled antibody. Both bands at the right size (85KDa) and confirm that CEPU-Fc-V5-His6 molecule was formed. The 3rd and the 4th blots stained with rat OBCAM antisera and secondary anti-rat HRP and anti-myc antibody with secondary anti-mouse HRP-labelled which means that OBCAM-Fc-myc-His6 was secreted in the medium.

In figure 3.13, a curve represents an ELISA assay on 10 fold concentrated CEPU-Fc-V5-His6 obtained by transient transfection and concentrated using a Spin column. Anti-V5 antibody was used to capture the V5 tag on the first chain of the molecule, which was then detected using the second V5 tag on the other chain of the molecule using anti-V5HRP labelled antibody as described in the diagram. As shown in this figure, there is a relation between the dilution factor of the protein and the absorbance at 450mm optical density. The dilution range was between 0.01 and 0.001 dilutions. The linear range was between 0.001 to 0.005 dilutions.

The ELISA assay on 10 times concentrated OBCAM-Fc-myc-His6 supernatant obtained by transient transfection is shown in figure 3.14. The diagram explains how anti-myc captures the recombinant protein and the anti-myc HRP detects the second epitope tag. There is a relation between the concentration of the protein and the absorbance at OD 450mm. The protein was diluted in serial dilutions; the linear range was between 0.1 to 0.001.which differs from the linear range for CEPU-Fc-V5-His6. This might be due the detection sensitivity of antibodies.

Having demonstrated that both constructs were correct and specified the synthesis of the correct epitope-tagged proteins the next step was to carry out a transient double transfection of CHO cells with both constructs to test for the formation of CO-Fc heterodimer.

CHO cells were transiently co-transfected with both pcDNA6-CEPU-1-Fc-V5 and pBudCE4.1-OBCAM-Fc-myc constructs in order to test whether the heterodimeric protein is assembled in these cells. The medium was collected from the co-transfected CHO cells after 7 days. The neat, 1+4 and 1+7 dilutions were assayed in an ELISA that revealed that CO-Fc heterodimeric protein gives high absorption at 450mm OD, while CC-Fc and OO-Fc give low absorption in all dilutions (figure 3.15).

DISCUSSION:

The aim of this chapter was to test the viability of constructing a heterodimeric protein using the Fc human IgG domain, by transient single and double transfection of CHO cells with pBudCE4.1-OBCAM-Fc-myc and pcDNA6-CEPU-Fc-V5 constructs.

Western blotting confirmed that the epitope tags had been cloned into the plasmids in frame and that CEPU-1 and V5 formed part of the same polypeptide chain as did OBCAM and myc. This was confirmed by the presence of CEPU-Fc-V5-His6 and OBCAM-Fc-myc-His6 following transient transfection of CHO cells.

The ELISA assay was developed in order to be able to detect CO-Fc as well as the two homodimers. These assays proved that transient double transfected CHO cell secreted CO-Fc heterodimer, CC-Fc and OO-Fc homodimers

In the ELISA assay, the homodimers may be underestimated due to a possibility of capture of both tags instead of one tag only of the homodimer. This leaves no chance for the HRP-labelled antibody to detect the second tag of the homodimer. For example, OO-Fc homodimer has two myc tags, which may be detected by the anti-myc antibody at the same time. In this case, the anti-myc-HRP labelled antibody will not be able to detect the second myc tag of the homodimer. In contrast, this cannot happen for CO-Fc heterodimer due to the presence of two different tags on the complex; myc and V5 tags. For example, the myc tag will be detected by the primary anti-myc antibody where the secondary anti-V5-HRP labelled antibody will detect the V5 tag of the other chain of the complex.

Furthermore, in double transfection; there was variability in the detection of CO-Fc according to the order of the antibodies. For example, when anti-V5 antibody used as the capture antibody instead of anti-myc antibody and anti-myc-HRP labelled

antibody used as the detection antibody instead of anti-V5 HRP-labelled antibody, the apparent concentration of CO-Fc was different. This point confirms that anti-V5-HRP labelled antibody was most sensitive.

Following confirmation that CO-Fc exists as heterodimer using ELISA assay, the next step is the generation of a stable cell line, which produces CO-Fc heterodimeric chimeric recombinant protein.

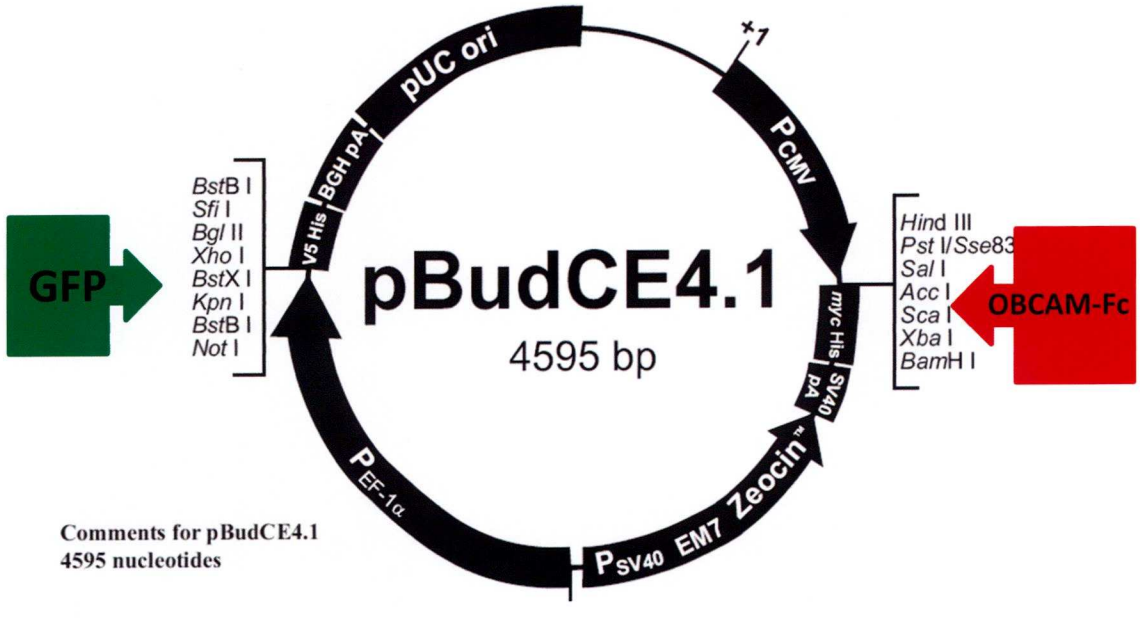

Figure 3.1: pBud vector plasmid map

The map of pBudCE 4.1 (4595bp) vector (Invitrogen) shows the cloning site of OBCAM-Fc downstream under CMV promoter between HIND III and Xba1 restriction sites. This location ensured that OBCAM-Fc was synthesised in frame with myc epitope tag. On the other side, GFP was cloned downstream under EF-1α promoter.

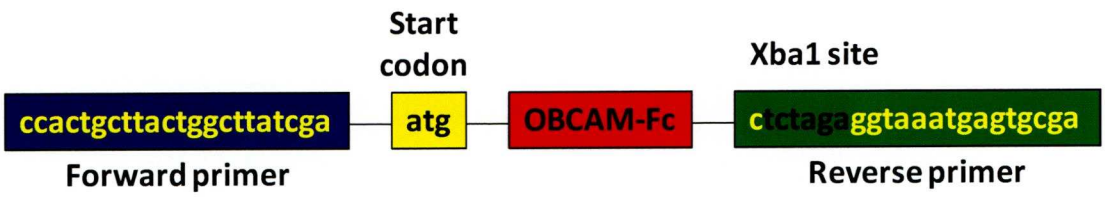

Figure 3.2: Modified sequence of OBCAM-Fc primers

This diagram describes the modified sequence for OBCAM-Fc showing the forward modified primer (blue) followed by the start codon (yellow) of OBCAM-Fc (red).The reverse primer which include Xba1 site (in black) is located before the stop codon of the Fc sequence. This allows the myc-His6 tag of the pBudCE4.1 to be added in frame to the OBCAM-Fc sequence.

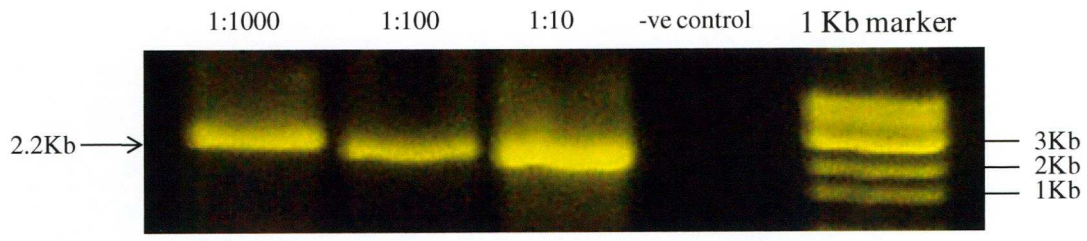

Figure 3.3: PCR amplification of OBCAM-Fc in pcDNA3

1% agarose gel shows three bands representing the PCR products produced using three dilutions 1:10, 1:100 and 1:1000 of the original OBCAM-Fc in pcDNA3 plasmid as template. PCR products prepared using pfx Taq polymerase (Invitrogen) are located at the expected size (2.2Kb). Both forward and reverse primers were used at annealing temperature 56°C and extension temperature was 68°C. The most diluted plasmid was selected (1:1000 dilution).The negative control showed no DNA band.

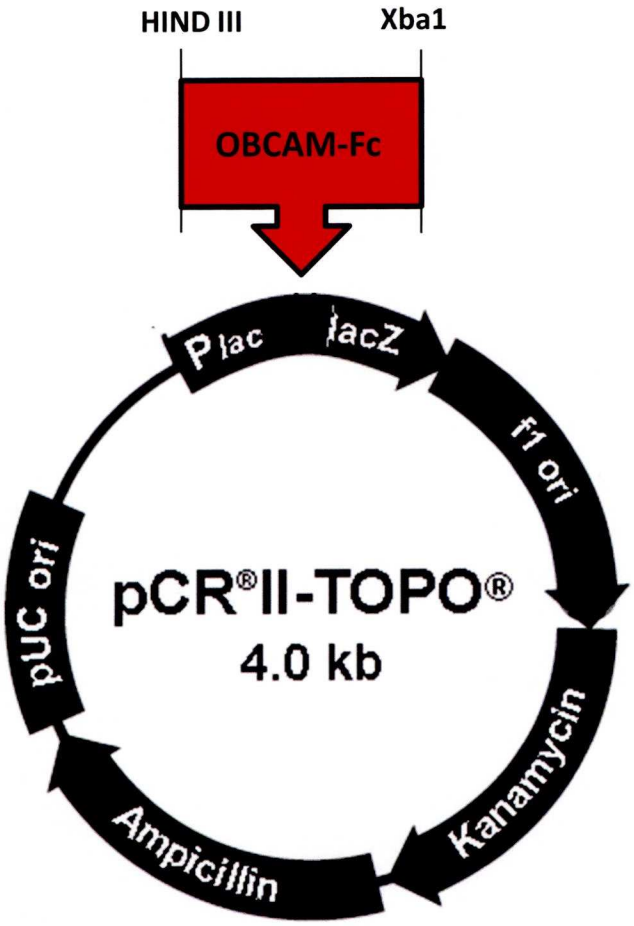

Figure 3.4: TA cloning of OBCAM-Fc PCR product into pCR® II-TOPO®

OBCAM-Fc construct was cloned into cloning site downstream under lacZ promotor of pCR® II-TOPO® as intermediate vector using T/A cloning kit (Invitrogen).

Figure 3.5: PCR screen for OBCCAM-Fc in pCRII TOPO vector

An agarose gel (1%) shows the results of the PCR screen using Taq polymerase (Sigma) for 10 selected colonies of transformed DH5-α-T1® competent bacteria. Colonies were selected on Kanamycin LB agar plates at 37°C overnight following TA cloning of OBCAM-Fc into pCRII TOPO intermediate vector. There were two different sizes of PCR products in five colonies (1, 2, 3, 6 and 9). The No.6 colony was selected which was strong and at the right size for Miniplasmid prep (Sigma). Therec was no DNA band in negative control lane.

A)

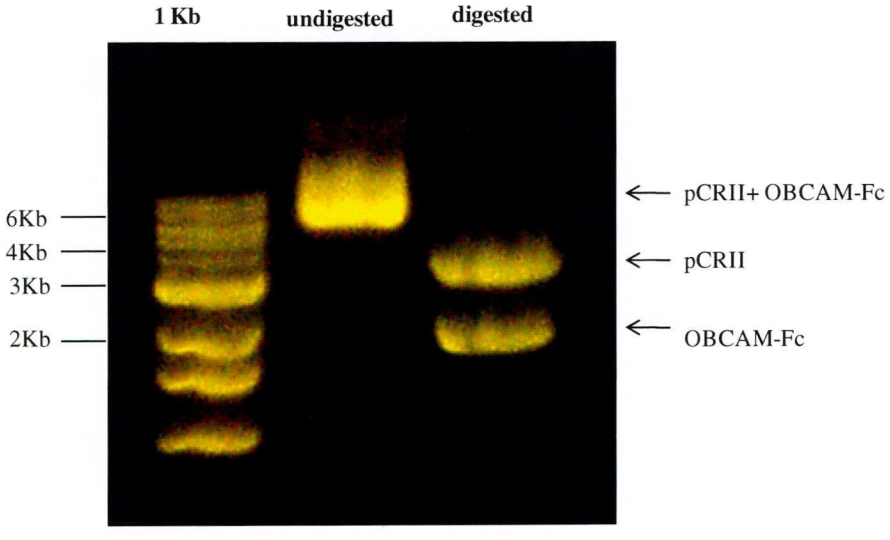

B)

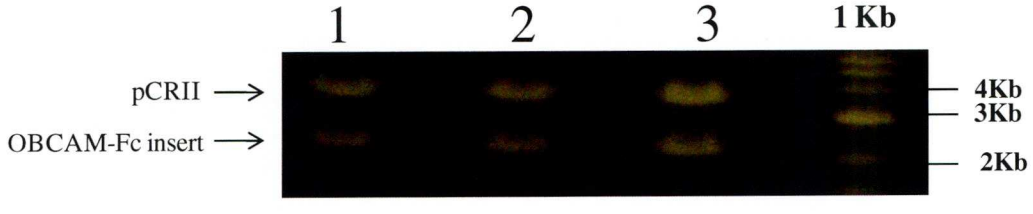

Figure 3.6: Double digestion of OBCAM-Fc from the pCRII vector

A) 1% Agarose gel shows the products of the double digestion of OBCAM-Fc pCRII vector using Hind III and Xba1 restriction enzymes. In the 1st lane 1Kb marker, in the 2nd lane, undigested OBCAM-Fc in pCRII. In the 3rd lane, there are two bands, the plasmid backbone pCRII and the insert OBCAM-Fc

B) OBCAM-Fc was prepared from the 1% Agarose gel ready for the next cloning step. The three insert bands were combined.

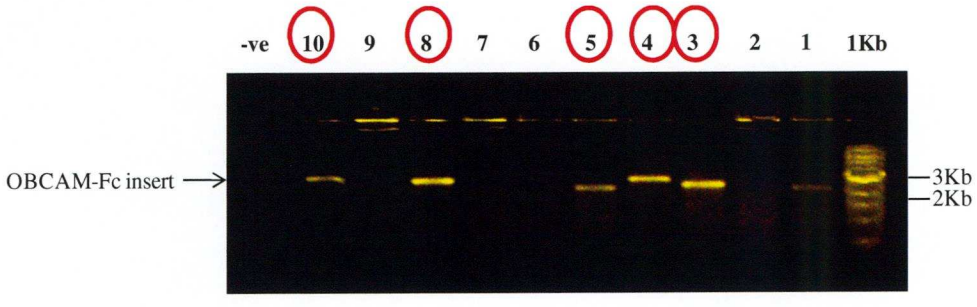

Figure 3.7: PCR screen for OBCAM-Fc in pBudCE4.1

1% Agarose gel shows PCR screen using Taq polymerase (Sigma) for 10 selected colonies which have been grown on Zeocin low salt LB agar overnight. Five colonies with the right size (2.2Kb) were selected as shown for Miniplasmid prep (Sigma).

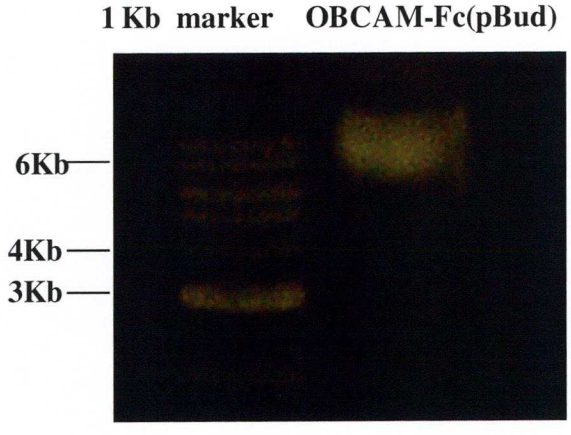

Figure 3.8: Miniplasmid prep of OBCAM-Fc-myc-His6 in pBudCE4.1 final vector

1% Agarose gel shows a band of OBCAM-Fc-myc-His^6 in pBudCE4.1 at the right size (6Kb). It was obtained from a Miniplasmid prep (Sigma) of an overnight culture of the colony number (3)

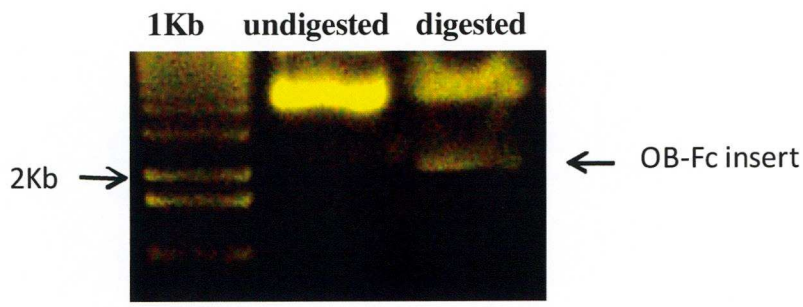

Figure 3.9: Confirmatory double digestion of OBCAM-Fc from pBud CE4.1

1% Agarose shows in the 1st lane markers, lane 2, undigested OBCAM-Fc in pBudCE4.1 at 6 Kb and 3rd lane, the OBCAM-Fc (2.2Kb) and pBudCE4.1plasmid digested with HINDIII and Xba1 restriction enzyme (Invitrogen).

```
Query  19       GTACCATCCTGCCTGCTGG-T--TNCGTCACCGCCACCACTGCCCTGCTCTTCATCCCAG  75
                 |||||||||||||||||| |  | | ||||||||||||||||||||||||||||||||
Sbjct  2408464  GTACCATCCTGCCTGCTGGATCGT-CTTCACCGCCACCACTGCCCTGCTCTTCATCCCAG  2408406

Query  76       G  76
                 |
Sbjct  2408405  G  2408405

Query  73       CAGGAGTGCCCGTGCGCAGCGGAGATGCCACCTTCCCCAAAGCTATGGACAACGTGACTG  132
                 ||||||||||||||||||||||||||||||||||||||||||||||||||||||||||||
Sbjct  2035468  CAGGAGTGCCCGTGCGCAGCGGAGATGCCACCTTCCCCAAAGCTATGGACAACGTGACTG  2035527

Query  133      TGCGGCAAGGGGAGAGTGTC-CGCTCAGGT  161
                 |||||||||||||||||| | |||||||||
Sbjct  2035528  TGCGGCAAGGGGAGAGTGCCACGCTCAGGT  2035557

Query  157      CAGGTGTACCGTGGATGACAGGGTGACGCGGGTAGCGTGGTTGAACCGCAGCACCATCCT  216
                 ||||||||||||||||||||||||||||||||||||||||||||||||||||||||||||
Sbjct  2164932  CAGGTGTACCGTGGATGACAGGGTGACGCGGGTAGCGTGGTTGAACCGCAGCACCATCCT  2164873

Query  217      TTATGCTGGCAATGACAAGTGGTCTATAGACAACCGCGTGGTCATCCTCTCCAACACTAA  276
                 |||||||||||||||||||||||||||||||||||||||||||||||||||||||||| ||
Sbjct  2164872  TTATGCTGGCAATGACAAGTGGTCTATAGACAACCGCGTGGTCATCCTCTCCAACACCAA  2164813

Query  277      AACCCAGTACAGCATCAAGATCCACAACGTGGATGTGTACGATGAGGGGCCCTACACCTG  336
                 |||||||||||||||||||||||||| ||||||||||||||||||||||||||||||||
Sbjct  2164812  AACCCAGTACAGCATCAAGATCCACAATGTGGATGTGTACGATGAGGGGCCCTACACCTG  2164753

Query  337      CTCTGTGCAGACAGACAATCACCCCAAAACATCGCGCGTCCACCTCATCGTGCAAG  392
                 ||| ||||||||||||||||||||||||||||||||||||||||||||||||||
Sbjct  2164752  CTCCGTGCAGACAGACAATCACCCCAAAACATCGCGCGTCCACCTCATCGTGCAAG  2164697

Query  387      TGCAAGTCCCCCCTCAGATTGTCAACATCTCATCAGACTTCGCCGTGAACGAAGGCAGCA  446
                 ||| |||||||||||||||||||||||||||||||||| || ||||||||||||||||||
Sbjct  2151390  TGC-AGTCCCCCCTCAGATTGTCAACATCTCATCAGACATCACCGTGAACGAAGGCAGCA  2151332

Query  447      GTGTGACCCTCATGTGCTTGGCCTTTGGG-G-CCGGAGCCCACTGTCACGTGGCGGCATC  504
                 |||||||||||||||||||||||||||| | ||||||||||||||||||||||||||||
Sbjct  2151331  GTGTGACCCTCATGTGCTTGGCCTTTGGGAGGCCGGAGCCCACTGTCACGTGGCGGCATC  2151272

Query  505      TCTCTGGGAAAGG  517
                 |||||||||||||
Sbjct  2151271  TCTCTGGGAAAGG  2151259

Query  515      AGGGCAAGGCTTTGTGAGTGAGGATGAGTACCTGGAGATCACGGGCATCACACGGGAGCA  574
                 ||||||||||||||||||||||||||||||||||||||||||||||||||||||||||||
Sbjct  2151075  AGGGCAAGGCTTTGTGAGTGAGGATGAGTACCTGGAGATCACGGGCATCACACGGGAGCA  2151016

Query  575      GTCGGGCGAGTATGAGTGCAGTGCTGTCAATGACGTGGCCGTCCC  619
                 |||||||||||||||||||||||||||||||| ||||| |||||
Sbjct  2151015  GTCGGGCGAGTATGAGTGCAGTGCTGTCAATGATGTGGCTGTCCC  2150971
```

Figure 3.10: OBCAM-Fc construct blasted against OBCAM sequence:

OBCAM-Fc sequence (Query) which is cloned into pBudCE4.1. This is sequenced by LARK Cogenics with T7P forward primer. It was blasted in www.ncbi.com website and the match showed more than 98% similarity to the OBCAM sequence (subject).

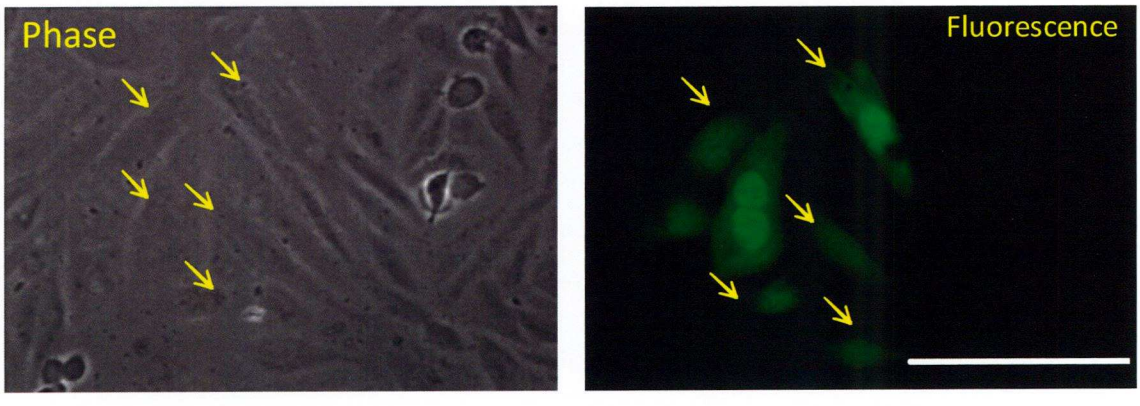

Figure 3.11: Transfected CHO cells with OBCAM-Fc-myc-His6 (pBudC4.1) (GFP)

Phase and fluorescence photographs show CHO cells that are transiently transfected with pBudCE4.1 where OBCAM-Fc construct was cloned under CMV promoter and GFP under EFα1 promoter. GFP was used to measure the transfection efficiency of pBudCE4.1 (50μm scale bar).

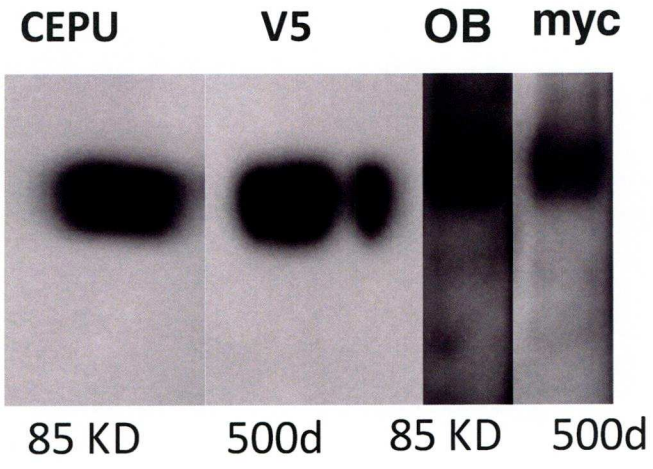

Figure 3.12: Western Blot for transient single transfection for OBCAM-Fc-myc-His6 and CEPU-Fc-V5-His6 respectively

The first blot was stained with rat anti CEPU-1 antisera (1:5000) with secondary HRP-labelled anti-rat antibody 1:5000, the second blot stained with mouse anti-V5 antibody 1:2000 with secondary HRP-labelled antimouse antibody 1:2000, both shows CEPU-Fc-V5 protein was secreted by singly transfected CHO cells. The third blot was stained with rat anti-OBCAM antisera 1:5000 with secondary anti rat HRP-labelled antibody 1:5000, the last blot stained with mouse anti-myc antibody (1:2000) and secondary anti-mouse-HRP-labelled (1:2000). Both show OBCAM-Fc-myc-His6 chimeric protein was secreted by singly transfected CHO cells.

A)

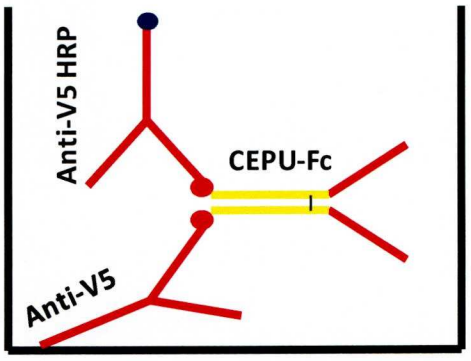

B)

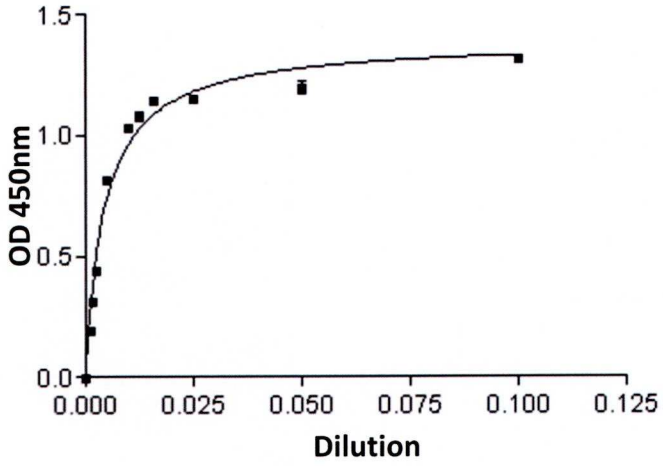

Figure 3.13: CEPU-Fc-V5-His6 Transient Single transfection

A) A diagram to describe the interaction between the anti-V5 antibody and anti-V5 HRP labelled antibody with CEPU-Fc-V5-HIS6 recombinant protein in ELISA assay.

B) A figure shows a curve for the relation between dilutions of CEPU-Fc-V5 His6 and the absorption at 450 nm optical density. CEPU-Fc-V5-His6 protein was diluted from 0.1 to 0.001 dilutions. (n=3)

A)

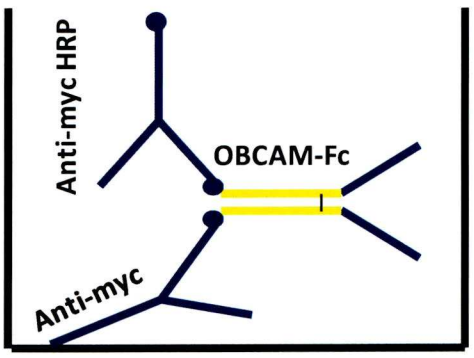

B)

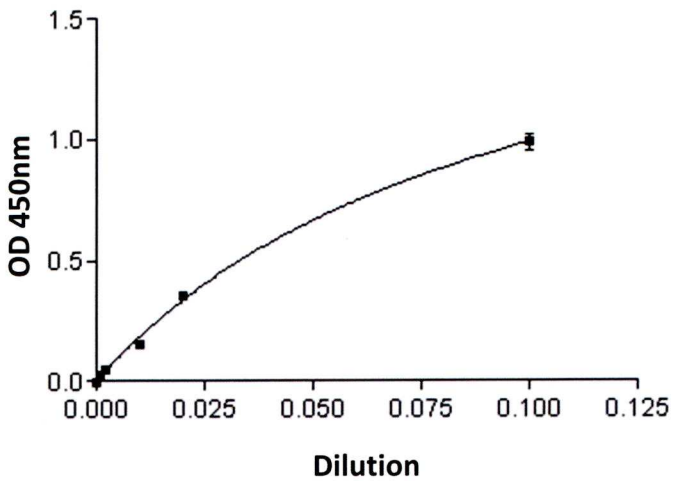

Figure 3.14 OBCAM-Fc-myc-His6: transient single transfection

A) A diagram to describe the interaction between anti-myc antibody and anti-myc HRP labelled antibody with OBCAM-Fc-myc-His6 recombinant protein in ELISA assay.

B) A figure shows a curve for the relation between dilutions of OBCAM-Fc-myc-His6 recombinant protein and the absorption capacity at 450 nm OD. (n=3)

A)

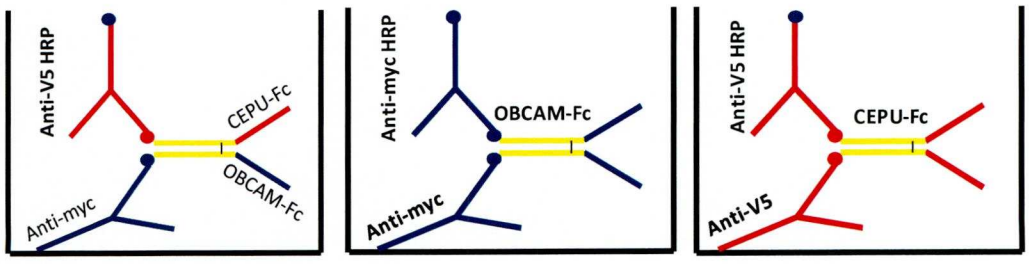

B)

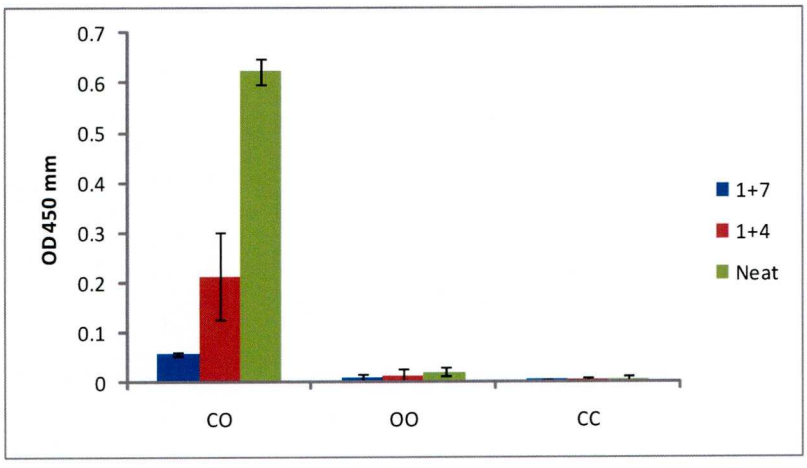

Figure 3.15: Transient double CEPU-OBCAM-Fc transfection

A) Diagrams describe the interaction between antibody (1:300) and HRP labelled antibody (1:500) with CO-Fc, OO-Fc and CC-Fc recombinant proteins in ELISA assay.

B) A figure shows a curve for the relation between the dilution of CO-Fc-myc-His6 recombinant protein and the absorption capacity at 450 nm OD. There are three different dilutions, neat (green bar), 1+4 (red bar) and 1+7 (blue bar). CO-Fc heterodimeric chimeric protein concentration is more than six fold more than the concentration of either OO-Fc or CC-Fc homdimeric proteins. (n=3)(SD=CO-Fc (0.025502, 0.08778, 0.003786) OO-Fc (0.008718, 0.011136, 0.007506) CC-Fc (0.004359, 0.003055, 0.001528) respectively.

Chapter Four

Production and Characterisation of CO-Fc heterodimeric recombinant protein

INTRODUCTION:

In this chapter, a stable cell line transfected with both pcDNA6-CEPU-Fc-V5 and pBudCE4.1-OBCAM-Fc-myc constructs will be prepared to generate the CO-Fc heterodimeric recombinant chimeric protein. There are many types of cells that can be used to establish this cell line. For example, CHO cells or mouse J558L myeloma cells have been used previously. However, the amount of the protein synthesised by the CHO cells is less than the amount of protein that is produced by the myeloma cell line. In addition, the myeloma cell line is normally used for the synthesis of antibodies and our protein is similar to an antibody in structure. They are considered as suspension cell type; therefore, a miniperm bioreactor can be used to scale up the concentration of the protein by accumulation of the protein in the culture medium. On other hand, the disadvantage of the myeloma cell line is that they are difficult to transfect especially with two plasmids (Lodge et al., 2000), while the CHO cell line is easy to transfect and has good growth. In case of adherent cell type such as CHO cells, a scale up method by expansion over large culture area can be used to get the appropriate yield of the recombinant protein. The aim is to attempt to make a doubly transfected cell line using mouse J558L cells but CHO cells can be used if necessary.

The cells doubly transfected with both pcDNA6-CEPU-Fc and pBudCE4.1-OBCAM-Fc constructs will be screened by using antibiotic resistance in both pcDNA6 plasmid and pBudCE4.1 plasmid. pcDNA6 has Blasticidin antibiotic resistance while the pBudCE4.1 has Zeocin resistance. Use of both antibiotics will select the stably transfected cell line.

Statistically, a mixture of heterodimeric and homodimeric chimeric recombinant proteins is expected to be produced by the double transfected cell line, with a ratio of two for CO-Fc heterodimeric protein to one for each of OO-Fc and

CC-Fc homodimeric proteins (2:1:1 ratio). In the previous chapter, the outcome of the transient double transfection of CHO cells was successful, where the ratio of CO-Fc heterodimer to the CC-Fc or OO-Fc homodimers was more than that expected. However, this ratio might be variable according to the efficiency of the transfection.

It may therefore be necessary to purify the putative CO-Fc heterodimeric protein of the contamination caused by homodimeric proteins. Anti-myc and anti-V5 antibodies can be coupled with the beads to assemble affinity columns that can be used in purification of the CO-Fc heterodimeric protein from the CC-Fc-V5 and OO-Fc-myc homodimeric recombinant chimeric proteins.

Characterisation of CO-Fc heterodimeric chimeric recombinant proteins will be required. Firstly, screening of the master clone of the transfection by dot blotting will ensure that both chains of the protein are secreted by the doubly transfected cell line. The ELISA assay is a sandwich type of ELISA using anti-myc antibody and anti-V5-HRP labelled antibody to detect CO-Fc as a complex. In addition, Western blotting will be used to identify the size of protein. Secondly, characterisation of the ratio of CO-Fc heterodimeric protein to the CC-Fc and OO-Fc homodimeric protein that are secreted by the cell line using ELISA will be necessary.

RESULTS:

Killing curves were carried out for wild type CHO cells at $1x10^5$ cell/ml and J588L mouse myeloma cells at $12x\ 10^4$ in 24 well plate at 50% confluency with Blasticidin and Zeocin at different concentrations for one week of incubation; the best concentration was 200µg/ml for Zeocin and 5 µg/ml for Blasticidin. Each antibiotic killed about 60% of the cells during the first three days (figure 4.1). Usually the process of generation of the stable cell line takes a long time, so a higher concentration of the antibiotic might affect their growth especially when both antibiotics are used together.

Because of the advantages of the mouse J558L myeloma cell line, transfection was attempted first, using the nucleofection method (Amaxa). Initially, single transient transfections with pBudCE4.1 were carried out to compare different programmes and buffers. The conclusion was that T-016 was the most efficient buffer (data not shown). Then, double transfection with both plasmids (pcDNA6-CEPU-Fc-V5 and pBudCE4.1-OBCAM-Fc-myc) was carried out by using T-016 programme on J558L myeloma cells at cell count $2x10^6$ cell/ml in the Amaxa cuvette. The electrporated cells were transferred immediately to a 24 well plate and incubated for 2 days at 37°C 10 % CO_2 and then transferred to a 6 well plate at which point both Zeocin and Blasticidin antibiotics were added to select for the co-transfected cells. pBudCE4.1 has two separate polylinkers into which OBCAM-Fc sequence was cloned under the CMV promotor and GFP sequence under EFα1 promotor (figure 3.2). Using an inverted fluorescence microscope, the transfection efficiency (20%) was assessed by counting the number of green cell that expressing GFP of pBud plasmid. Most of the non-transfected cells died after few days in selection medium whereas the transfected cells started to grow in colonies.

The transfected cells were subcloned into two 96 well plates (100cell/ plate-1000cell/plate) in half the concentration of antibiotics used previously to encourage the cell growth. After one week of incubation, both plates were screened for pBudCE4.1-OBCAM-Fc transfected colonies using the inverted fluorescence microscopy since GFP was expressed under the second promoter of the pBud plasmid. Next dot blots were used to screen the transfected colonies using anti-myc and anti-V5 antibodies (figure 4.2). Only nine colonies expressing OBCAM-Fc-myc, CEPU-Fc-V5 and GFP and displaying good growth were transferred into a 24 well plate. In figure 4.3, dot blot for supernatants of clones thought to express CO-Fc were stained with both anti-V5 and anti-myc antibodies to check the stability of expression of both chains. However, some clones showed stable expression of both chains while others lost either CEPU-Fc-V5 or OBCAM-Fc-myc chain. The ELISA assay was used to test the existence of the CO-Fc heterodimer complex and to estimate the ratio between heterodimeric and homodimeric protein using anti-myc and anti-V5 antibodies. In figure 4.4, the ELISA revealed that the concentration of produced protein from the myeloma was low and showed that the myeloma cells had failed to form the dimeric protein. These results suggested these cells were unable to assemble the CO-Fc heterodimer complex. This might be due to difficulties in co-transfection with both plasmids or in dimeric protein formation. Therefore, CHO cells were chosen to establish the stable CHO cell line.

Figure 4.5, shows the steps required for double transfection of CHO cells in 6 well plate with both pcDNA6-CEPU-Fc and pBudCE4.1-OBCAM-Fc using ExGen500 transfection reagent. Transfection efficiency was again monitored by the number of cells expressing GFP compared to the total number of cells counted across three microscope fields. The transfected cells survived due to the resistance to both

Blasticidin and Zeocin antibiotics. Care was taken to ensure that both antibiotics were effective by transferring cells to a larger dish to keep the number of cells below 50% confluency. The resistant transfected colonies were established and grown in the selective antibiotic medium and then subcloned in two 96 well plates (figure 4.6). Then 24 clones were expanded in a 24 well plate and were screened by ELISA assay for CO-Fc. There was sufficient medium to screen for CO-Fc in parallel to OO-Fc and CC-Fc in the medium of 24 well plate. The assay for the best clone out of 24 clones revealed that the concentration of both OO-Fc and CC-Fc homodimeric proteins was higher than the concentration of CO-Fc heterodimeric protein (figure 4.7). In view of previous results with transient double transfections in the previous chapter, a second round of subcloning was carried out in two 96 well plates, the first one with 100cell/plate and the other with 200cell/plate.

The 96 well plates were screened for single green colonies using the inverted Leica fluorescent microscope. A neat sample of medium from each positive well was used to characterise the supernatant of the transfected colonies. The medium was tested by dot blot to identify cells or wells that produce CEPU-Fc-V5-His or OBCAM-Fc-myc-His6 using anti-V5 and anti-myc antibodies. Dot blot assays showed that some of these clones secreted equal amount of both proteins and others that secreted unequal amount of each protein (figure 4.8). The next question was did these proteins exist as a complex and what is the ratio of CO-Fc heterodimeric protein, CC-Fc or OO-Fc homodimeric proteins? ELISA was used to answer this question, by characterising neat samples of the supernatant secreted by the previously mentioned clones in 96 well plates. To identify the CO-Fc complex anti-myc antibody was used as first layer to capture the myc tag of the OBCAM-Fc chain whereas the anti-V5-HRP labelled antibody was used to detect the V5 tag of the

other chain of the molecule which is CEPU-Fc. ELISA assay revealed that most of the selected clones secreted CO-Fc heterodimeric protein. The concentration varied from the maximum, which was 1D6 clone with 0.6 OD to IG12 clone which produced the lowest concentration just above zero OD. There was only one clone that did not produce CO-Fc which is IE11 (figure 4.9).

In figure 4.10, all the previously tested clones in 96 well plates were transferred to 24 well plates and allowed to grow for 2 days until they become confluent, and then analysed again by ELISA to identify the ratio between the CO-Fc heterodimeric protein and the OO-Fc or CC-Fc homodimeric proteins. Some clones such as ID1, ID6, IH3, IIG4, IIG7, IIH9 and IIH11 secreted high concentration of CO-Fc but still there were variable concentrations of OO-Fc and CC-Fc secreted by these clones.

The above-mentioned clones were transferred into six well plates; the supernatants were rechecked for the stability of the secretion of CO-Fc heterodimeric protein against the OO-Fc or CC-Fc homdimeric proteins. ID6 clone when assayed for CO-Fc gave an OD of 1.3; while CC-Fc gave an OD of 1.2 OO-Fc was 0.8 OD. This clone had the highest concentration of CO-Fc. The ID1 produced almost the same concentration of CO-Fc and CC-Fc, which was about 1.0OD, and OO-Fc was about 0.8 OD. The rest of the clones produced CO-Fc about 1.0 OD, OO-Fc about 0.8 OD and CC-Fc around 0.6 OD (figure 4.11).

Six clones that secreted higher concentrations of CO-Fc and lower concentrations of OO-Fc or CC-Fc were transferred into small sized flasks. At this stage, IIG4 was considered the best clone because the CO-Fc concentration was about 0.9 OD, OO-Fc and CC-Fc about 0.5 OD. Although, ID6 produced the highest

concentration of CO-Fc which was about 1.1 OD, the problem was the concentration of CC-Fc was about 0.8 OD which was considered to be too high (figure4.12).

Finally, IIG4 clone was selected to be the best clone according to the expected ratio(2:1:1) that produced the CO-Fc heterodimeric recombinant protein at about 1.0 OD with a contamination with CC-Fc and OO-Fc homodimeric proteins about 0.5 OD (figure 4.13).The rest of clones were frozen down and kept as a backup in liquid nitrogen.

A large quantity of CO-Fc is required for experiments so, one vial of the frozen final clone (IIG4) was thawed, spun and then resuspended in small flask in culture medium with 10% FCS for 24 hours at 37 °C and 5% CO2. When they become confluent, then transferred into medium sized flask for another 24 hours, then split the cells into four medium sized flasks with a lower concentration of FCS of 5% to be ready for the next step. Each flask was expanded into five (15 cm dishes) to get finally 20 X 15cm dishes which were cultured in 2% low IgG serum (Hyclone) because the normal serum contain about 5.0 mg/ml of IgG which will interfere with protein A agarose beads during purification. Protein A agarose beads were used to concentrate and purify 500ml of supernatant of the stably transfected CHO cell line cultured for 1 week in 2% low IgG. It was important to adjust the pH of the medium to pH8 prior to the addition of the beads to improve the binding. CO-Fc was kept in contact with the beads on the rotator for 2 to 24 hours at 4°C to increase the chance of the binding of CO-Fc to the beads (figure 4.14a). In figure 4.14b, serial fractions of the elution of the protein A agarose column were dotted and dried on a filter paper, and then stained with Coomassie stain for few minutes, followed by several washes with destain solution. High concentration of the protein was shown by most

of the dots. All factions with detectable proteins were included together and concentrated by spin column to 1ml.

Because CO-Fc heterodimeric protein could not be isolated free from IgG in the culture medium beside the CC-Fc and OO-Fc homodimeric proteins, it was necessary to devise a method to be able to compare the quantity of CO-Fc in different samples. Firstly, the linear range of the ELISA was established. (figure 4.15a). In figure 4.15b, an arbitrary unit was introduced from a normalised curve for ELISA assay at the linear range for CO-Fc heterodimeric protein, OO-Fc homodimeric protein and CC-Fc homodimeric proteins. It was decided that CO-Fc, OO-Fc and CC-Fc that gave absorption of 0.5 at 450nm was 1 AU/ml. Hence, if a 1:1000 dilution gave an OD of 0.6 then the neat solution would have a concentration of 1200 A.U. (1.2 A.U. would give an OD of 0.6). Using A.U. for the concentration of CC-Fc and OO-Fc would also mean that the concentration of both could be compared in different samples.

The next step was the purification of the CO-Fc heterodimeric chimeric recombinant protein from either OO-Fc or CC-Fc homodimeric proteins. This was necessary for binding experiments but not for outgrowth assay experiments where C-Fc and O-Fc do not interfere in these experiments. Both epitope V5 and myc tags may play a role in the process of purification; anti-myc column was assembled to be used in purification of CO-Fc heterodimeric protein of the contamination of CC-Fc homodimeric protein (figure 4.16).

In figure 4.17a, an anti-myc affinity column was used to purify the CO-Fc and OO-Fc away from the CC-Fc. In the elution (1ml), CO-Fc, OO-Fc and CC-Fc were assayed in different dilutions. All readings were in the linear range. The flow through of the column was analysed for CO-Fc, OO-Fc and CC-Fc in different dilutions and

indicated that the column eliminates most of the CC-Fc but there was unexpected loss of CO-Fc (figure4.17b).

Anti-V5 affinity column was used also as a second trial to purify the CO-Fc from OO-Fc (figure 4.18). In figure 4.19a, ELISA assayed CO-Fc, OO-Fc and CC-Fc in different dilutions. The flow through of the anti-V5 affinity column was analysed and indicated the same problem as the antimyc column (figure4.19b). In figure 4.20, a table summarises the data of the elution and flow through for both column in arbitrary unit (AU/ml) which revealed that both columns purified CO-Fc. However, a high level of contamination remained in the elution of each column.

The concentration of CO-Fc is not known, so to ensure that a comparable amount of CO-Fc was used to coat cover slips in outgrowth assay experiments, Western blotting was used to compare the concentration of the total Fc recombinant protein in the mixture of CO-Fc, OO-Fc and CC-Fc, in addition to the bovine IgG. C-Fc and O-Fc single recombinant proteins were run alongside the CO-Fc. The concentration of the total Fc protein was estimated from previous experience of production of recombinant protein by adherent cells similar to CHO cells. The Western blot indicated that the band for total amount of Fc recombinant protein was similar to either band for C-Fc or O-Fc, whereas CO-Fc is the higher concentration in the total Fc recombinant proteins based on ELISA assay (figure 4.21a). The western blot was scanned using Image J software and the density profile was printed onto paper. The appropriate peaks were cut out and weighed using an analytical balance. In figure 4.21b, the graph shows the relationship between the dilutions of chimeric protein and the weight of the peaks, generated by scanning each track with imageJ software. Three samples gave relatively similar peaks confirming that a the CO-Fc

concentration was comparable to the C-Fc and O-Fc concentrations used in previous neurite outgrowth experiments.

DISCUSSION:

It proved to be difficult to produce a doubly transfected myeloma cell line. The transfection efficiency was low compared with CHO cells and even the Amaxa nucleofector (electroporation) failed to give better than ExGene500 (polyethylinamine) transfection efficiency as judged by the number of GFP expressing cells after 48hours. Strangely, the double transfected cells also exhibited instability such that subcloned colonies showed increasingly unbalanced expression of the recombinant proteins. Finally it was decided to use CHO cells to generate the doubly transfected cell line. CHO cells were transfected with both V5 epitope tagged CEPU-Fc in pcDNA6 and myc epitope tagged OBCAM-Fc in pBudCE4.1. Both Zeocin and Blasticidin antibiotics were used to screen the cells transfected with both pBudCE4.1 and pcDNA6. 60% of the cells died with Zeocin at concentration 200μg/ml and 5 μg /ml of Blasticidin in the first three days, and the rest of the cells died after one week. During a stable cell line generation, high concentration of antibiotics will slow the growth of the transfected cells. Although some non-transfected cells may continue to grow, they will be eliminated during subcloning process.

The level of expression of CC-Fc and OO-Fc was higher in the CO-Fc stably transfected cells compared to the transiently co-transfection. The best clone (G9) of the first round subclone secreted much higher CC-Fc and OO-Fc than CO-Fc. This might be due to presence of more than one cell in one well of subcloning plate that are singly transfected and produced only either CC-Fc or OO-Fc homodimers. Therefore, a second round of subcloning was carried out, and successfully, the final clone (G4) of the second round secreted higher CO-Fc than CC-Fc and OO-Fc.

The recombinant chimeric protein was expanded into 20X 150 cm dishes for a week instead of using miniperm because the transfected CHO cell line is an adherent cell type and the outcome of the miniperm bioreactor was not promising when used previously by our group for adherent cell lines.

The concentration for CC-Fc is (900AU/ml) which less than CO-Fc (1300AU/ml) and OO-Fc (500) is the least. The shallower gradient may be a reflection of CC-Fc and OO-Fc assay being less efficient than CO-Fc because the same antibody is used for both capture and detection and the capture antibody might occupy both epitope tags. The difference between CC-Fc and OO-Fc may be due to efficiency of HRP labelling of the secondary antibody.

Anti-myc and anti-V5 coupled beads columns were used to attempt to purify the CO-Fc heterodimer protein from the CC-Fc and OO-Fc homodimers. The idea of use of the affinity columns was to preserve the CO-Fc with one of homodimers and then discard the other homodimer according to which column was used. Then either anti-myc or anti-V5 antibodies can be used to detect the CO-Fc protein alongside the flow through of the columns will be used as negative control. For example, anti-myc antibody can be used to detect the CO-Fc isolated using the anti-V5 column where the expected OO-Fc in the flow through can be used as negative control. However, the presence of the same tags on the homodimers either CC-Fc or OO-Fc may increased the chance of their binding to the columns against the chance of binding of CO-Fc heterodimer which has two different tags and this may have led to a loss of CO-Fc through both columns. For example, in the case of the myc column, the chance of binding of OO-Fc with two myc tags might be greater than the chance of CO-Fc, which has one myc tag.

The reason for the CC-Fc appearing in the elution from the anti myc column is unclear, it could be due binding of CC-Fc to OO-Fc via head groups. However, there was less OO-Fc than CC-Fc (Fig 4.13). The same reason may account for OO-Fc appearing in elution of myc column. As conclusion, myc and V5 columns were not useful as CO-Fc was lost from both and neither efficiently removed the contaminant expected.

The recombinant protein mixture used for neurite outgrowth assays was not a problem as CC-Fc and OO-Fc have been shown to have no effect. For the cell binding experiments the myc antibody could be used as OO-Fc was previously shown to have minimal binding to neurons.

In the next chapters, anti-myc antibody will be used to detect CO-Fc heterodimeric chimeric recombinant protein at neat concentration to investigate its binding to neurons, frozen sections and IgLON transfected cell lines with recombinant proteins produced from single transient transfections as negative control. Anti myc will not detect CC-Fc hence CC-Fc will not interfere in these experiments.

(A)

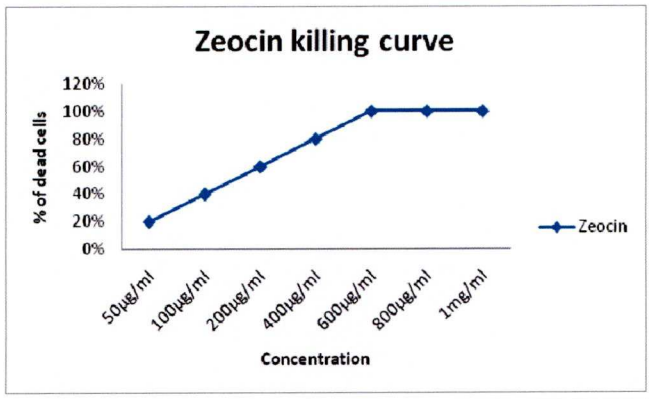

(B)

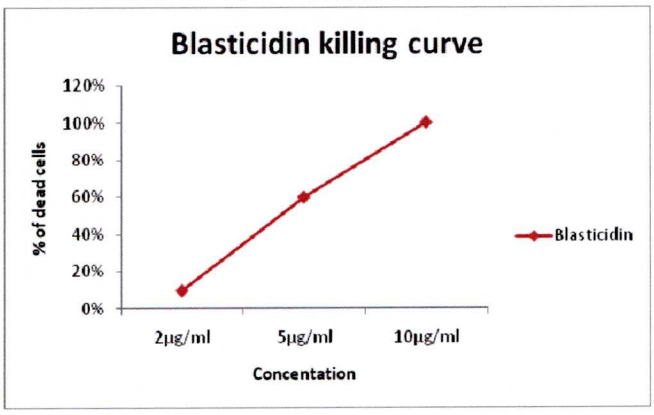

Figure 4.1: Blasticidin and Zeocin Killing Curves

A) The killing curve for Zeocin antibiotic with Wild type CHO cells or at 50% confluency with serial dilutions; 50ug/ml, 100ug/ml, 200ug/ml, 400ug/ml, 600ug/ml, 800ug/ml and finally 1mg/ml after 3 days of incubation at 37°C and 5% CO_2. The number of dead cells increased gradually with the increasing concentration of the antibiotic. Most of the cells died between 200ug/ml to 400ug/ml while the entire cell population died at 600ug/ml.

B) The killing curve for Blasticidin antibiotic with Wild type CHO cells at 50% confluency with serial dilutions; 2ug/ml, 5ug/ml and 10ug/ml after 3 days of incubation at 37°C and 5% CO_2 10% of the cells had died at 2ug/ml. At 5ug/ml, most of cell had died and 10ug/ml was aggressive on the cells since all died on the first day.60 % of cells died in the first three days with 200ug/ml Zeocin and 5ug/ml and 100% cell died after 8-10 days.

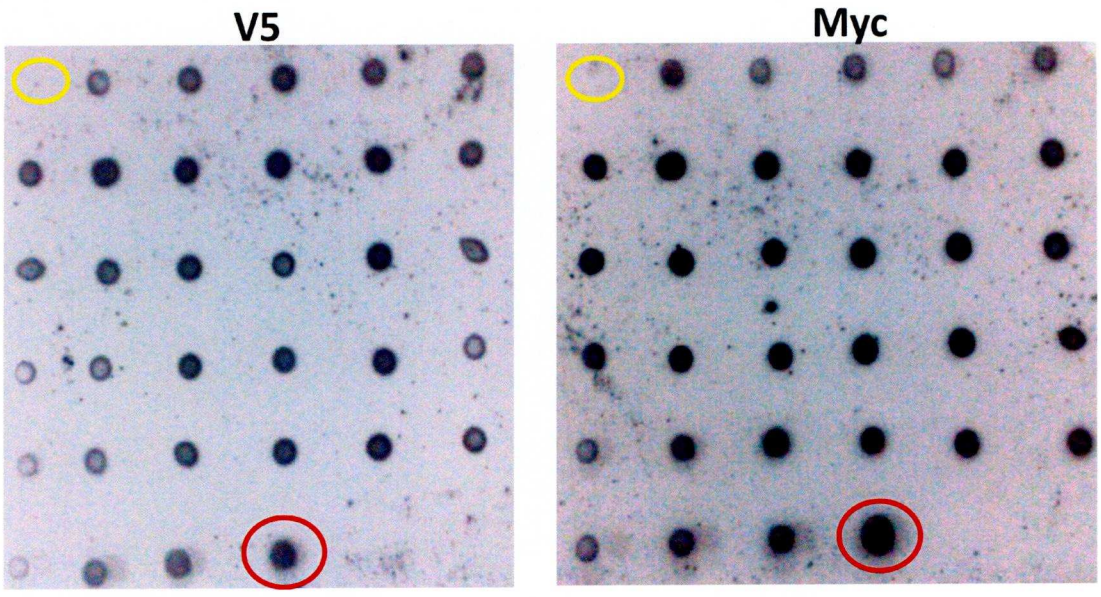

Figure 4.2: Dot blot for myeloma cell line subclones from 96 well plates:

The supernatants of different clones of CO-Fc myeloma cell line dotted on a nitrocellulose membrane. They were stained with both mouse antiV5 and antimyc antibodies (Invitrogen) (1:2000). Anti-mouse HRP was used as secondary antibody (Dako) (1:2000). The red circles represent the positive control, which is CO-Fc transient transfection while the yellow circles are negative control.

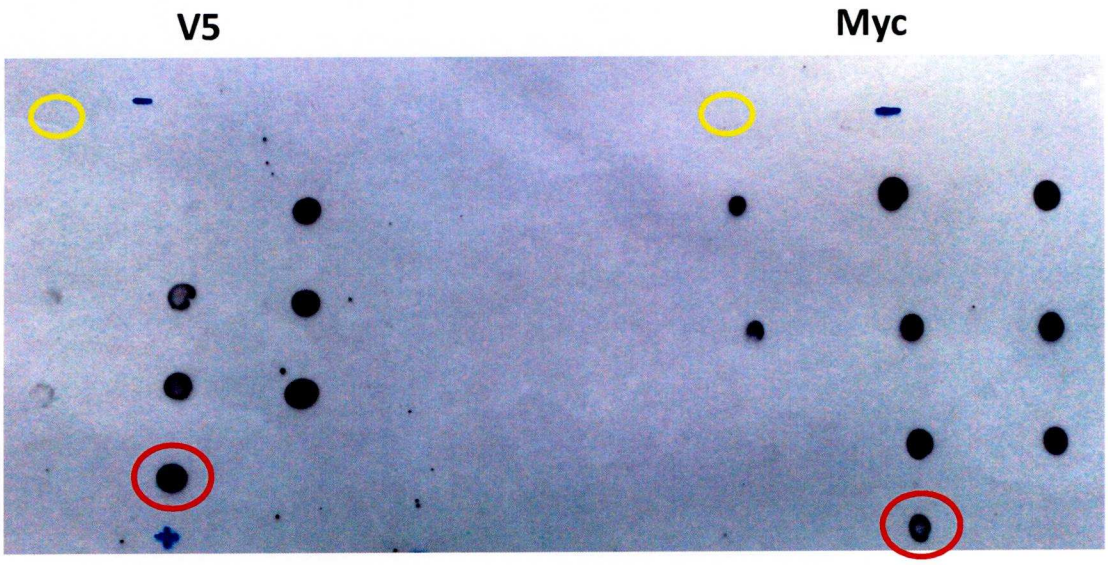

Figure 4.3: Dot blot for CO-Fc myeloma cell line from 24 well plate

The supernatants of different clones of CO-Fc myeloma cell line dotted on a nitrocellulose membrane. They were stained with both mouse antiV5 and antimyc antibodies (Invitrogen)(1:2000). Anti-mouse HRP was used as the secondary antibody (Dako)(1:2000). The red circles represent the positive control which are CO-Fc transient transfection while the yellow circles are negative control. There are some clones that express both myc and V5 where other clones express only myc while no or low expression of V5 which means un equal expression of both CEPU-Fc-V5 and OBCAM-Fc-myc.

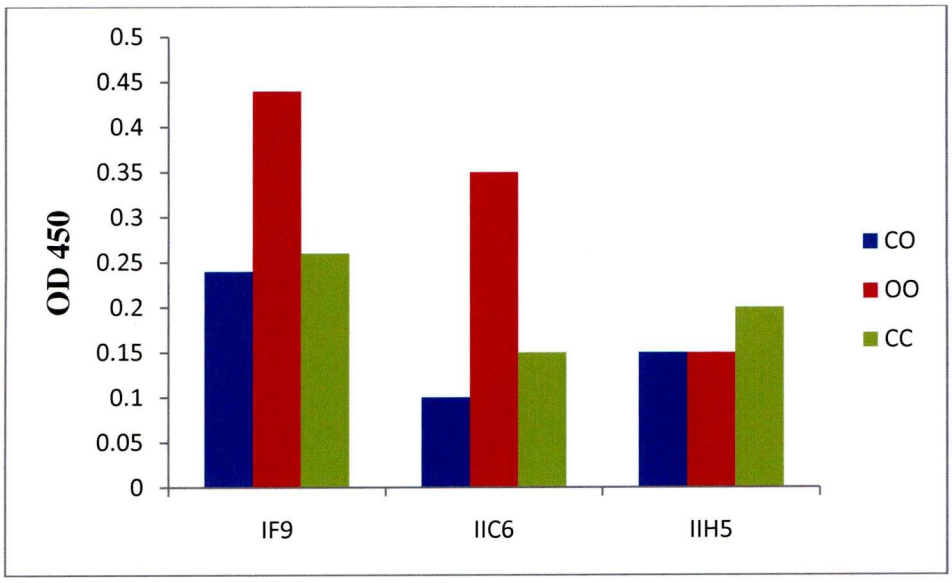

Figure 4.4: ELISA Assay for best clones of CO-Fc myeloma cell line:

ELISA assay for 10 x concentrated of 10 ml of supernatants of the three clones (IF9-IIC6-II H5) were assayed by using anti-myc or anti-V5 antibodies as primary antibody (Invitrogen) (1:300). Anti-myc or anti-V5 –HRP labelled antibodies (Invitrogen) (1:500) were used as secondary antibody. The concentration of CO-Fc heterodimer from three clones was low (0.1-0.2 OD) while the concentration of OO-Fc and CC-Fc homodimers are higher than CO-Fc but still low.

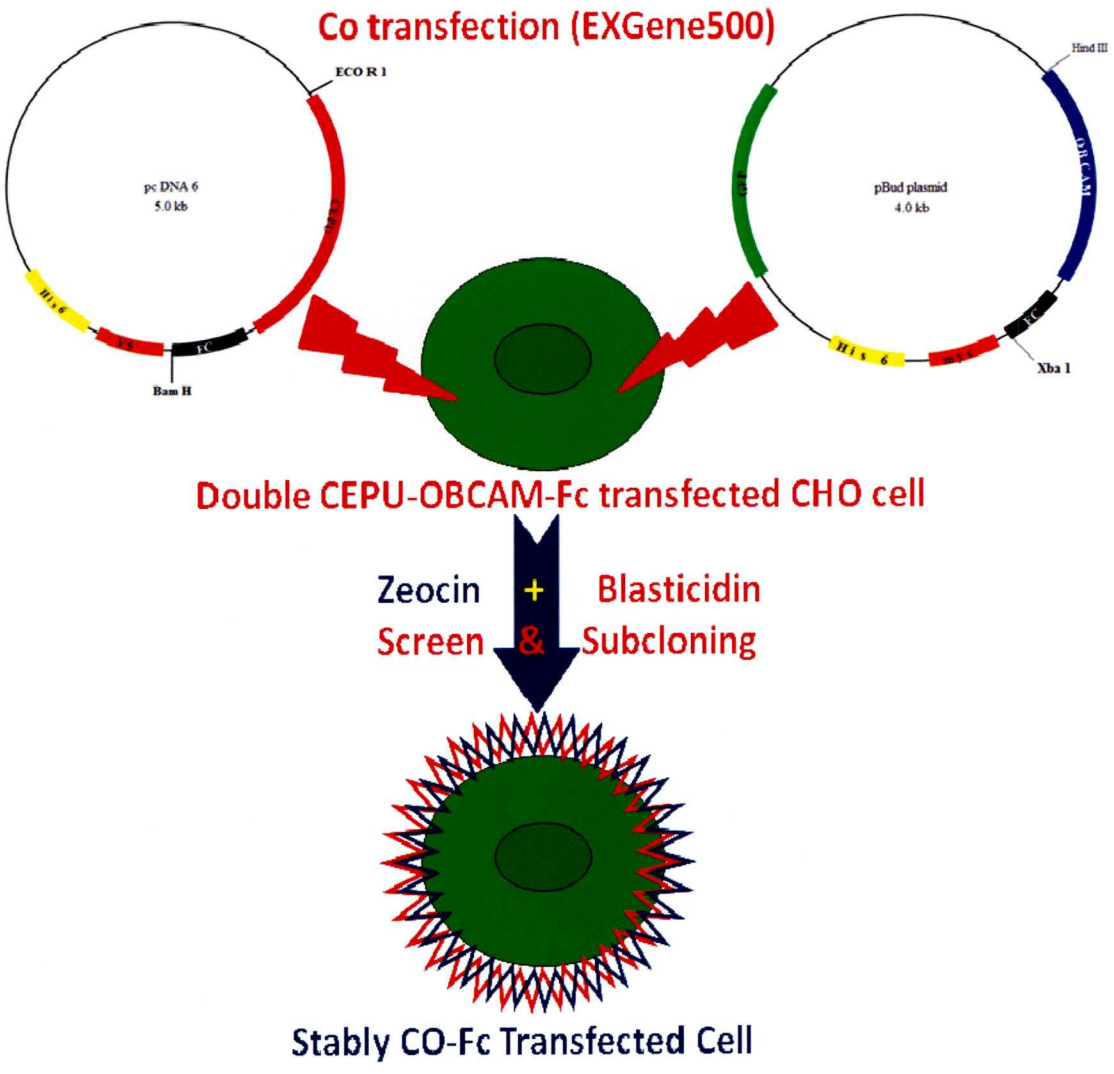

Figure 4.5: CO-Fc Stable transfection of CHO cell line

A diagram describes the steps of the CO-Fc stable transfected CHO cell line CEPUFc (pcDNA6) (1µg/µl) and OBCAM-Fc (pBudCE4.1) (1µg/µl) using ExGEN500 (Fermentas). The next step was screening for pcDNA6 which is resistant to Blasticidin (5µg/ml), and pBudCE4.1 which is resistant to Zeocin (200ug/ml). Finally, CO-Fc stably transfected clone after a number of subclones were selected.

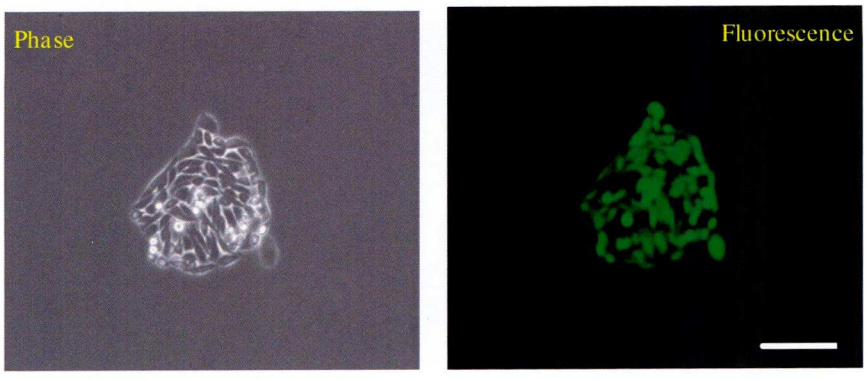

Figure 4.6: CO-Fc transfected selected clone

The first photograph is a phase picture for a selected clone in 96 well plate, the second one is a fluorescent picture for the same clone with GFP fluorescent protein which was used to check the transfection with OBCAM-Fc in pBudCE4.1 (scale bar50μm).

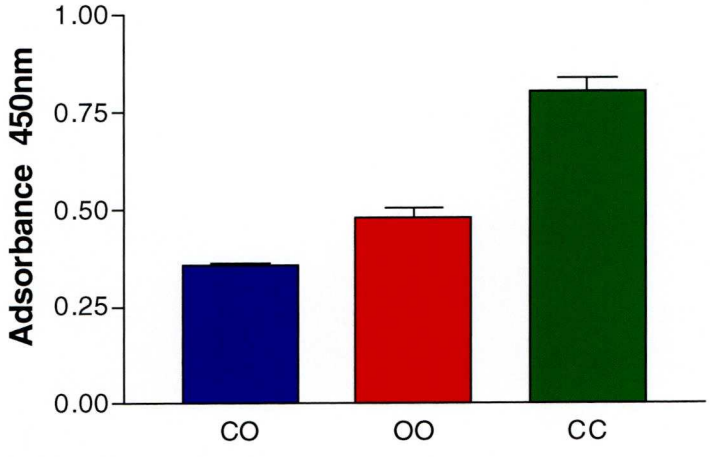

Figure 4.7: final clone (G9) of the first round of subcloning

A graph shows an ELISA assay for CO-Fc using anti-myc antibody as capture antibody and anti-V5-HRP labelled antibody as detection antibody.CO-Fc concentration (blue bar) in the medium was about 0.35 OD. Anti-myc and anti-myc-HRP labelled antibodies were used for detection of OO-Fc. OO-Fc concentration (red) was about 0.5 OD. For CC-Fc detection, anti-V5 and anti-V5-HRP labelled were used (green) about 0.8 OD. The ratio is two for CC-Fc to one for CO-Fc and OO-Fc. It was expected to be two for CO-Fc heterodimer and one for each homodimer. (n=3)(SEM= CO-Fc 0.0064, OO-Fc 0.025, CC-Fc 0.038).

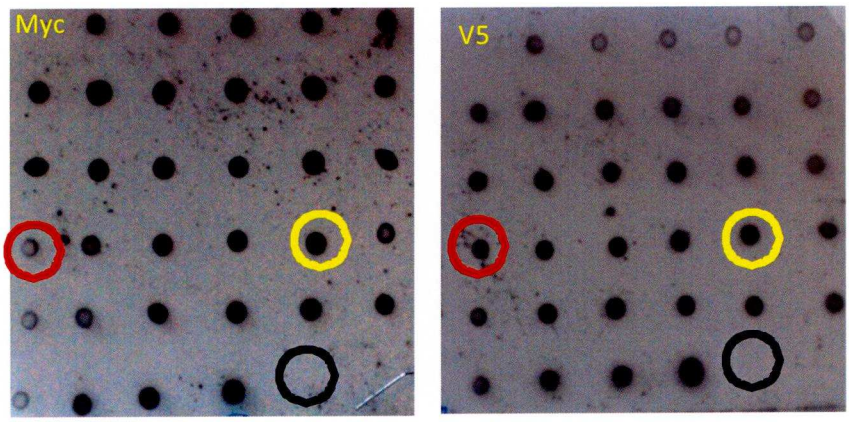

Figure 4.8: Dot Blot for CO-Fc subclones with antimyc and antiV5 antibodies

Dot blots for the selected colonies from 96 well plate. The first blot was stained with mouse anti-myc antibody (1:2000) (Invitrogen) to test the generation of OBCAM-Fc-myc-His6 protein, and the second one was stained with mouse anti-V5 antibody (1:2000) for CEPU-Fc-V5-His6. Secondary anti-mouse HRP labelled (1:2000) (Dako) was used. The yellow circles represent colonies with equal expression of CEPU-Fc-V5-His6 and OBCAM-Fc-myc-His6, while red circles represent unequal expression of both chains. Negative controls were encircled by black circles.

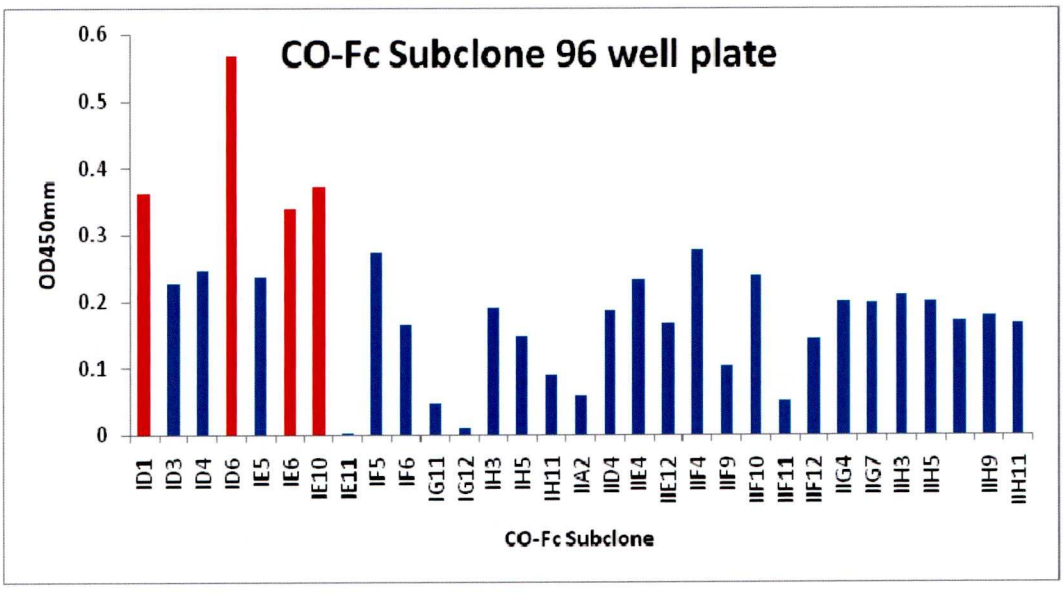

Figure 4.9: ELISA assays for the selected colonies from 96 well plates

A graph shows an ELISA assay for a number of selected colonies from 96 well plates using anti-myc antibody (1mg/ml) (1:300) as first capture layer for OBCAM-Fc-myc-His6 chain and anti-V5 HRP labelled antibody (1:500) to detect the CEPU-Fc-V5-His6 chain to test for CO-Fc heterodimer recombinant protein secreting colonies. An ELISA micro plate reader was used at 450mm wavelength. The red bars represent the colonies that produced the highest concentration of CO-Fc; ID1, ID6, IE6 and finally IE10.

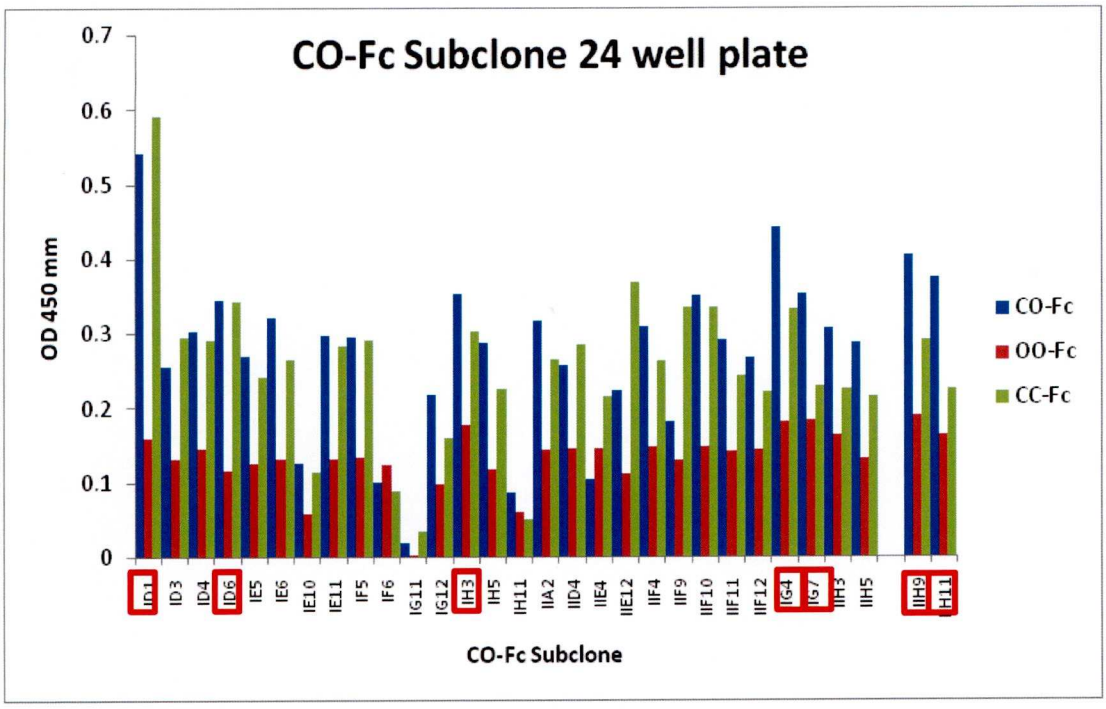

Figure 4.10: ELISA assay for the selected colonies from 24 well plates for CO-Fc heterodimer, OO-Fc homodimer and CC-Fc homodimer

A graph for ELISA assay shows the ratio of the secreted CO-Fc heterdimer (blue) using anti-myc and anti-V5HRPantibodies to the OO-Fc (red) using anti-myc and anti-mycHRP antibodies and CC-Fc (green) using anti-V5 and anti-V5HRP antibodies. ID1, ID6, IH3, IIG4, IIG7, IIH9 and IIH11 clones(red reqtangles) were selected that produce CO-Fc more than OO-Fc and CC-Fc to be transferred to a 6 well plate.

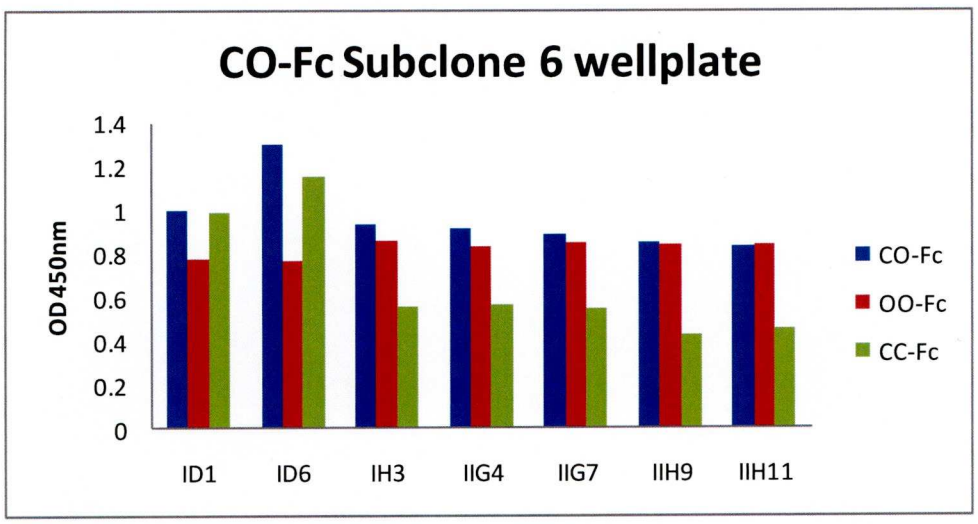

Figure 4.11: ELISA assay for the selected colonies in 6 well plate

A graph shows an ELISA assay for the selected clones. The CO-Fc concentration varies from one clone to another. ID1, ID6, IH3, IIG4, IIG7, IIH9 and IIH11 were transferred to small flasks because they secret more CO-Fc heterodimer than OO-Fc or CC-Fc homodimers.

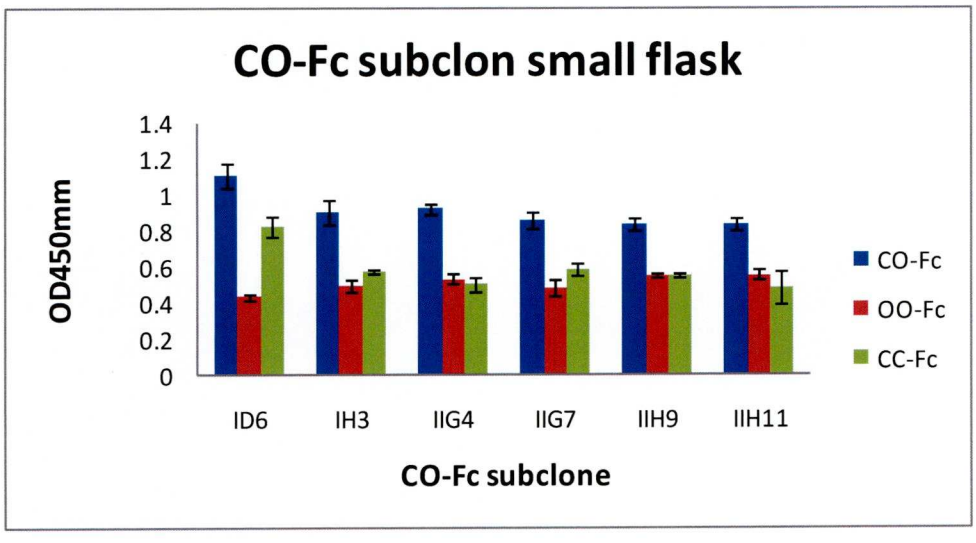

Figure 4.12: ELISA assay for the selected subclones in small sized flasks

A graph shows an ELISA assay for the selected clones in small flask. The best clone is IIG4 that produce twice as much CO-Fc (blue) (0.9 OD) as the OO-Fc (red) or CC-Fc (green) (0.5OD).The other clones still produce higher concentration of CO-Fc but the concentration of the homodimers is still more than IIG4. (n=3)(SD= ID6 0.0674, 0.0160, 0.057-IH3 0.071501, 0.03245, 0.01305-IIG4 0.02700, 0.0308, 0.04087- IIG7 0.0449, 0.0485, 0.03178- IIH9 0.03439, 0.0094, 0.0087-IIH11 0.0334, 0.0269, 0.09603 for CO-Fc, OO-Fc and CC-Fc respectively.

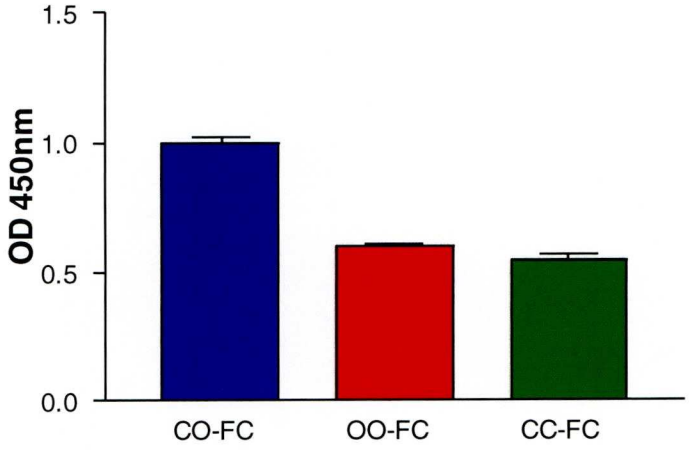

Figure 4.13: ELISA assay for the Final clone of CO-Fc

A graph shows an ELISA assay for the final clone which is IIG4 after many subclones. The ratio of the CO-Fc concentration is double (1.0 OD) the concentration of OO-Fc or CC-Fc homodimers (0.5) in large flask which prove the stability of the cell line. (n=3) (SEM= CO-Fc 0.024, OO-Fc 0.010, CC-Fc 0.024)

A)

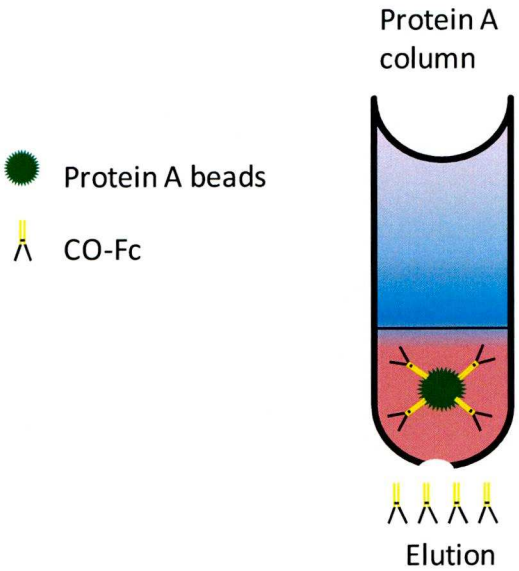

B)

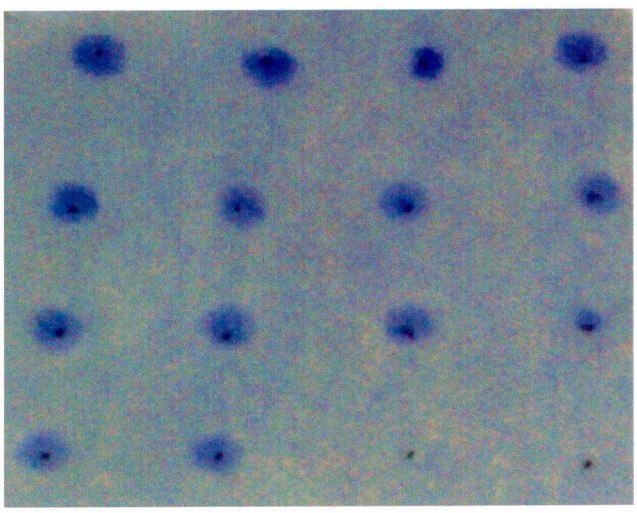

Figure 4.14: Purification of CO-Fc with Protein A agarose beads column

(A) The first diagram describes the structure of the protein A agarose beads (Sigma) column. The CO-Fc heterodimeric protein interacts with beads with the human Fc tail of the complex.

(B) The second picture shows a Coomassie stain for serial fractions of the elution of the protein A beads column (100µg/ml) on a filter paper. The concentration of the protein gradually decreased until it disappears in the last two fractions.

A)

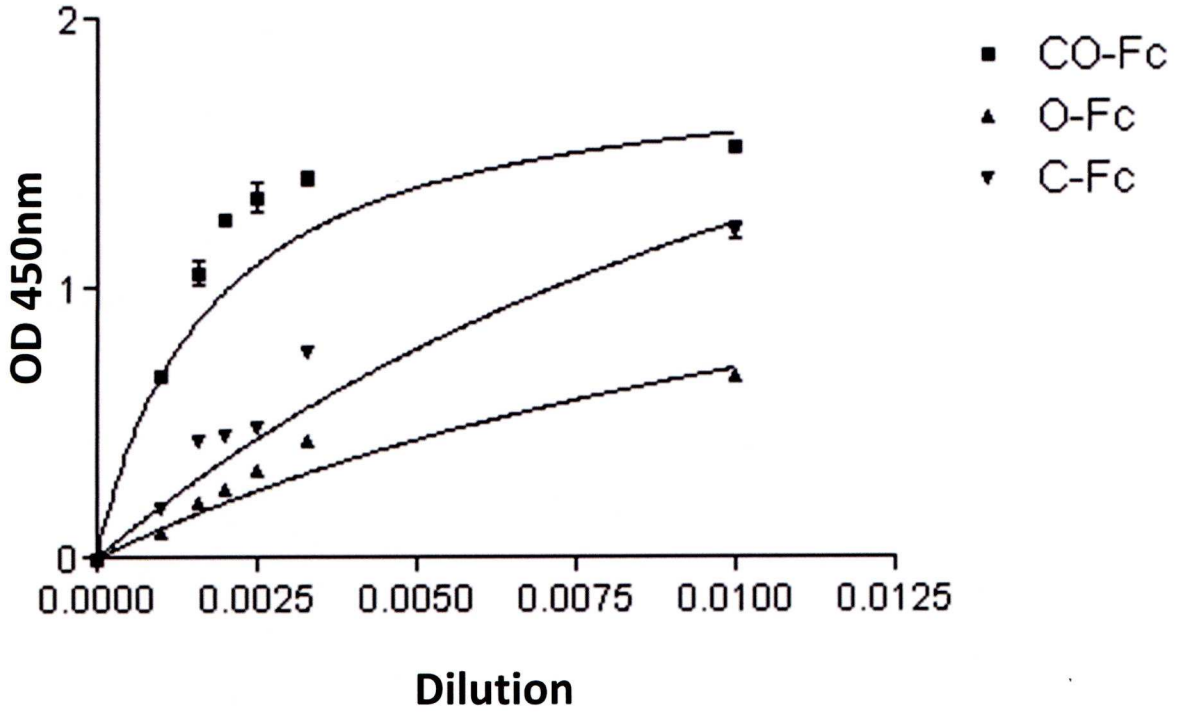

Figure 4.15: ELISA assays for the elution of Protein A agarose beads column

A graph shows a normalised curve for ELISA assay for the elution of protein A beads column. The concentration of CO-Fc heterodimeric recombinant protein is still higher than the concentration of the OO-Fc or the CC-Fc homodimers. The linear range is between 0.001 to 0.003 dilutions.

An arbitrary unit (AU/ml)was introduced to measure the concentration of the recombinant protein from the ELISA curve at the linear range, 0.5 OD equal 1 AU/ml. CO-Fc is about 1300AU/ml CO-Fc, OO-Fc is 500AU/ml and CC-Fc is 900AU/ml.

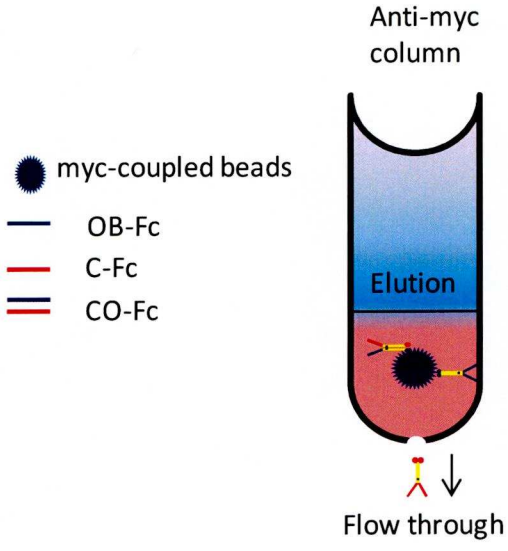

Figure 4.16: an illustration describes the principle of an anti-myc column

This diagram describes the purification of CO-Fc by anti-myc column which is composed of myc coupled beads. The myc tags of both CO-Fc and OO-Fc will bind to the beads and be located in the elution of the column, while the CC-Fc will not bind to myc beads and will be in the flow through of the column.

A)

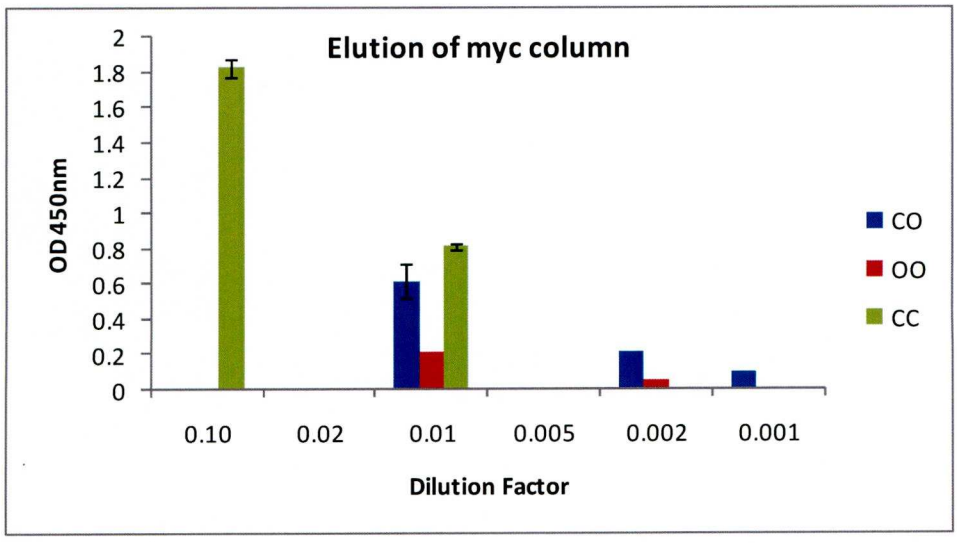

B)

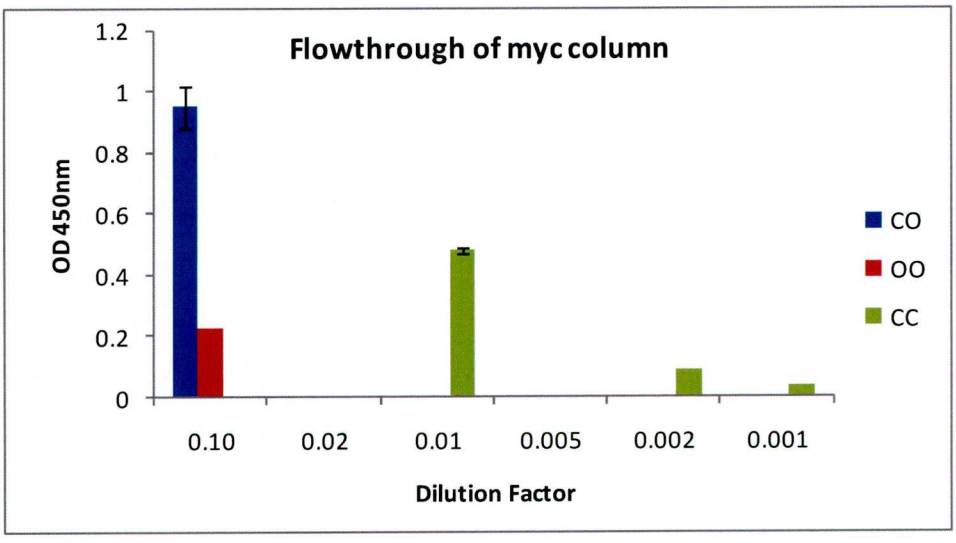

Figure 4.17: Purification of CO-Fc with anti-myc column

A) A graph show the elution of anti-myc affinity column, CO-Fc (blue) at 0.01 and 0.002 and 0.001, OO-Fc (red) at 0.01 and 0.02 and CC-Fc (green) at 0.1 dilutions.

B) A graph shows the flow through of anti-myc column CO-Fc (blue) at 0.01, OO-Fc (red) 0.1, CC-Fc (green) at 0.01, .0.02 and .001dilutions.

The arbitrary units for both elution and flow through will be in table in figure 4.15.

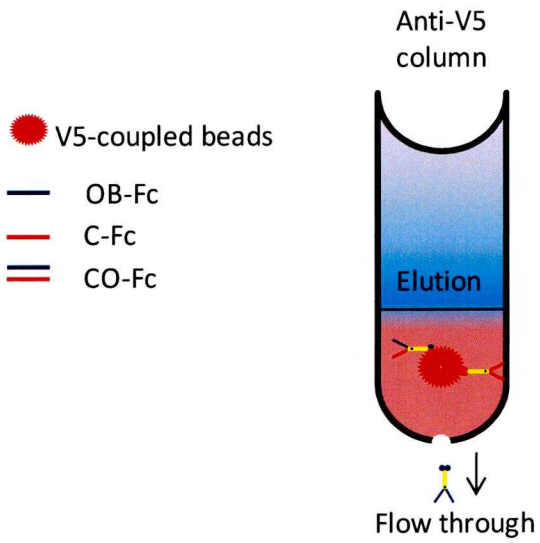

Figure 4.18: an illustration describes the principle of an anti-V5 column

This diagram describes the purification of CO-Fc by anti-V5 column which is composed of V5 coupled beads. The myc tags of both CO-Fc and CC-Fc will bind to the beads in the elution of the column, while the OO-Fc will not bind to myc beads and will be flow through of the column.

A)

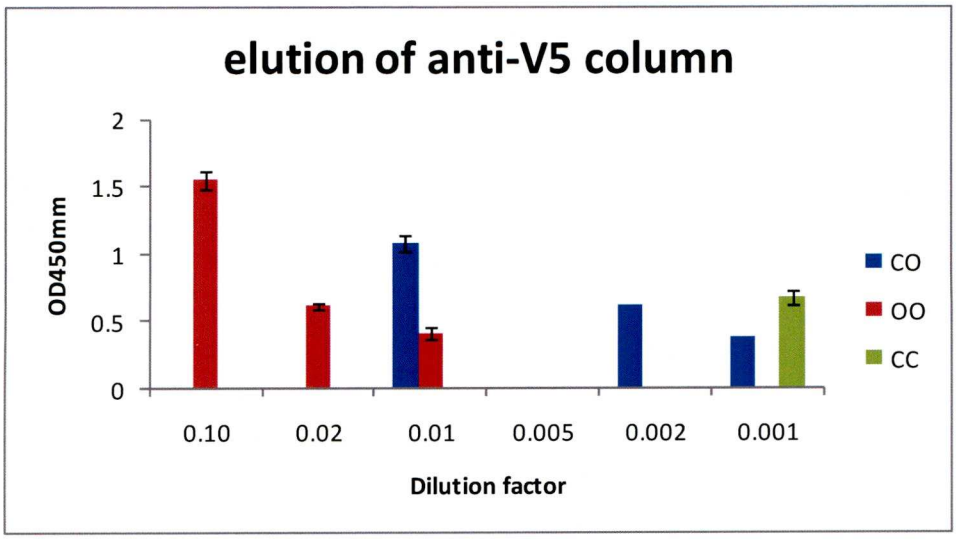

B)

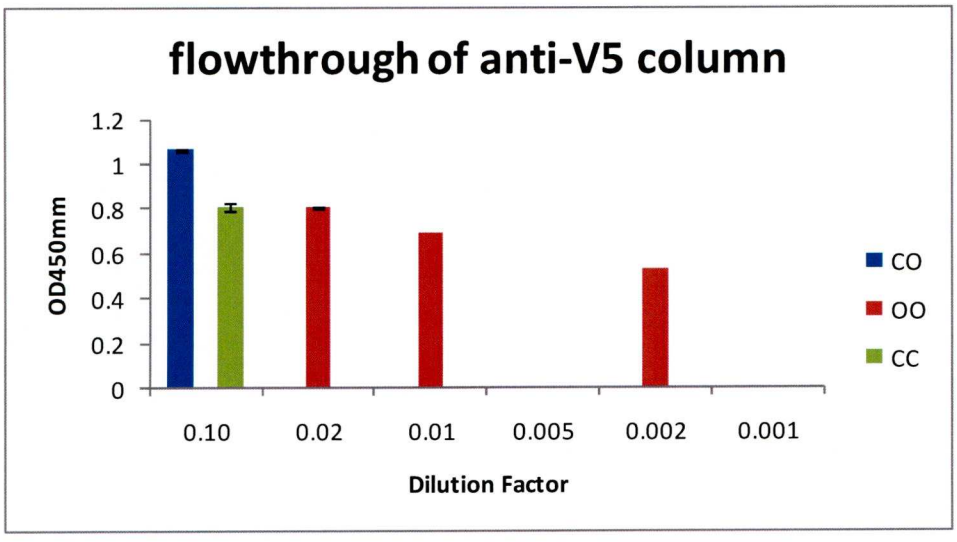

Figure 4.19: Purification of CO-Fc by antiV5 affinity column

A) A graph shows the elution of anti-V5 affinity column, CO-Fc (blue) at 0.01, 0.002 and 0.001 dilutions. OO-Fc (red) at 0.1, 0.02 and 0.01 dilutions and CC-Fc (green) at 0.001dilution.

B) A graph shows the flow through of the anti-V5 affinity column, CO-Fc (blue) at 0.1 dilution, OO-Fc (red) at 0.02, 0.01 and 0.002 dilutions, CC-Fc (green) at 0.1 dilution. The arbitrary units for both elution and flow through will be in table in figure 4.17.

A) Antimyc column

Protein	*Elution*	*Flow through*
CO-Fc	*120AU/ml*	*20AU/ml*
OO-Fc	*40AU/ml*	*4AU/ml*
CC-Fc	*160AU/ml*	*100AU/ml*

B) Anti-V5 column

Protein	*Elution*	*Flow through*
CO-Fc	*216AU/ml*	*22AU/ml*
OO-Fc	*83AU/ml*	*80AU/ml*
CC-Fc	*1340AU/ml*	*16AU/ml*

Table 4.20: table listing the concentration of the elution and flow through for anti-myc and anti-V5 columns in AU/ml

(A)

(B)

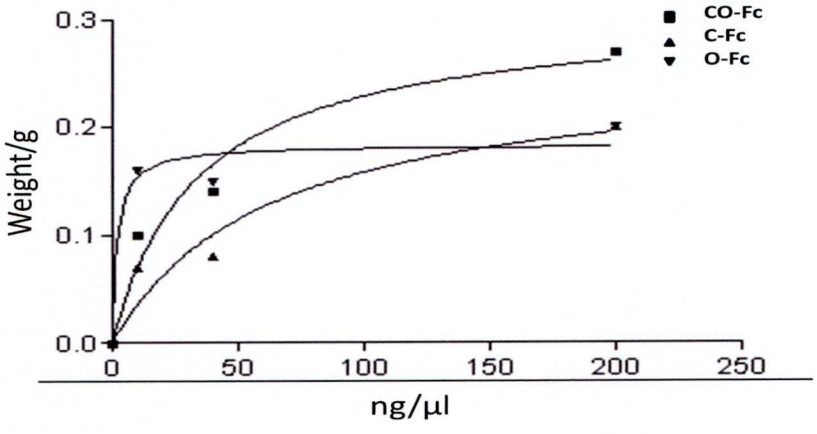

Figure 4.21: Western blot to estimate the concentration of CO-Fc heterodimeric protein

A) A western blot shows bands for CEPU-Fc (1st lane), OBCAM-Fc (2nd lane) single recombinant protein (200ng/ml) and CO-Fc heterodimeric protein (1:10). The CO-Fc concentration that was loaded onto the gel was estimated from previous experience of production of recombinant protein by adherent cell line. The blot stained by primary rabbit anti-human Fc antibody (1:1000) and secondary anti-rabbit HRP-labelled (1:2000). West Pico (Pierce) was used and exposure time was 1 minute. The blot revealed similar concentration of C-Fc, O-Fc and CO-Fc recombinant proteins in three lanes.

B) A graph shows the relation between dilution factor of each band of the three proteins and their weight when they scanned with image J software. The concentration of all three chimeric proteins used for the outgrowth assays were relatively similar.

Chapter Five

The activity of CO-Fc heterodimeric recombinant protein

INTRODUCTION:

In the previous chapter, CO-Fc heterodimeric chimeric recombinant protein was generated by stable transfection of wild type CHO cell line with both pcDNA-6-CEPU-1-Fc-V5 and pBudCE4.1-OBCAM-Fc-myc. In this chapter, the activity of the CO-Fc heterodimeric protein will be tested on the outgrowth of the neurons in comparison with the effect of the CO double transfected CHO cell line.

Previously, GP55 protein which is a mixture of IgLONs inhibited the neurite outgrowth from DRG and forebrain neurons. This suggested that GP55 contained heterodimeric complexes (DigLONs), since there was no or minimal effect on the neurite outgrowth with either single CEPU-1 or OBCAM (Clarke and Moss, 1994, 1997) (McNamee et al., 2002). In addition, the CEPU-1-OBCAM (CO) double transfected CHO cell line inhibited the initiation of the neurite outgrowth from a subpopulation of cerebellar granule cells (CGC) (Reed et al., 2004). These data suggested that IgLONs become active when present as a heterodimer complex (DigLON). There is indirect evidence to suggest that CO, CL and LO DigLONs could be formed (Reed et al., 2004). A DigLON is a combination between two different members of the group. There are six possible combinations of IgLONs and hence they may be six different DigLONs (Reed et al., 2004).

Recently it has been shown that initiation of neurites from E7/E8 forebrain neurons were inhibited when they were grown on double transfected CO and CL CHO cell line (Christine McNamee PhD Thesis University of Liverpool 2008), while no inhibition with single IgLONs was observed.

The inhibition of the initiation of neurites could have occurred due to interaction between the DigLON expressed on transfected cell lines and IgLONs or DigLON that are expressed on the surface of the neurons. However, this requires that

the IgLONs should be able to signal to the neuronal cytoskeleton and since they do not have a cytoplasmic domain, the mechanism in this case is unclear.

A second possibility is that the receptor could be a transmembrane receptor that has a cytoplasmic domain that can initiate the signaling pathway. The third possibility is that DigLON bind to a complex formed by transmembrane receptor beside IgLON (figure 5.1).

To investigate whether IgLONs form part of the receptor, the response of neurons to DigLONs will be tested with and without surface IgLONs. IgLONs can be removed from the surface of the neurons by treatment of the neurons with PI-PLC that cleave the GPI anchor. This is an advantage of the CO-Fc recombinant protein as tool since this experiment is not possible with CO-CHO transfected cell line (Marg et al., 1999; McNamee et al., 2002).

MATERIALS AND METHODS:

PIPLC Treatment: Phosphatidyl inositol-specific phospholipase C (Molecular Probe)

IgLONs are cell adhesion molecules attached to the cell membrane by GPI anchored protein.

PI-PLC was used to cleave IgLONs from the surface of the neurons at GPI anchor site while keep the neurons alive.

E8 chick forebrain dissociated neurons were incubated in forebrain culture medium that contain PI-PLC (1.0 U/ml) for 1 hour at 37°C and 5%CO_2. Then, the treated neurons were resuspended in forebrain culture medium that contains (0.1U/ml) PI-PLC. Instantly, the treated neurons were counted and then plated in a 24 well plate that has precoated cover slips with Poly-Lysine, protein A (Sigma) which is responsible for the orientation of IgLON heads and then coating standard single chimeric proteins such as CEPU-Fc, OBCAM-Fc or CO-Fc heterodimeric chimeric recombinant protein for neurite outgrowth assay experiments (Gil et al., 1998).

RESULTS:

Neurite outgrowth assay experiments were used to investigate the activity of the CO-Fc heterodimeric recombinant protein. It was used as a substrate on nitrocellulose coated cover slips alongside the standard chimeric protein CEPU-Fc or OBCAM-Fc as negative controls.

The first experiment was on E8 forebrain neurons (figure 5.2), the graph shows a normalised relation between the percentage of the neurite outgrowth with different chimeric proteins CEPU-Fc (100μg/ml), OBCAM-Fc (100μg/ml) and CO-Fc heterodimeric protein. The concentration of CO-Fc was 700AU/ml based on a correlation between ELISA assay and western blotting. 50% of the neurons were inhibited from extending their neurites due to the effect of CO-Fc heterodimeric chimeric protein while minimal inhibition occurred with CEPU-Fc and no inhibition with OBCAM-Fc standard chimeric proteins. The forebrain neurons that extend neurites with length double the diameter of the cell body were counted. In figure 5.3, photographs represent the inhibition of outgrowth assay experiment for forebrain neurons at E8. Photographs showed that most of the neurons were able to initiate their neurites with polyLysine, CEPU-Fc or OBCAM-Fc single chimeric proteins while on CO-Fc a subset of neurons were inhibited by CO-Fc heterodimeric protein.

In figures 5.4, E10 dorsal root ganglion neurons were cultured on cover slips that were coated with CEPU-Fc (100μg/ml), OBCAM-Fc (100μg/ml) or CO-Fc (700AU/ml) alongside a positive control with laminin. The first bar on the graph represents the percentage of neurite outgrowth on laminin only, which was about 90 %. Neither CEPU-Fc nor OBCAM-Fc inhibited the neurite outgrowth which was almost similar to the normal outgrowth on laminin. No inhibition occurred when CO-Fc used at the same concentration used with E8 forebrain (700 AU/ml). This result

was similarly to that observed previously where E10 DRG neurons extended axons on CO-CHO cells. However, significant inhibition occurred with the 4xfold concentration of CO-Fc heterodimeric protein (2700AU/ml), 75% of the neurons were not able to initiate their neurites (figure 5.5). The photographs showed that neurite outgrowth occurred with laminin, C-Fc or OB-Fc while CO-Fc (2700AU/ml) inhibited the neurite outgrowth (figure5.6).

In figure 5.7, the lower concentration of CO-Fc (700AU/ml) failed to inhibit the neurite outgrowth from E10 sympathetic neurons, while 4 fold higher concentration of CO-Fc heterodimeric protein (2700AU/ml) inhibited the outgrowth of E10 sympathetic neurons, approximately, 80% of the neurons were inhibited to extend their neurites (figure 5.8). In both cases CEPU-Fc or OBCAM-Fc were unable to prevent the neurons from extending their neurites which was similar to those neurons grown on the laminin control. CO-Fc as seen in photograph (CO-Fc) inhibited the outgrowth from the neurons whereas no inhibition occurred with laminin, C-Fc or OB-Fc photographs (figure5.9). All experiments were carried out in triplicate. The number of counted neurons was about 300 in each experiment. Prism software was used to produce these graphs.

Finally, to investigate whether IgLONs are involved in the formation of the putative receptor complex, E8 chick forebrain neurons were treated with PI-PLC. PI-PLC treatment is used to release the GPI anchored proteins including IgLONs from the surface of the neurons.

In figure 5.10, fluorescent photographs showed that IgLONs are expressed on the cell bodies, axons and dendrites of E8 chick forebrain neurons. The staining of the PI-PLC treated E8 forebrain neurons with IgLONs antisera (anti-CEPU-1, anti-OBCAM and anti-LAMP) revealed that no IgLONs still expressed on the surface of

the neurons after the treatment with PI-PLC (figure5.11). In the outgrowth assay experiment, there was a significant difference between PI-PLC treated and untreated forebrain outgrowth with CO-Fc, while no significant difference in treated and untreated forebrain neurite outgrowth with C-Fc and O-Fc standard chimeric protein was observed (figure5.12). This suggests that GPI-anchored protein including IgLONs/DigLONs may have a role in the formation of the putative receptor for CO-Fc heterodimeric protein, however further investigations are required to support this evidence.

DISCUSSION:

The initiation of the neurite outgrowth from forebrain, DRG or sympathetic neurons was inhibited by the action of CO-Fc heterodimeric chimeric recombinant protein while no inhibition occurred with single CEPU-Fc or OBCAM-Fc or mixed together. This data supported the evidence that GP55 may contain heterodimeric complexes which inhibit the outgrowth from DRG neurons (Clarke and Moss, 1994). Protein A was used in these experiments to orient the protein to allow the IgLONs heads of the CO-Fc complex to contact with the neurons. The fact that CO-Fc heterodimeric protein preparation was contaminated with CC-Fc and OO-Fc homdimeric protein was not a problem in this experiment, since no inhibition occurred with CEPU-Fc or OBCAM-Fc recombinant proteins controls. The concentration of the CO-Fc was comparable to that used for CEPU-Fc and OBCAM-Fc based on the correlation between the ELISA assay and the western blot results for CEPU-Fc, OBCAM-Fc and CO-Fc using anti-human Fc antibody. Furthermore, no inhibition of the initiation of the neurite outgrowth of forebrain neurons occurred when both CEPU-Fc and OBCAM-Fc single recombinant proteins were mixed together (McNamee et al., 2002) (Michael Lyons).

The inhibition occurring with CO-Fc is similar to that observed with double transfected (CO) CHO cell line in case of forebrain neurons (Christine McNamee PhD Thesis University of Liverpool 2008). On other hand, CO-CHO and CO-Fc were unable to inhibit the neurite outgrowth of DRG or sympathetic neurons. However, significant inhibition occurred on both DRG and sympathetic neurite outgrowth when 4xfold concentration of CO-Fc was used. Surprisingly, the 4x fold concentration difference goes from 0 to 75% inhibition whilst only 50% forebrain

neurons were inhibited. This might be due to heterogeneity of forebrain neurons versus DRG and sympathetic neurons.

IgLONs are expressed in different part of the forebrain; CEPU-1 is expressed in the ventricular surface of the anterior part of E8 forebrain section, while OBCAM is expressed in posterior part of E6 forebrain section. Furthermore, E8 forebrain is a site for co-expression of IgLONs, LAMP-CEPU-1 are co-expressed posteriorly, where the anterior part of the forebrain showed a co-expression of LAMP and OBCAM (Sahar Youssef PhD thesis Liverpool University 2007). In addition, IgLONs are expressed by both dorsal root ganglion and sympathetic chain neurons (Gil et al., 1998; McNamee et al., 2002). This evidence suggests that CO-Fc may interact with IgLONs on the surface of forebrain, DRG and sympathetic chain neurons. There is expression of IgLONs in E7 chick spinal cord; LAMP, OBCAM and CEPU-1 are co expressed in dorsal roots (Sahar Youssef PhD thesis Liverpool University 2007). IgLONs may promote the preganglionic neurons to innervate the sympathetic chain through *trans* homophilic or heterophilic interactions.

In vivo, CEPU-1 is expressed early during the development of neurons; the intensity of staining of CEPU-1 varies from faint in the anterior ectoderm and mesenchyme region of chick embryo to more intense in the neural plate (Jungbluth et al., 2001; Kimura et al., 2001). With development, a broad band of CEPU-1 mRNA expression is situated to the area of forebrain, midbrain and anterior hindbrain. However, it became more localised at the isthmus or midbrain-hindbrain boundary at (E2) embryonic day (Jungbluth et al., 2001). During migration of the neurons, CEPU-1 is expressed in primary sensory and motor regions of the rat brain, mainly, restricted to postmitotic neurons that increase in the rat forebrain from the age of E15 (Gil et al., 2002; Struyk et al., 1995). On other hand, OBCAM is expressed later than

CEPU-1 mainly in the cerebral cortical plate and hippocampus regions of the brain (Struyk et al., 1995). In addition, in situ hybridization data showed that CEPU-1 and OBCAM expressed in the notochord and floor plate in chick embryo at E3 (Sahar Youssef PhD thesis Liverpool University 2007).

CO-Fc heterodimeric protein may bind to the putative receptor complex on the surface of the neurons to inhibit the initiation of the neurite outgrowth. IgLONs could be part of this complex. Because they don't have cytoplasmic domain, a transmembrane receptor may be required to form a complex with IgLON to signal to the cytoskeleton (figure5.10). Removal of the GPI anchored protein including IgLONs from the surface of the neurons suggested that IgLONs may have a role in the formation of a putative receptor complex for CO-Fc heterodimeric chimeric recombinant protein. Hence CO-Fc requires the interaction with GPI anchored proteins on the surface of the neurons to inhibit their neurite outgrowth.

In the next chapter, the nature of the putative receptor complex for CO-Fc heterodimeric protein will be investigated using immunofluorescence studies investigating its interaction with E8 forebrain, E10 dorsal root ganglion and sympathetic neurons. In addition, the interaction E18 chick retina frozen sections which is a common site for expression of IgLONs will also be investigated. Analysis of the binding of CO-Fc to IgLON transfected cell lines will provide insight into the IgLONs specificity and which IgLONs may be are involved in the receptor complex. Finally, binding experiments to neurons treated with PILPC to remove the GPI anchored proteins will confirm the loss of binding of CO-Fc to the surface of the neuron in absence of IgLONs.

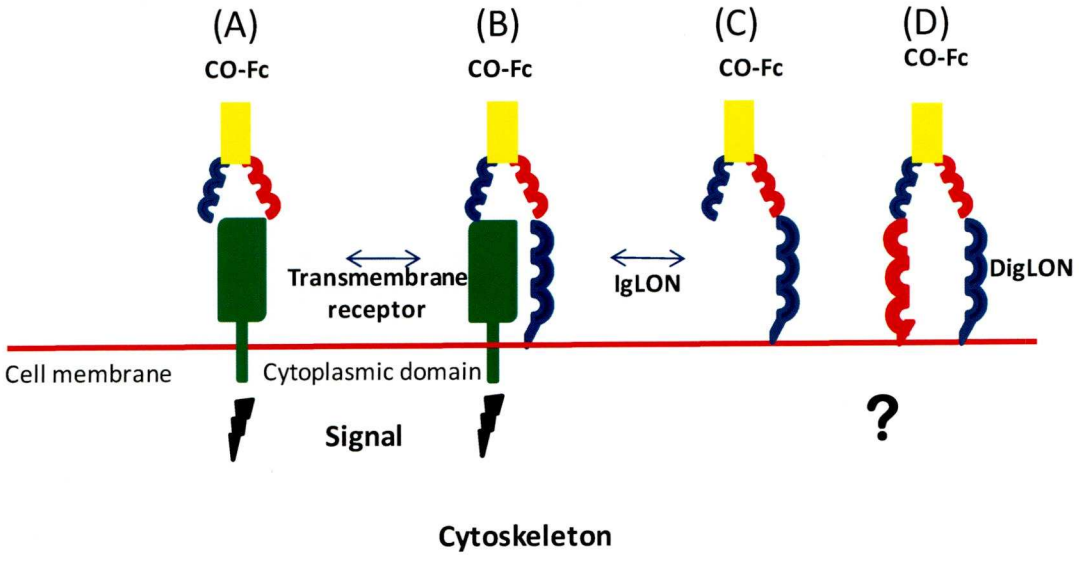

Figure 5.1: Diagram to describe the proposed options for the nature of the putative receptors for CO-Fc heterodimeric protein

A) The first option is that CO-Fc binds a transmembrane receptor with a cytoplasmic domain that initiates the signalling pathway without IgLONs.

B) The second option is that CO-Fc binds to both IgLON and transmembrane receptor that can signal through to the cytoskeleton.

C) The third option is that CO-Fc binds to IgLON alone, however the mechanism of signaling in this case in unknown.

D) The last option that CO-Fc binds to DigLON and the mechanism of signalling is again unknown.

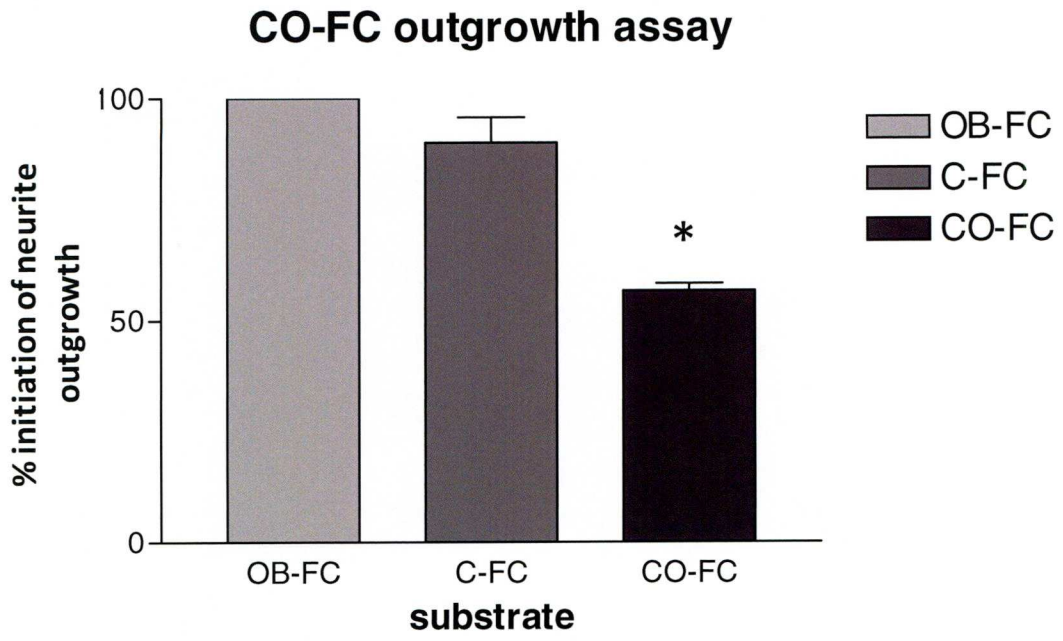

Figure 5.2: CO-Fc inhibits neurites outgrowth from E8 Forebrain neuron

E8 Forebrain neurons were cultured on coated cover slips with L- polylysine (10µg/ml), protein A (100µg/ml) and chimeric proteins OB-Fc (100µg/ml) C-Fc (100µg/ml) and CO-Fc heterodimeric protein (700AU/ml). It was normalised against the higher control (OB-Fc) to 100%. There is a significant difference between CO-Fc, C-Fc and OB-F c (p value<0.05) while no significant difference between C-Fc and OB-Fc (p value>0.05). (n=3) (SEM= OB-Fc 0, C-Fc 5.774, CO-Fc 1.667).*

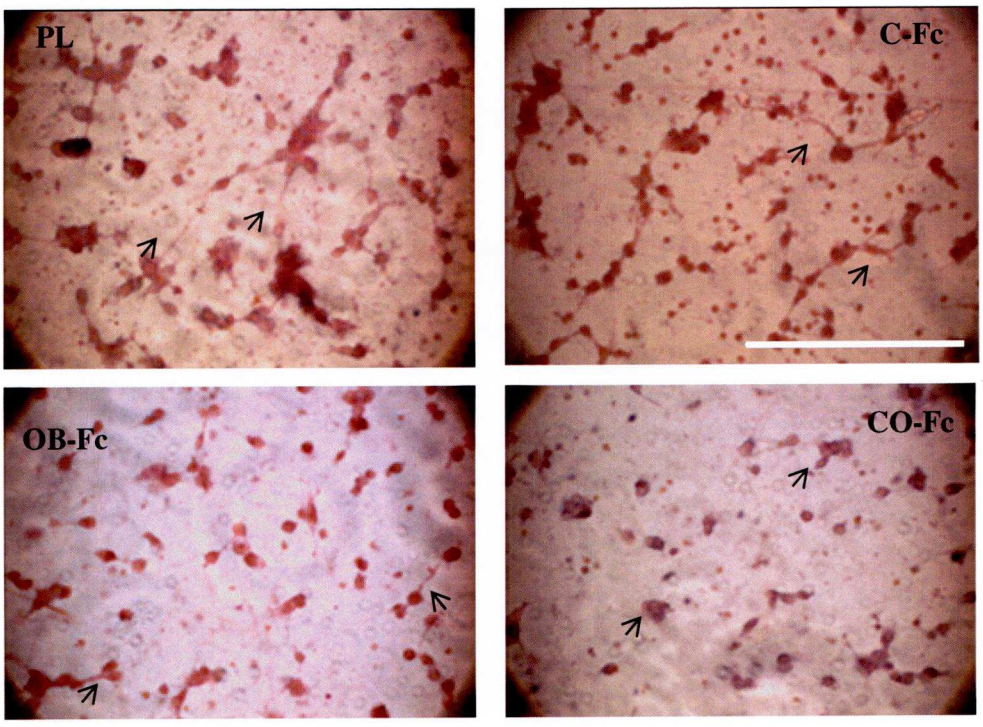

Figure 5.3: E8 Forebrain neurite outgrowth assay

Photomicrographs show that forebrain neurons were cultured on coated cover slips with nitrocellulose, polylysine, protein A (100µg/ml) and standard IgLON chimeric protein; OB-Fc) or C-Fc(C) as well as CO-Fc heterodimeric chimeric protein. CO-Fc inhibits the initiation of their neurites when compared with C-Fc, OB-Fc and PL (scale bar 50µm). 300 cells were counted double blind in three separate microscopic fields.

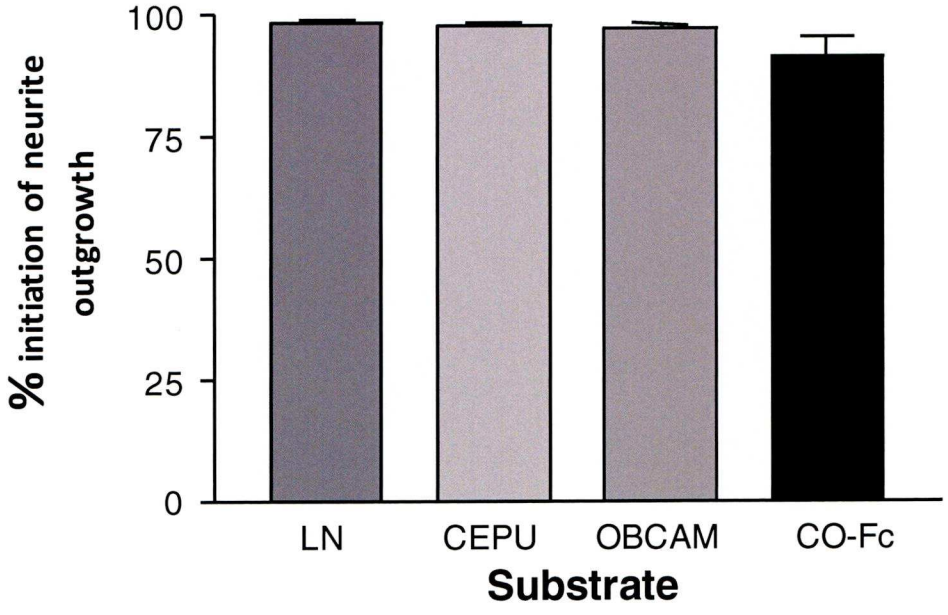

Figure 5.4: CO-Fc does not inhibits neurite outgrowth from E10 dorsal root ganglion neurons (DRG) at low concentration

E10 dorsal root ganglion neurons were cultured on coated cover slips with nitrocellulose, Laminin, protein A (100µg/ml) and chimeric protein C-Fc (100µg/ml), OB-Fc (100µg/ml) and CO-Fc heterodimeric protein (700AU/ml). The 1st bar is for neuron grown on laminin only, the 2nd bar for the neurons grown on C-Fc substrate, the 3rd for neurons grown on OB-Fc substrate. The last bar for neurons were grown on CO-Fc substrate, there was no inhibition of neurite outgrowth. No significant difference between CO-Fc, OB-Fc, C-Fc and LN (p value >0.05).(n=3) (SEM= LN 0.882, C-Fc= 1.202, O-Fc 0.667, CO-Fc 4.177).

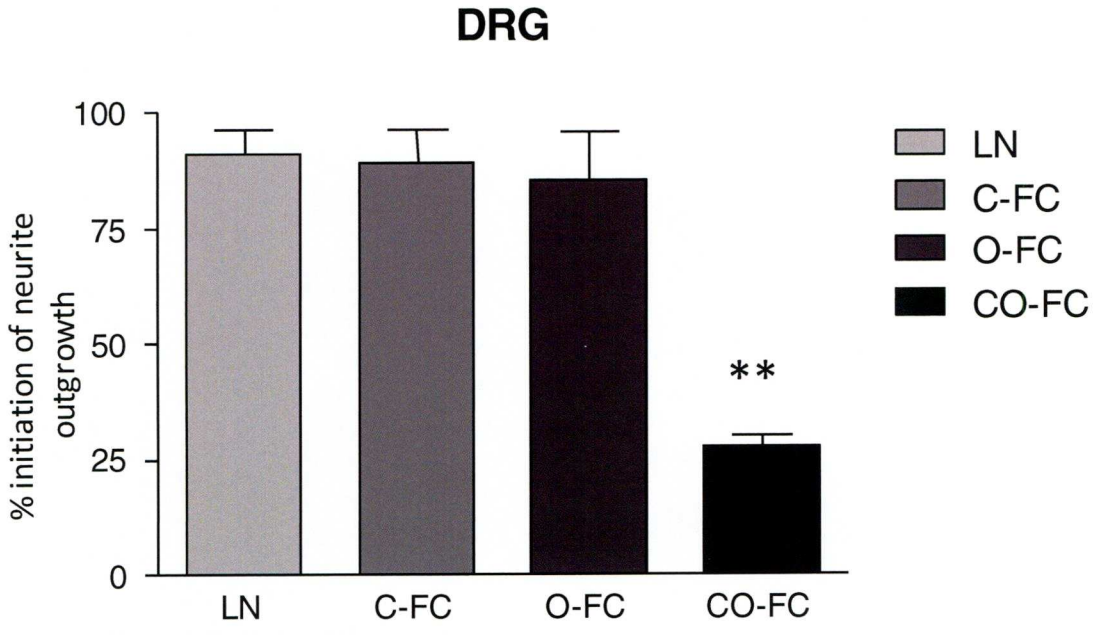

Figure 5.5: CO-Fc inhibits neurite outgrowth from Dorsal root ganglion neurons (DRG) at high concentration

*E10 dorsal root ganglion neurons were cultured on coated cover slips with nitrocellulose, Laminin, protein A (100µg/ml) and chimeric protein C-Fc (100µg/ml), OB-Fc (100µg/ml) and CO-Fc heterodimeric protein (2700AU/ml). The 1st bar is for neuron grown on laminin only; the growth is about 90%, the 2nd for the neurons grown on C-Fc substrate, the 3rd for neurons grown on OB-Fc substrate. The last bar is for neurons were grown on CO-Fc substrate, there was about 75% inhibition of neurite outgrowth. There is a significant difference between CO-Fc and O-Fc, C-Fc and LN (p value<0.01**), while no significant difference between O-Fc, C-Fc and LN (p value>0.05.). (n=3) (SEM= LN 5.568, C-Fc 7.506, OB-Fc 11.015, CO-Fc 2.500).*

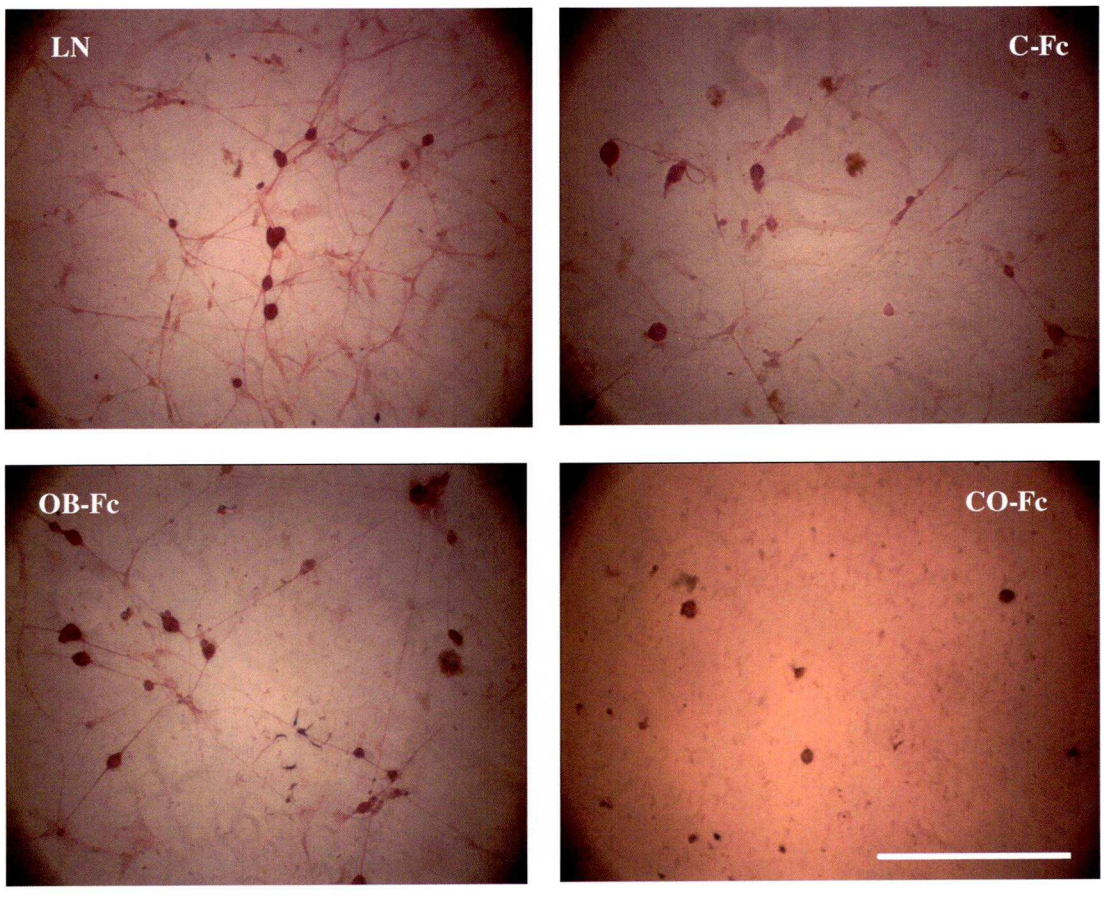

Figure 5.6: E10 DRG neuron outgrowth assay

Photographs show that the initiation of neurite outgrowth from E10 Dorsal root ganglion neurons was inhibited due to the effect of CO-Fc heterodimeric recombinant protein. The standard single chimeric IgLON chimeric proteins such as C-Fc and OB-Fc failed to inhibit while normal growth was observed with Laminin (50μm scale bar).

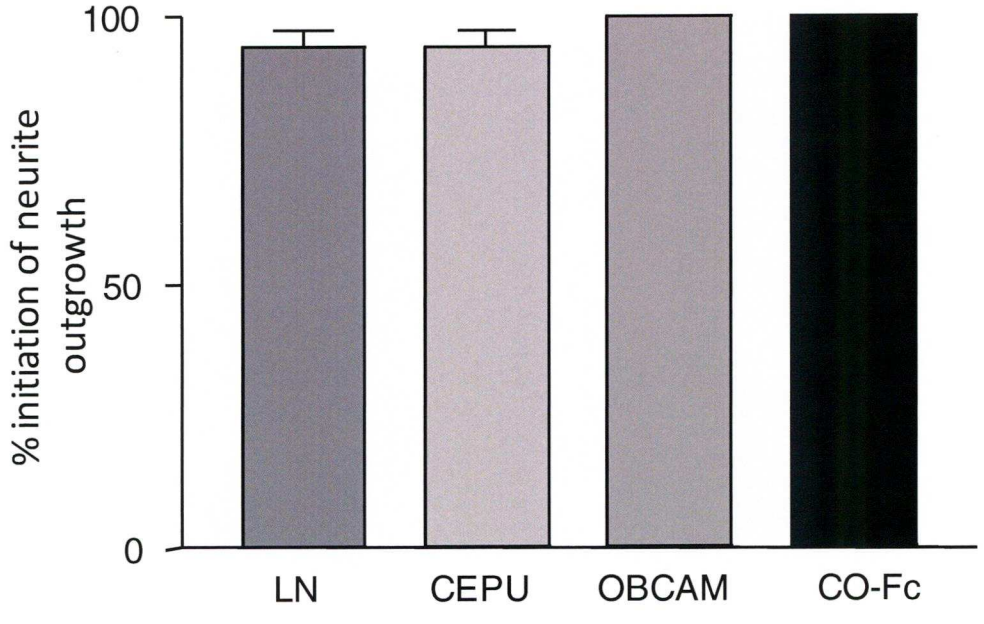

Figure 5.7: CO-Fc does not inhibits neurite outgrowth from E10 Sympathetic neurons at low concentration

E10 Sympathetic neurons were cultured on coated cover slips with nitrocellulose, Laminin, protein A (100µg/ml) and chimeric protein C-Fc (100µg/ml), OB-Fc (100µg/ml) and CO-Fc heterodimeric protein (700AU/ml). The 1st bar is for neuron grown on Laminin only; the growth is about 90%, the 2nd bar for the neurons grown on C-Fc substrate, the 3rd for neurons grown on OB-Fc substrate. The last bar for neurons were grown on CO-Fc substrate, there was no inhibition of neurite outgrowth. No significant difference between CO-Fc, C-Fc, O-Fc and Laminin (p value>0.05) (n=3) (SEM=LN 3.180, C-Fc 3.180, OB-Fc 0, CO-Fc 0).

.

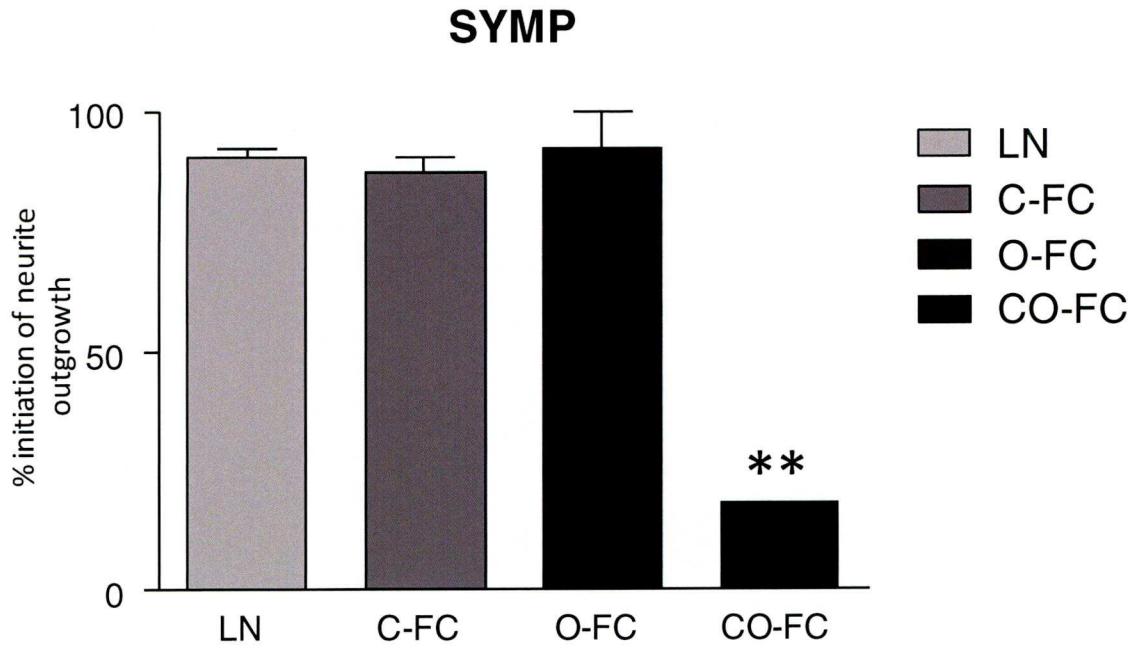

Figure 5.8: CO-Fc inhibits neurite outgrowth from E10 Sympathetic neurons at high concentration

*E10 Sympathetic neurons were cultured on coated cover slips with nitrocellulose, Laminin, protein A (100µg/ml) and chimeric protein C-Fc (100µg/ml), OB-Fc (100µg/ml) and CO-Fc heterodimeric protein (2700AU/ml). The 1st bar is for neurons grown on Laminin only; the growth is about 90%, the 2nd bar for the neurons grown on C-Fc substrate, the 3rd for neurons grown on OB-Fc substrate. The last bar for neurons were grown on CO-Fc substrate, there was about 80% inhibition of neurite. There is a significant difference between CO-Fc, O-Fc, C-Fc and LN (p value<0.01**), while no significant difference between O-Fc, C-Fc and LN (p value>0.05).*

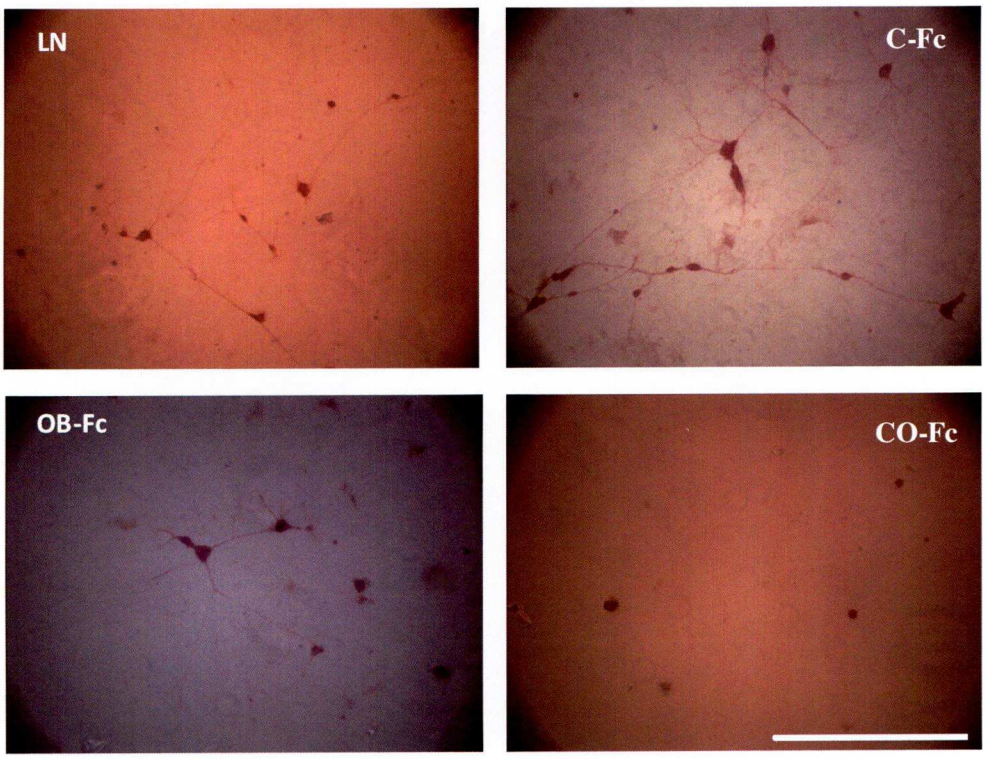

Figure 5.9:E10 Sympathetic neurons outgrowth assay

Sympathetic neurons (E10) were cultured on cover slips that were coated with nitrocellulose, Laminin and IgLON chimeric proteins. The initiation of neurite outgrowth was inhibited with CO-Fc heterodimeric recombinant protein (D). The standard chimeric protein; C-Fc and OB-Fc did not inhibit (B and C) similar to normal growth on Laminin (50μm scale bar).

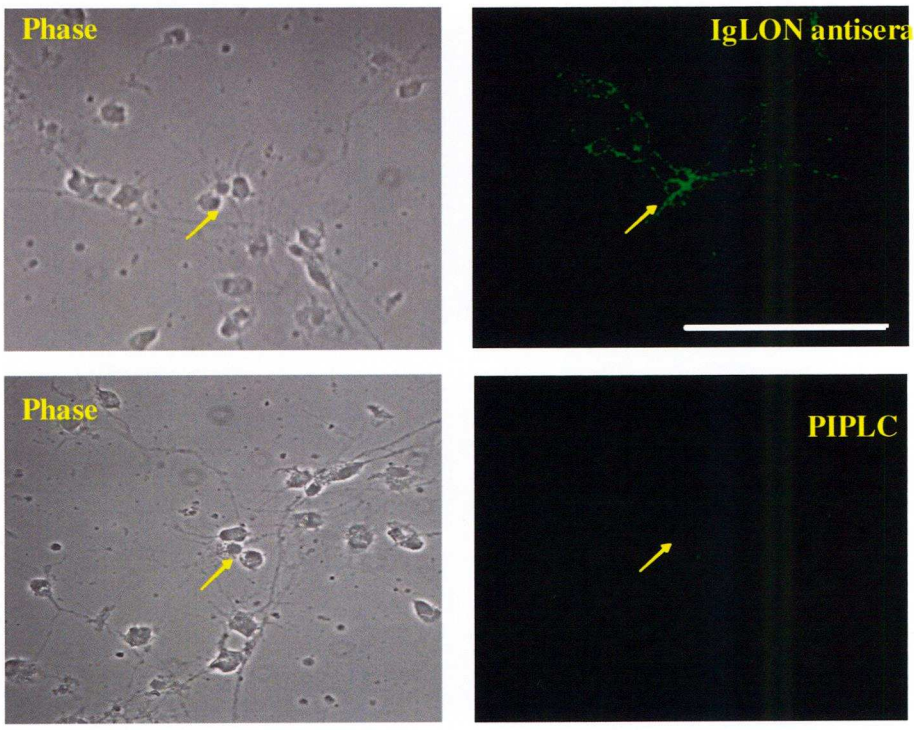

Figure 5.10: E8 Forebrain neurons stained with IgLON antisera Pre and Post PI-PLC treatment

A) E8 chick forebrain neuron were stained with IgLON antisera (1:50) and secondary anti-rat Alexa Fluor 488 (1:200). IgLONs were expressed in cell bodies, axons and dendrites.

B) After PI-PLC treatment of E8 forebrain neurons, no staining with IgLON antisera was observed indicating that IgLONs were now undetectable on the surface of the neurons (scale bar50μm).

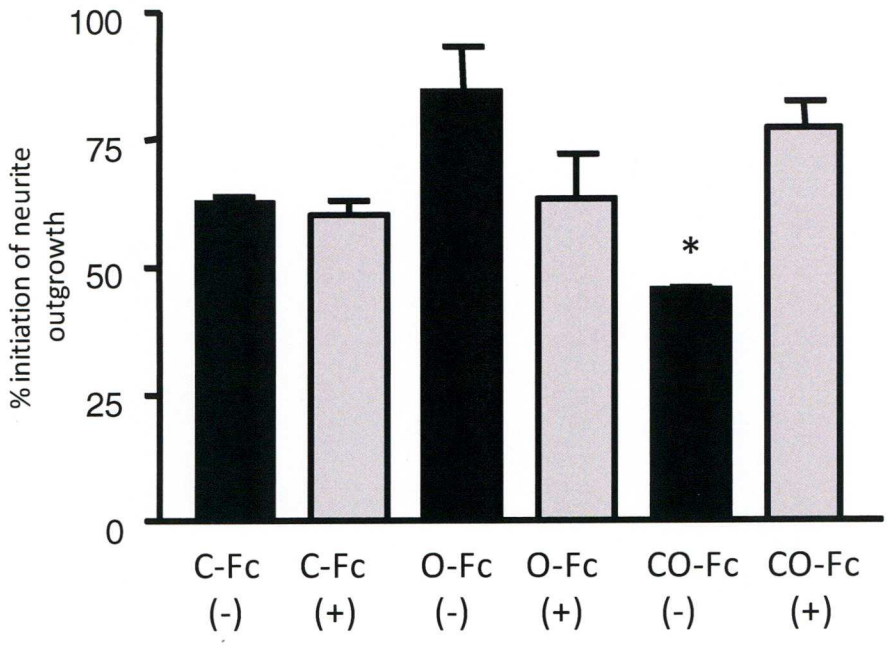

Figure 5.11: Neurite outgrowth assay PIPLC treatment of PI-PLC treated or untreated E8 Forebrain neurons with.

PI-PLC treated and untreated E8 forebrain neurons were cultured on a nitrocellulose, polylysine (10µg/ml), protein A beads (100µg/ml) then coated with either C-Fc, O-Fc (100 µg/ml) or CO-Fc (250AU/ml). The dark bars represent the neurite outgrowth of untreated neurons, while the light bars represent the neurite outgrowth of neurons treated with PI-PLC.

There is a significant difference between CO-Fc (-) (untreated) and CO-Fc (+) (treated ($p<0.01$), while no significant difference was observed between O-Fc (untreated and treated) or C-Fc (untreated and treated) ($p>0.05$). This suggests that GPI-anchored proteins have a role in the formation of the receptor complex for CO-Fc.*

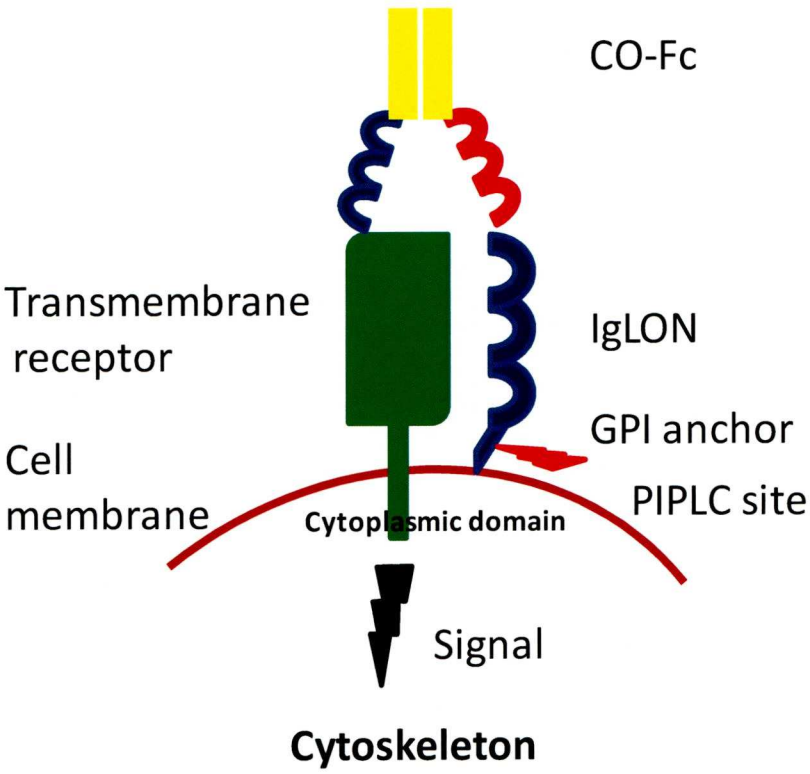

Figure 5.12: Diagram to describe the proposed role of IgLONs in the putative receptor complex for CO-Fc heterodimer

This is an illustration of an IgLON and associated transmembrane receptor in lipid raft in the cell membrane of neuron. The green structure represents a transmembrane receptor with a cytoplasmic domain that could interact with an IgLON to initiate the signalling pathway to the cytoskeleton. Results of PI-PLC treatment suggested that IgLONs have a role in the formation of the putative receptor, either with a transmembrane receptor as shown above or alone.

Chapter Six

The interactions of CO-Fc heterodimeric recombinant protein

INTRODUCTION:

In this chapter, immunofluorescence studies will be used to show the interaction of the CO-Fc heterodimeric chimeric recombinant protein with the IgLONs and/or putative receptor complex on the surface of the cell membrane of neurons, retina frozen sections or other IgLON transfected cell lines.

IgLONs are cell adhesion molecules that are expressed in lipid rafts on the surface of the neurons, and interact with each other either in *cis* and/or in *trans* on the plane of the cell membrane. Binding assay between IgLON-Fc and the corresponding IgLON transfected cell lines have shown that CEPU-1, OBCAM and LAMP have either homophilic or heterophilic trans interactions (Brummendorf et al., 1997; Lodge et al., 2000; Reed et al., 2004). Ntm-Fc (CEPU-1) and OBCAM-Fc interacted heterophilically with LAMP-CHO cells (Gil et al., 2002). No interaction occurred with other Ig superfamily members tested so far such as, N-CAM and contactin recombinant-Fc protein. CO-Fc heterodimer complex can be used to investigate the interaction between a putative DigLON, as it is formed of CEPU-1 head and OBCAM-Fc head held together at the disulfide bridge of human IgG Fc tail and specific IgLONs/DigLONs.

The CO-Fc complex could interact with IgLONs expressed on the surface of the neurons. However, a transmembrane receptor may be required to form a receptor complex in order to signal to the cytoskeleton.

Anti-myc or anti-V5 antibodies can be used to detect the binding of the CO-Fc complex, but because there is a mixture of CO-Fc heterodimeric, OO-Fc and CC-Fc homodimeric recombinant proteins anti-myc was preferred to be used to detect CO-Fc heterodimeric protein and not anti-V5 antibody. This is because previous work showed that OBCAM binding is weak. While it revealed strong binding of CEPU-1.

Based on the results in previous chapter, IgLONs may act as a part of the putative receptor complex for the CO-Fc heterodimer protein. Therefore, immuno-staining of neurons after PI-PLC treatment will be used to support the hypothesis of role of IgLONs in formation of the receptor complex. Because the contaminating O-Fc precludes the absolute certainty that the binding observed with the anti-myc antibody is solely due to the CO-Fc, preliminary FRET experiments will be carried out to try to confirm the specific binding of CO-Fc to retina.

The aim of FRET is to distinguish between the binding of CO-Fc heterodimeric recombinant protein which is tagged with both myc and V5 epitope tags, and either OO-Fc or CC-Fc homodimeric recombinant proteins which are tagged by either two myc tags or two V5 tags.

FRET can be used to specifically detect CO-Fc because of the proximity between the myc and V5 tags. Direct labelling V5 with anti-V5 Alexa 488 and myc with anti-myc Alexa 555 will result in FRET while single O-Fc or C-Fc will not. It is important to confirm that a mixture of both O-Fc and C-Fc will not result in FRET.

Material and Methods:

The materials that are required for FRET experiment are anti-V5 Alexa Fluor 488-labelled antibody as donor (ABD serotec) and anti-myc Alexa Fluor 555 labelled as acceptor antibody (Millipore). There is an overlap between the emission of the donor and the excitation of the acceptor (figure 6.11a). The R_0 for both antibodies fluorphors is 7nm at which about 50% of the energy that initiated by the excitation of the donor will be transferred to the adjacent fluorphor which will result in excitation of the acceptor (figure6.11 b).

Transient transfection of CHO cells in 15cm dishes at cell count $1x10^7$ cell/ml in 5% FCS with either pcDNA6-CEPU-Fc-V5 or pBudCE4.1-OBCAM-myc endotoxin free plasmid (1μg/μl) was carried out using TransIT (Mirus) transfection reagent. The transfection efficiency was 60% and the medium was changed to low IgG medium which incubated for one week before collection of the supernatant of each transfection. Concentration of the supernatants was carried out by spin columns (Sartorius) 10 times.

FRET between the two fluorphors was measured using FRET package on the Leica (DM IRE2) confocal microscope. The fluorescence of the Alexa 488 (donor) and the Alexa Fluor 555(acceptor) was measured, and then the acceptor was bleached and the fluorescence of the donor was measured again. The increase in donor fluorescence was a measure of the FRET that had occurred initially.

In order to measure the ratio of energy transfer between two fluorphors for CO-Fc, live staining of LAMP CHO cells was carried out using anti-V5 Alexa Fluor as donor and anti-myc Alexa Fluor 555 as acceptor with either CO-Fc or a mixture of both CC-V5 and OO-myc recombinant proteins. Bleaching anti-myc Alexa Fluor 555 (acceptor) will allow the anti-V5 Alexa Fluor 488 (donor) to become brighter than

before bleaching due to the 50% (if R_0=7nm) of energy that was going to be transferred to the acceptor will be emitted by the donor due to close proximity between V5tag and myc tag of CO-Fc. In the case of CC-V5 and OO-myc mixture, no FRET was expected to occur due to distance between two fluorphors. No change will occur between the emission of the donor before and after the bleaching of the acceptor (figure 6.12).

The following equation is required to measure the ratio of FRET:

$$FRET = \frac{\mathrm{D}post - \mathrm{D}pre}{\mathrm{D}post}$$

RESULTS:

In this chapter, the interaction of CO-Fc heterodimeric chimeric recombinant protein was investigated by immunofluorescence studies with different types of cells and tissues. CO-Fc heterodimeric recombinant is contaminated with OO-Fc and CC-Fc homodimeric recombinant proteins. Anti-myc antibody was used to detect the interaction of the CO-Fc; however, OO-Fc will be detected as well due to the presence of the epitope myc tag in both proteins. It was important to perform control experiments with OO-Fc alongside the CO-Fc, and the concentration used in these experiments was based on the western blot that estimated the concentration of the total Fc recombinant proteins in CO-Fc to the concentration of either C-Fc or O-Fc single recombinant proteins (figure 4.18 a, b).

E8 chick forebrain neurons were stained with single recombinant chimeric proteins; CEPU-Fc and OBCAM-Fc (10μg/ml) (control), CEPU-Fc was brighter than OBCAM-Fc (figure 6.1). In figure 6.2, CO-Fc heterodimeric bound to the surface of E8 chick forebrain neurons when live stained with CO-Fc using mouse anti-myc antibody to detect the myc tag on the CO-Fc heterodimer complex. The single standard chimeric protein, CEPU-Fc and OBCAM-Fc were tested by live staining of

E10 dorsal root ganglion and sympathetic chain neurons, there was staining with CEPU-Fc using anti-human Fc fluorescent labelled antibody (figure6.3a), whereas no staining occurred with OBCAM-Fc (figure6.3b). Interestingly, CO-Fc heterodimeric protein (1300AU/ml) bound to small fraction of E10 dorsal root ganglion and sympathetic chain neurons when detected with the anti-myc antibody while no glial cells stained with CO-Fc (figure6.4) (figure 6.5).

In conclusion, CO-Fc may bind to E8 forebrain (but this is not conclusive because O-Fc bound also). The evidence that CO-Fc binds to E10 dorsal root ganglion and E10 sympathetic neurons is stronger e, while OO-Fc did not bind to E10 dorsal ganglion neurons or sympathetic neurons.

Chick retina is a well-characterised site for expression of IgLONs, as they are expressed in different layers of the retina. LAMP and Neurotractin are co-expressed in both outerplexiform and inner plexiform layers, while CEPU-1 is expressed only in the outerplexiform layer and OBCAM in the inner plexiform layer of the retina at E18 age (Lodge et al., 2000).

The retina could be an interesting site for interaction of the putative CO-Fc heterodimer complex. In figure 6.6, the structure of the retina is described which is formed of 10 layers comprised of different types of cells. Prefixed frozen sections of E18 chick retina were stained with CO-Fc heterodimeric protein (1300AU/ml). The outer plexiform and inner plexiform layers of the retina were the prominent areas for the binding of CO-Fc and C-Fc single recombinant protein, while O-Fc single recombinant protein bound prominently to the outer plexiform layer of the retina with weak binding to the inner plexiform layer (figure 6.7).

IgLONs could be a part of the putative receptor complex for the CO-Fc heterodimeric chimeric protein. Therefore, CEPU-CHO, OBCAM, LAMP-CHO,

CL-CHO and CO-CHO alongside wild type CHO cells were live stained with CO-Fc to investigate its interaction with GPI anchored IgLONs or DigLONs (figure6.8). CO-Fc was detected by mouse anti-myc antibody and Alexa Fluor 488 secondary antibody on the surface of IgLON transfected CHO cells except CO-CHO cells while no staining of wild type cells was observed.

In the previous chapter, CO-Fc heterodimeric protein failed to inhibit the neurite outgrowth from E8 forebrain neurons in the absence of IgLONs after successful PI-PLC treatment of E8 forebrain neurons (figure 6.9). Furthermore, treated and untreated E8 forebrain neurons were stained with anti-CEPU, anti-OBCAM or anti-LAMP anti-sera to ensure that no more IgLONs exist on the surface of the neurons. The staining that occurred without the treatment disappeared after the treatment with PI-PLC (figure6.8) which confirmed the removal of IgLONs from the surface of the neurons (figure6.9). Interestingly, CO-Fc did not bind to the surface of the neurons following treatment with PI-PLC (figure6.9). This suggested that IgLONs, as GPI anchored proteins might be part of the putative receptor for CO-Fc heterodimer complex.

Fluorescence resonance energy transfer (FRET):

A key requirement to confirm the observation about CO-Fc putative binding to forebrain neurons is to show that the results observed are due specifically to CO-Fc and not to OO-Fc. One method to do this is to use FRET to distinguish between OO-Fc and CO-Fc binding. The first step is to test the fluorphors of each antibody before FRET experiment. In figure 6.13a, LAMP CHO cells were live-stained with CC-Fc-V5 recombinant protein, anti-mouse anti-V5 antibody and anti-mouse Alexa Fluor 488. Indirect immunofluorescence was used because the directly labelled anti-V5Alexa Fluor 488 did not work properly. There is an excitation at 488nm and emission at 520nm wavelength, but little emission at 580nm the peak of the acceptor emission. The directly labelled mouse anti-myc Alexa Fluor 555 bound to the myc epitope tags of OO-myc recombinant protein when used in live staining of LAMP CHO cells. The fluorphor was excited at 488nm whereas no emission at 580nm was observed, there was an emission at 580nm when the fluorphor excited at 560nm (figure 6.13b). Thus, the two fluorphors were appropriate to use for FRET experiment.

In addition, a positive control also required to ensure that the FRET technique is going to work when used with CO-Fc recombinant protein on LAMP CHO cells. The ratio of energy transfer will be measured between the mouse anti-myc Alexa Fluor 555 antibody as acceptor and anti-mouse Alexa 488 antibody as donor when bound to single OO-myc recombinant protein on LAMP CHO cells. In figure 6.14a and b, photographs for live stained LAMP CHO cells with single OO-myc recombinant protein that shows the emission of the acceptor (AF555) at 580nm and emission of the donor (AF488) at 520nm before bleaching of the acceptor. The edge of LAMP CHO cell was selected to bleach the acceptor (green rectangular) at 60 %.

No emission of the acceptor was detected at 580nm due to bleaching of the acceptor, while the donor becomes brighter than before bleaching when excited at 488nm because the energy was emitted rather than transferred to the already bleached acceptor (Figure 6.14c, d). In figure 6.14e, a photograph shows the brightness of the donor after bleaching the acceptor. The FRET ratio was variable according to the area and the intensity of bleaching and R_0 between the fluorphors. The maximum ratio of FRET that measured between two fluorphors was about 20% in this case. In figure 14 f, a diagram clarifies the mechanism of the positive control.

DISCUSSION:

The interaction of CO-Fc heterodimeric chimeric recombinant protein with putative receptors on the surface of forebrain and dorsal root ganglion and sympathetic neurons can be detected either with anti-human Fc which will detect the OO-Fc and CC-Fc beside CO-Fc. While using anti-V5 antibody will detect only CO-Fc and CC-Fc which is known to bind strongly to neurons and its concentration is high in the mixture of CO-Fc. The advantage of using anti-myc antibody is that will detect CO-Fc and OO-Fc which has weak binding to the neurons in addition to the point that the contamination caused by OO-Fc is not abundant in the mixture of CO-Fc. Therefore, the chance of detection of CO-Fc heterodimeric recombinant protein with anti-myc antibody is greater than using anti-V5 or anti-human Fc antibodies. However, CEPU-Fc standard chimeric protein bound to E10 DRG and sympathetic neurons using anti-human Fc antibody while OBCAM-Fc did not, suggesting that anti-myc was detecting the CO-Fc heterodimeric protein and not the OO-Fc homodimeric protein.

Data so far suggests that CO-Fc binds to IgLONs since different layers of the retina expressed different combinations of IgLONs. CO-Fc bound to the outerplexiform layer of E18 chick retina where LAMP, CEPU-1 and Neurotractin were expressed (Lodge et al., 2000) (Sahar Youssef PhD thesis University of Liverpool 2007). This data suggests that there might be interactions between CO-Fc and either LAMP, CEPU-1 or Neurotractin or combinations in the form of DigLONs.

The next experiment investigated the interaction of CO-Fc heterodimeric protein with different IgLON transfected cell lines; CEPU-1, OBCAM, LAMP, CO, CL or wild type CHO cells as control. This was carried out to clarify binding of IgLONs or DigLONs with CO-Fc heterodimeric recombinant protein. There was an

interaction between the CO-Fc with different cell lines with variable degree of staining using anti-myc antibody. However, OO-Fc might be detected with anti-myc as well that may explain the interaction with LAMP-CHO cells which should not interact with CO-Fc such as LAMP-Fc that did not bind to CO-Fc CHO cells. Surprisingly, CO-Fc did not bind to CO-CHO cells but did bind to CL-CHO cells. This is might be due to unbalanced expression of either LAMP or CEPU-1 on the surface of the CL-CHO cells or heterophilic interactions between DigLONs.

The loss of staining with CO-Fc heterodimeric protein due to removal of IgLONs from the surface of the neurons by PI-PLC treatment supported the result in the previous chapter, that CO-Fc did not inhibit the neurite outgrowth after the PI-PLC treatment as before the treatment. These results suggested the idea that IgLONs has a role in the formation of the putative receptor either alone or forming a complex with a transmembrane receptor.

The previous data suggested that CO-Fc interacts with putative receptors on the surface of the neurons. IgLON could be a part of this receptor. However, IgLONs do not have a cytoplasmic domain. Thus, IgLON plus a transmembrane receptor could form the putative complex receptors for the CO-Fc heterodimeric chimeric recombinant protein.

The presence of OO-Fc may interfere with these results making their interpretation difficult; therefore, we considered alternative ways of detecting CO-Fc binding alone.

The experiments also confirm that Alexa 488 and Alexa555 are suitable fluorphors for FRET and that direct labelling of the myc and V5 tags on CO-Fc with these fluorphor coupled antibodies should allow the measurement of FRET between them. It is unlikely that the indirectly labelled tags will result in the fluorphors being

close enough for FRET. Hence, it will be necessary to ensure that an anti-V5 Alexa Fluor 488 is obtained that labels CO-Fc directly. Completion of these experiments on forebrain neurons and retina will provide final confirmation that CO-Fc can bind to the surface of neurons

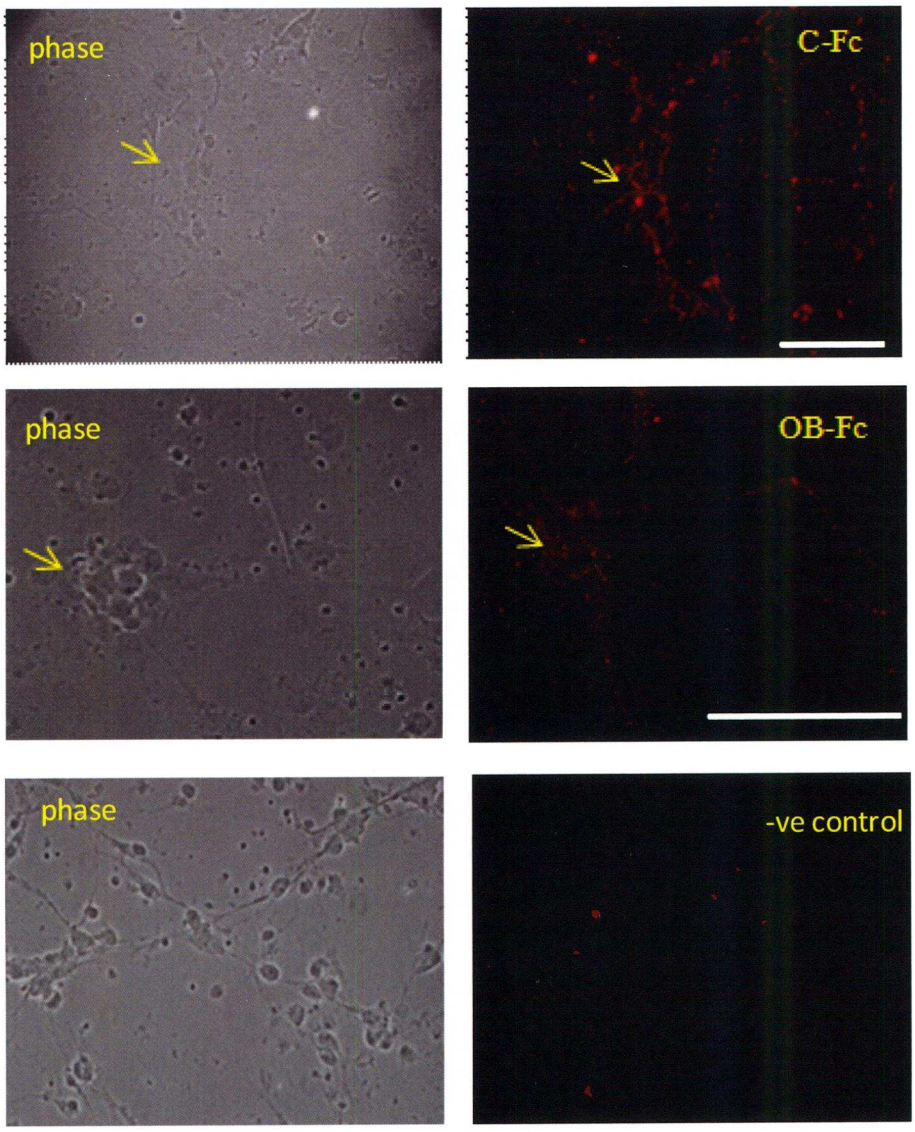

Figure 6.1: E8 Forebrain neurons stained with CEPU-Fc and OBCAM-Fc single standard chimeric proteins

E8 chick Forebrain neurons were stained with CEPU-Fc and OBCAM-Fc single standard chimeric proteins (10µg/ml). Antihuman Fc fluorescent labelled antibody (1.5mg/ml) (1:100) was used as secondary antibody. CEPU-Fc stained relatively brighter than OBCAM-FC. There was no staining in the negative control (Scale bar 50µm).

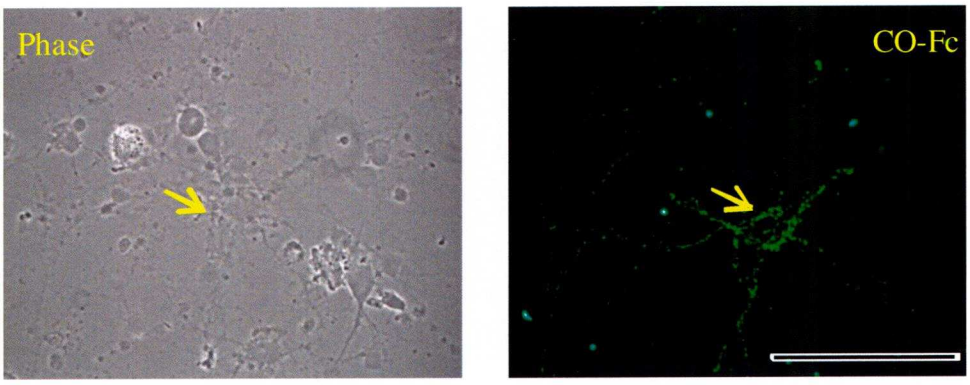

Figure 6.2: CO-Fc binds to E8 Forebrain neuron

A subset of E8 chick forebrain neurons were stained with CO-Fc heterodimeric chimeric protein (1333AU/ml). Primary mouse anti-myc (1mg/ml) (1:50) was used to detect CO-Fc and secondary antimouse Alexa Fluor 488 antibody (1:200). Cell bodies, axons and dendrites were stained (scale bar50μm).

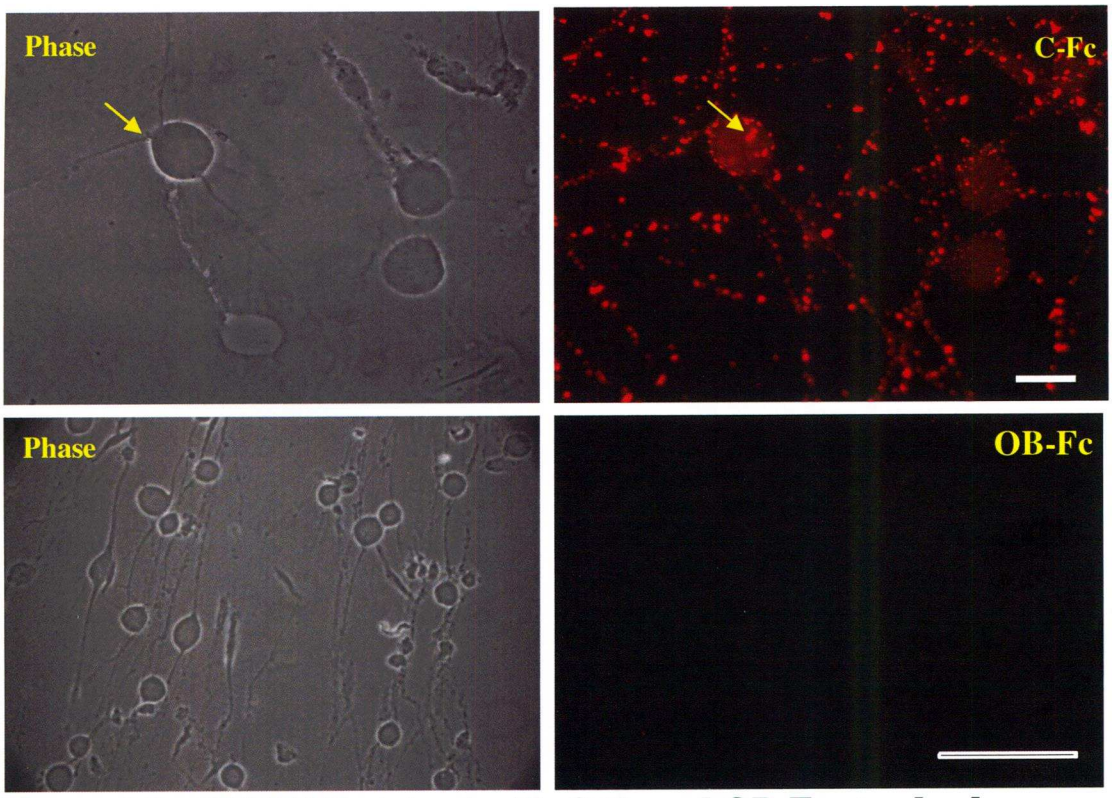

Figure 6.3.: E10 DRG stained with C-Fc and OB-Fc standard chimeric protein

E10 Dorsal root ganglion neurons were stained with CEPU-Fc standard single IgLON chimeric protein (10µg/ml) and OBCAM-Fc standard IgLON chimeric protein (10µg/ml). Secondary anti-human Fc fluorescent-labelled antibody at (1:100) was used. The neurons were stained with CEPU-Fc but not OBCAM-Fc. (50µm scale bar).

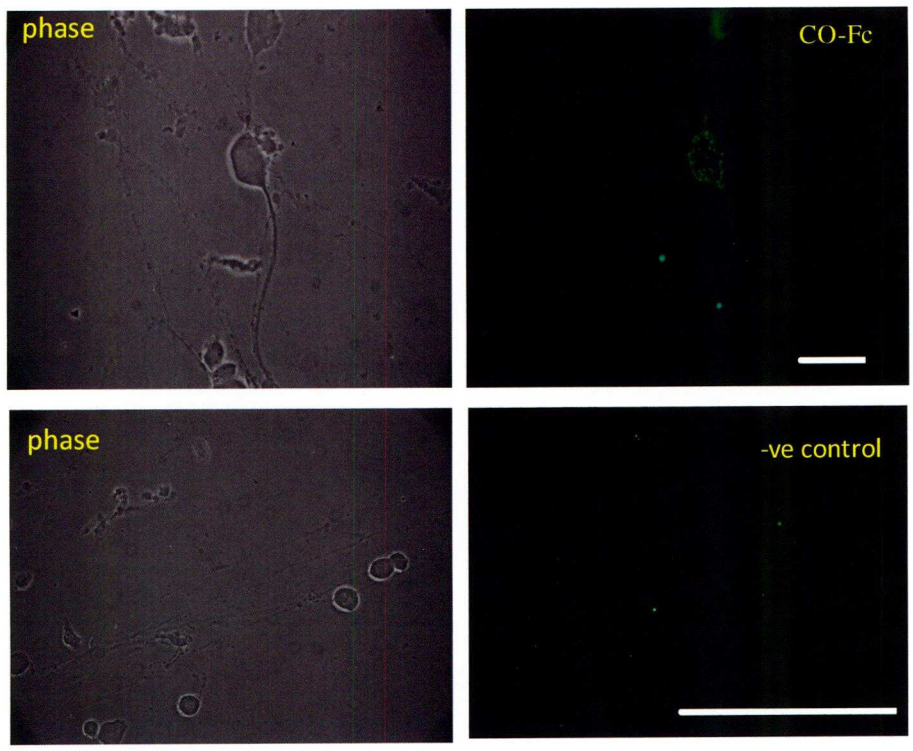

Figure 6.4: CO-Fc binds to E10 dorsal root ganglion (DRG)

CO-Fc heterodimeric chimeric recombinant protein (1300AU/ml) was used to stain E10 chick dorsal root ganglion neurons. Mouse anti-myc antibody as primary antibody (1:50), and secondary antimouse Alexa Fluor 488a antibody (1:200) were used. Both cell body and axon were stained (10μm scale bar).No staining in negative control (50μm scale bar).

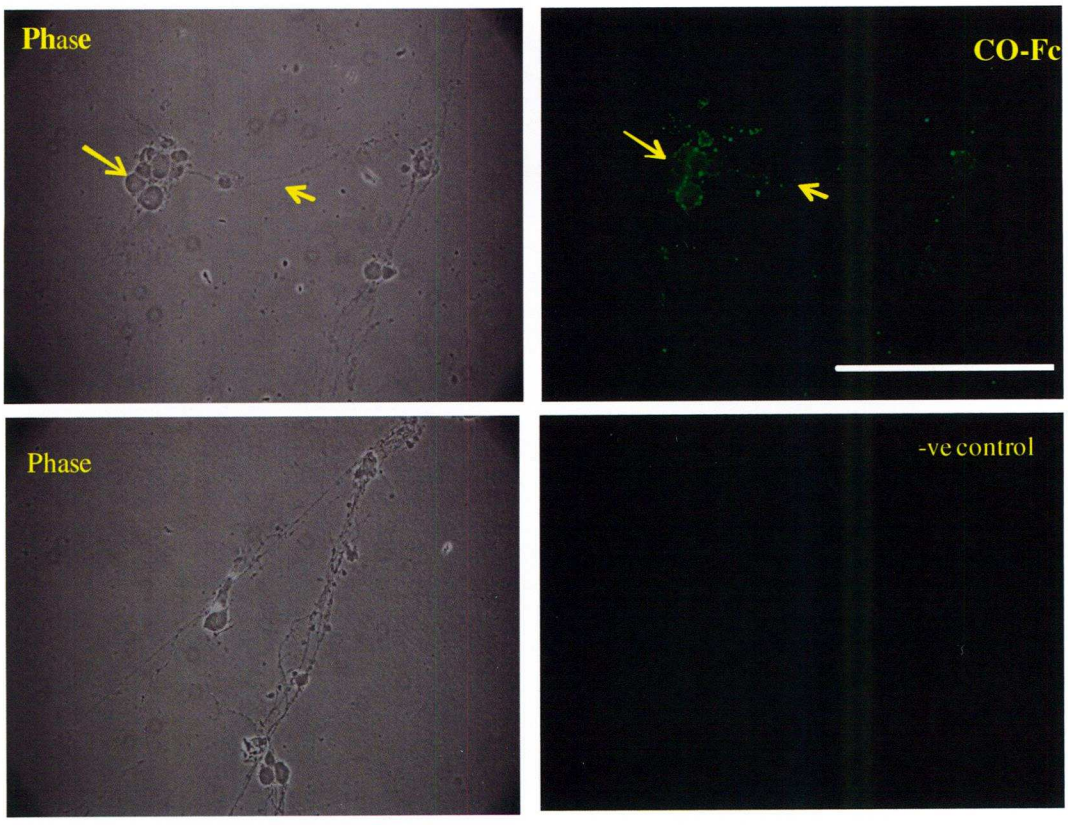

Figure 6.5: CO-Fc binds to E10 Sympathetic chain neurons

Photographs (phase and fluorescence) for E10 chick sympathetic neurons, all the neurons in the field were stained with CO-Fc protein (1300AU/ml) and primary mouse antimyc antibody (1mg/ml) (1:50), then secondary antimouse Alexa Fluor 488 (1:200). Both cell body and axons were stained. There was no staining in negative control (Scale bar 50μm).

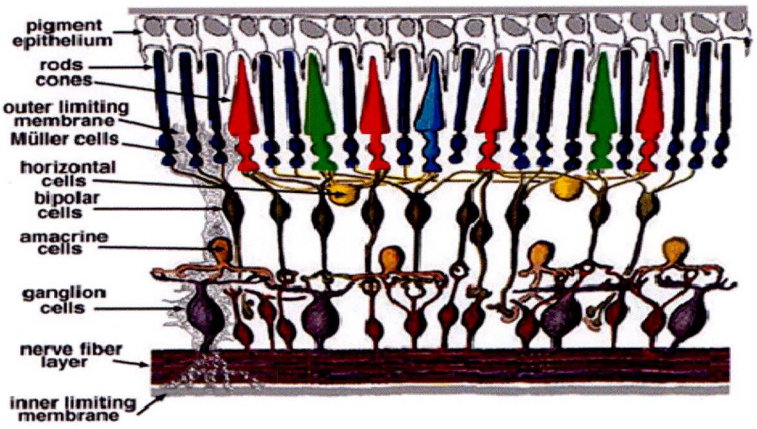

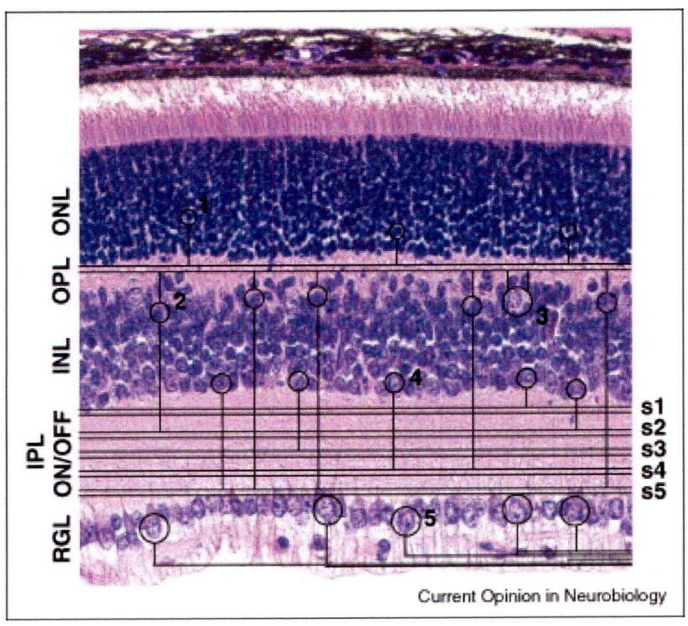

Figure 6.6: The structure of the retina

diagram and H&E stain cross section describes the structure of the retina which is composed of the pigmented epithelium, outerplexiform layer which contains rods and cons, Muller cells, horizontal cells, bipolar cells, amacrine cells, ganglion cells, nerve fibre layer and inner plexiform layer.

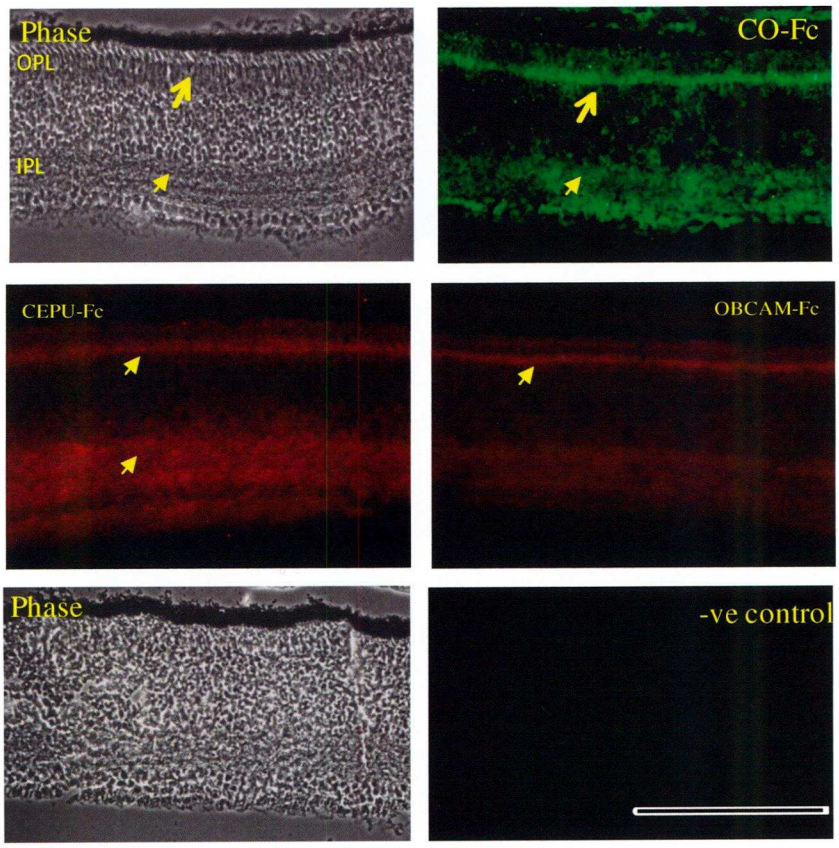

Figure 6.7: CO-Fc binds to the outerplexiform layer of the retina

E18 chick retina frozen section photographs (phase and fluorescence) which was stained with the CO-Fc heterodimeric protein (1333AU/ml) using mouse antimyc antibody (1:50) and antimouse Alexa Fluor 488 antibody (1:200). CO-Fc binds to the outerplexiform layer and inner plexiform layer (OPL, IPL) of the retina, as CEPU-Fc (10µg/ml), while OBCAM-Fc (10µg/ml) stained outerplexiform layer and faint staining in inner plexiform layer. Secondary anti-Fc fluorescent-labelled was used with single IgLON recombinant proteins (1:100).

Fluorescence photographs show no staining for a negative control using antimyc antibody (1:50) and antimouse Alexa Fluor 488 antibody (1:200 (50µm scale bar).

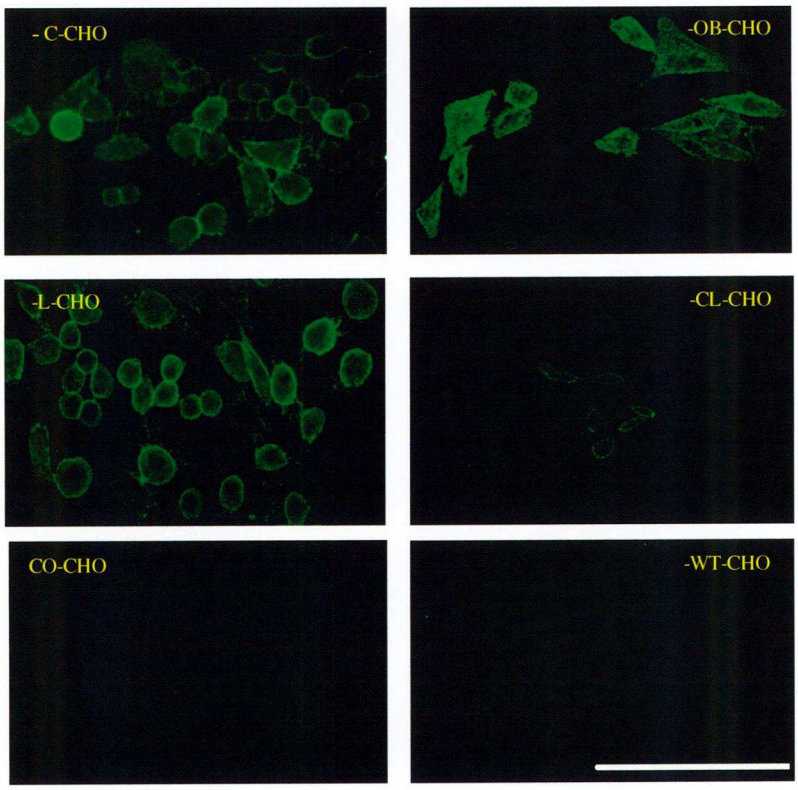

Figure 6.8: CO-Fc interacts with IgLONs transfected cell lines

CO-Fc heterodimeric protein (1300AU/ml) was used to test its interaction with different IgLON transfected cell lines. Anti-myc was used to detect the CO-Fc on the surface of the transfected CHO cells (1:50). Alexa Fluor 488 used as secondary antibody (1:200). CO-Fc binds to CEPU-CHO, OBCAM-CHO, LAMP-CHO and CL-CHO cells, but, it does not bind to CO-CHO or wild type CHO cells (scale bar 50 μm).

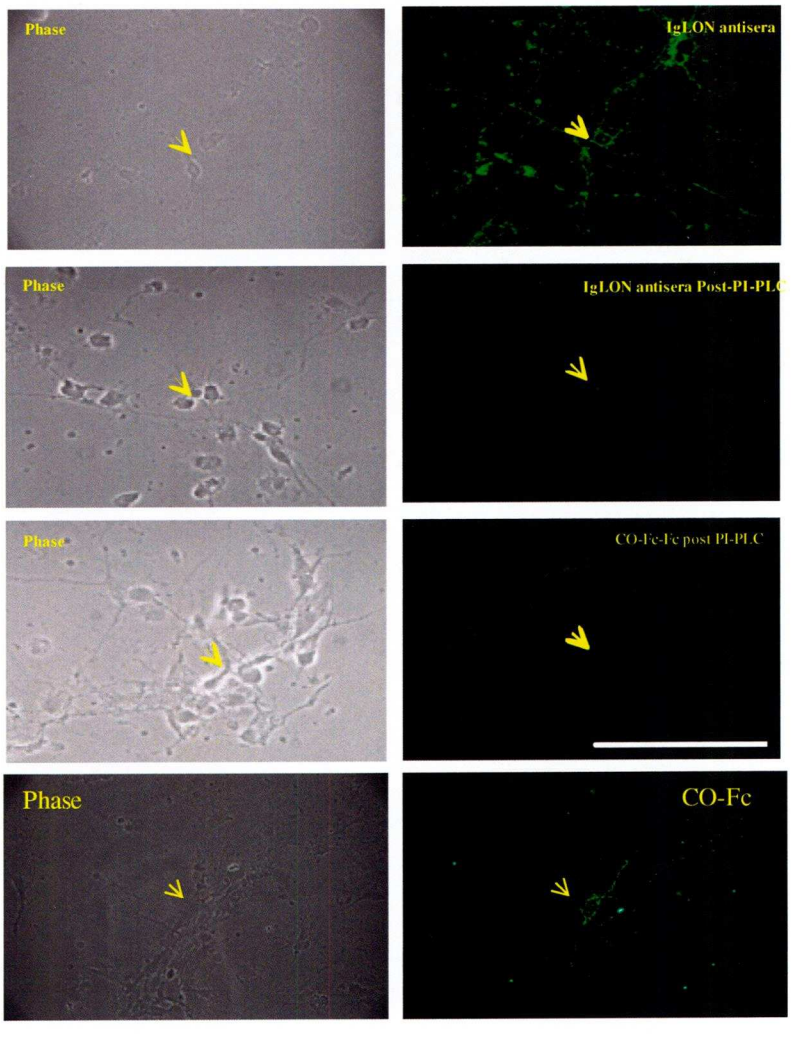

Figure 6.9: Loss of binding of CO-Fc after treatment with PIPLC

E8 Forebrain neurons stained with IgLON antisera pre and post PIPLC treatment (anti-CEPU-1, anti-OBCAM and anti-LAMP) at (1:50). Alexa Fluor 488 secondary antibody was at (1:200) used. Post PIPLC staining with IgLON antisera confirmed that no IgLONs on the surface of the neurons. At the same experiment, E8 forebrain neurons stained with CO-Fc(1333AU/ml) after treatment with PIPLC, CO-Fc binds to untreated neurons, but did not bind to the treated neurons with PI-PLC (scale bar 50μm).

	C-Fc	OB-Fc	CO-Fc
E8 Forebrain	staining	Faint staining	Staining
E10 DRG	staining	No staining	Staining
E10 Sympathetic	staining	No staining	Staining
E18 Retina	Staining OPL-IPL	Staining OPL –faint IPL	Staining OPL-IPL
CEPU-CHO	Staining	staining	staining
OBCAM-CHO	Staining	Faint staining	staining
LAMP-CHO	Staining	Staining	staining
CL-CHO	N/A	N/A	Few cell stained
CO-CHO	No staining	No staining	No staining
WT-CHO	No staining	No staining	No staining

Table6.10: summary table for interactions of CO-Fc in comparison to C-Fc and OB-Fc

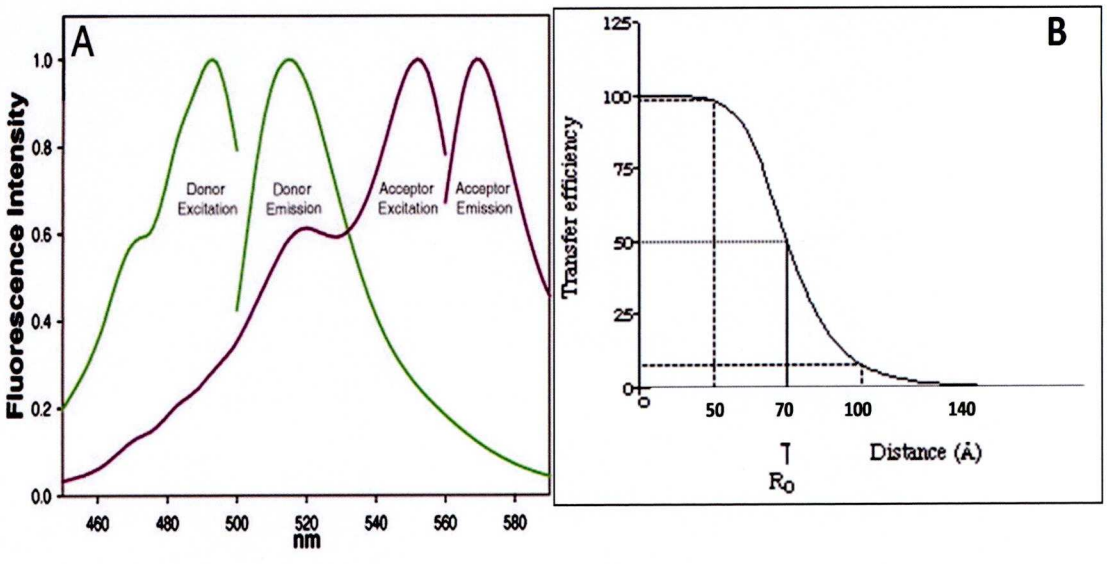

Figure 6.11: The method of Fluorescence resonance energy transfer (FRET):

A) A diagram describes the relation between the fluorescence intensity and the wavelength and excitation and the emission of the donor which overlapping with excitation of the acceptor. There will be an energy transfer between the donor and the acceptor (FRET).

B) A curve represents the R_0 for Alexa Four 488 and Alexa Fluor 555 at which 50% of energy transfer at 70Å that is equal 7nm.

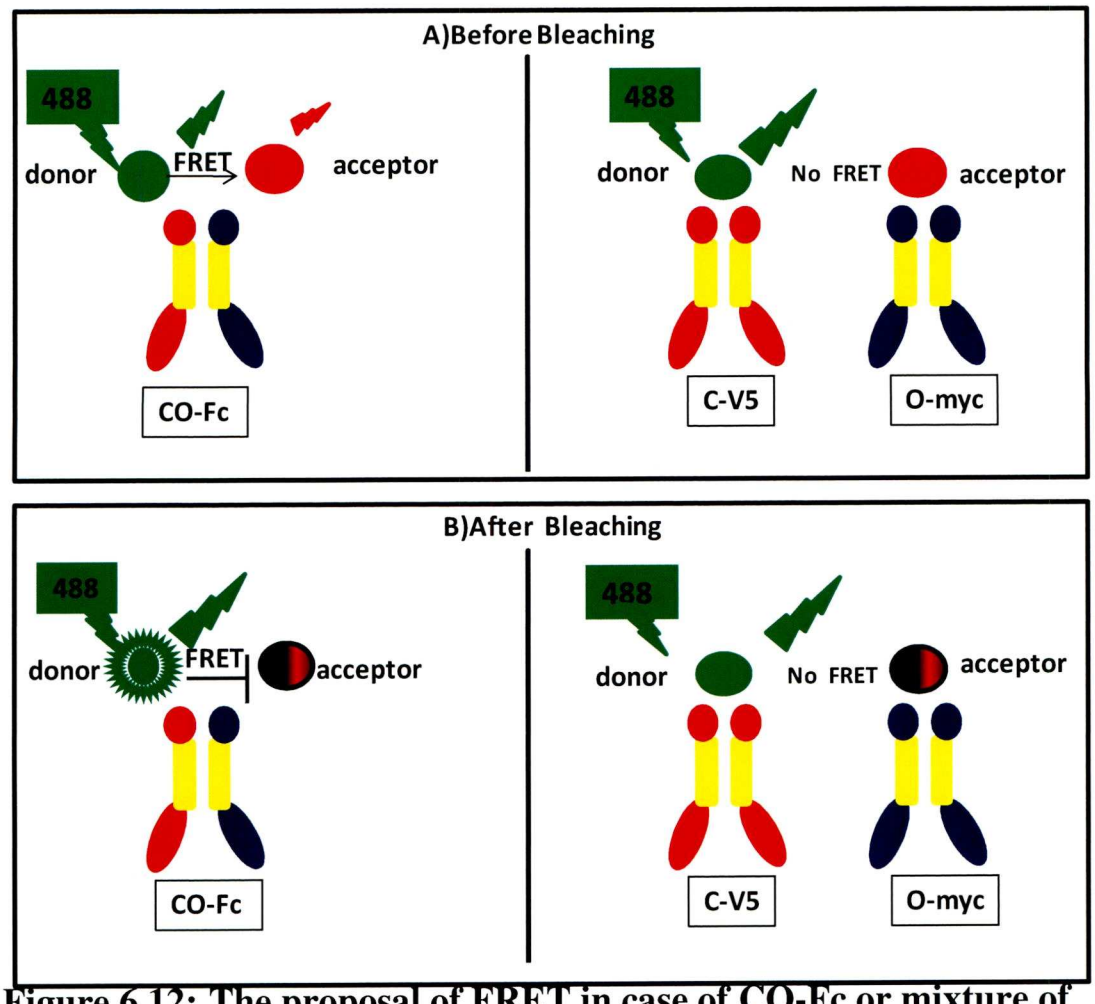

Figure 6.12: The proposal of FRET in case of CO-Fc or mixture of C-V5 and O-myc recombinant proteins:

A) Before bleaching the acceptor, when the donor is excited at 488nm, 50% of the energy will emit at 520nm and 50% will transferred to the acceptor in case of CO-Fc heterodimeric recombinant protein at close proximity. While in case of the mixture of CC-Fc-V5 and OO-Fc-myc, 100% of energy will emits at 520nm.

B) After Bleaching of the acceptor, 50% of energy will emits at 520nm plus 50% that was going to be transferred to the acceptor but due to bleaching which will lead to increase the brightness of donor more than before bleaching. While in case of the mixture the emission is equal to the emission before bleaching.

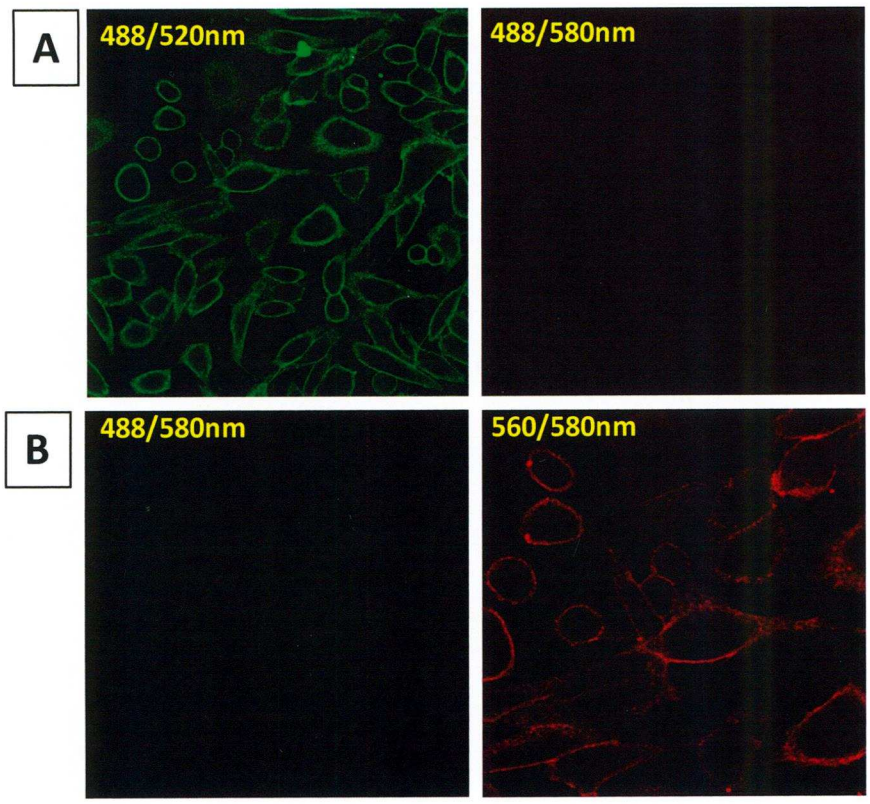

Figure 6.13: Testing the fluorphors of the antibodies:

A) *LAMP CHO cells were live stained with CC-V5 recombinant protein, follwoed by mouse anti-V5 antibody (Invitrogen) (1:50) and anti-mouse Alexa Fluor 488 (1:200). There is emission at 520nm following excitation at 488nm and no emission at 580nm.*

B) LAMP CHO cells were stained with transient OO-myc single transfection recombinant protein, mouse anti-myc antibody Alexa Fluor555 (Millipore) (1:250). No emission occured at 580nm, when the acceptor was excited at 488nm. While there was an emission at 580nm when the acceptor excited at 560nm.

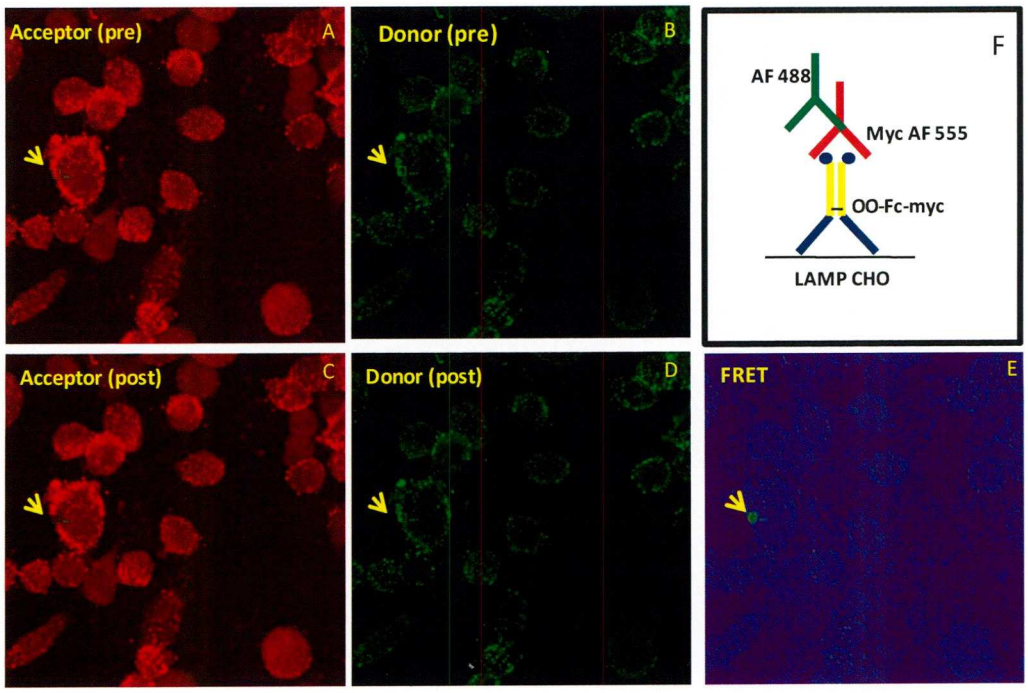

Figure 6.14: Positive control for FRET experiment:

LAMP CHO cells live stained with transient OO-myc single transfection recombinant protein, mouse anti-myc Alexa Fluor 555 (Millipore) (1:250) and antimouse Alexa Fluor 488 (Invitrogen) (1:200). (A)The acceptor was excited at 560nm and the donor (AF488) excited at 488nm before bleaching (B). A bright area at the edge of the LAMP CHO cell was selected (green square) to be bleached at 60%. (C)The selected bleached area becomes darker due to the bleaching of the acceptor whereas the donor becomes brighter after bleaching (D). An image shows the corresponding area for FRET (E). A diagram describes the mechanism of interaction between the donor and acceptor at close proximity when bind to OO-myc recombinant protein on LAMP-CHO cells (E)

Chapter Seven

Final Discussion

DISCUSSION:

CO-Fc heterodimeric recombinant protein (DigLON-Fc) was prepared as a tool in the investigation of the interaction of IgLONs/DigLONs and in the identification of the putative receptors. All previous results suggested the role of CO-DigLON, was to inhibit neurite outgrowth from a subpopulation of E8 forebrain neurons (Christine McNamee PhD thesis, University of Liverpool 2008). CO-transfected cell line also inhibited neurite outgrowth from cerebellar granule cells (Reed et al., 2004). In addition, previous evidence of GP55 chick glycoprotein that has a mixture of IgLONs inhibits the neurite outgrowth while no inhibition occurs with single IgLON (Clarke and Moss, 1994, 1997; McNamee et al., 2002), which suggests heterodimeric combination of IgLONs (DigLONs) is required (Reed et al., 2004).

CO-Fc heterodimeric recombinant protein is secreted as a physical dimer, held together by human Fc tail and tagged with epitope myc and V5 tags. These tags were used in characterisation of the complex. CO-Fc can be used as tool in identification of the putative receptor, by testing the activity and the binding of CO-Fc on PI-PLC treated and untreated neurons. In addition, the concentration of CO-Fc recombinant protein can be manipulated, whereas it is difficult to estimate the concentration of CO-DigLON that is expressed on the surface of CO-CHO cell line. CEPU-1 and OBCAM exist in close proximity in the CO-Fc complex, while on the surface of CHO cells the CEPU and OBCAM may reversibly dissociate and it may be hard to isolate the released complex.

Although there is evidence of DigLON formation in vitro, co-expression of two of more members of the family in the same cells is necessary for DigLONs to have a role in vivo. Co expression of both CEPU-1 and OBCAM protein in different area of the nervous system suggests the formation of CO-DigLON may occur in vivo

and they may have a role in the development of the nervous system. E8 optic fibre layer of chick retina is an area where both molecules are co-expressed, also cerebral cortex, retina and hippocampus (Gil et al., 2002; Miyata et al., 2003b; Struyk et al., 1995). In contrast, CEPU-1 expressed on the outer plexiform layer whereas OBCAM expressed in inner plexiform layer of E18 chick retina. Furthermore, double immunofluorescence and confocal microscopy studies suggest colocalisation of two members of IgLONs in the plane of the membrane of subpopulation of forebrain neurons (Sahar Youssef PhD thesis, University of Liverpool 2007) (Manuscript in preparation).

CO-Fc heterodimeric recombinant protein was produced from CHO stable cell line, which was transfected with both pcDNA6-CEPU-Fc-V5 and pBudCE4.1-OBCAM-Fc-myc constructs. These epitope tags were useful for characterisation and detection of the CO-Fc heterodimer complex. ELISA assays revealed that the cell line produced a mixture of CO-Fc heterodimeric protein, OO-Fc and CC-Fc homodimeric proteins. Therefore, anti-V5 and anti-myc affinity columns were tested for their ability to purify the CO-Fc from OO-Fc and CC-Fc. Anti-myc antibody was used to detect the CO-Fc because The failure of both anti-myc and anti-V5 columns to purify the CO-Fc totally from either C-Fc or O-Fc.

The first set of experiments was designed to test whether CO-Fc had the same activity as CO expressed together on CHO cells. CO-Fc inhibits the initiation of neurite outgrowth from E8 forebrain neurons in keeping with results with the CO-transfected CHO cell line, since no inhibitory activity occurred when CEPU-1 and OBCAM single recombinant proteins were mixed together (Michael Lyons). Therefore, CEPU-1 and OBCAM become active only when acting as a heterodimer

complex which suggests that CO-Fc will be a good tool to investigate binding to the receptor complex.

GP55 which may contain DigLONs inhibits the neurite outgrowth of DRG neurons (Clarke and Moss, 1994). However, CO CHO cell line and CO-Fc recombinant protein at (700AU/ml) failed to inhibit the outgrowth from E10 DRG and sympathetic neurons. Surprisingly, a high concentration of CO-Fc (2700AU/ml) significantly inhibits the initiation of outgrowth from essentially all DRG and sympathetic neurons. This suggests that the result might be due to the heterogeneity between forebrain, dorsal root ganglion and sympathetic neurons.

Having established that CO-Fc has the expected activity and must therefore interact with the surface of neurons, the binding properties were investigated. Since CEPU-Fc binds more strongly than OBCAM-Fc, anti-myc antibody was used rather than anti-V5 antibody in detection of CO-Fc heterodimeric protein in immunofluorescence binding assays. Different IgLON-transfected cell lines were used to test the interaction of CO-Fc heterodimeric recombinant protein. CO-Fc bound to CEPU-CHO, OBCAM-CHO and surprisingly to LAMP CHO cells, because LAMP-Fc did not bind to CO-CHO cells previously. However, a low level of OO-Fc homdimeric protein was present with CO-Fc heterodimeric protein after purification, and may have interfered and been detected with the anti-myc antibody in binding experiments. Interestingly, CO-Fc bound to CL-CHO cells and not to CO-CHO or Wt CHO cells suggesting that heterophilic interactions may be possible between DigLONs or CO-Fc may be binding to monomers or homodimers due to unbalanced expression of CEPU-1 or LAMP on the surface of CHO cells. The binding was significantly less than for the corresponding singly transfected CHO cells.

Since it proved difficult if not impossible to isolate CO-Fc from the OO-Fc and CC-Fc, it might have been a better idea to label CEPU-Fc with RFP (CEPU-Fc-RFP) and OBCAM-Fc with GFP (OBCAM-Fc-GFP). Then Fluorescence resonance energy transfer technique (FRET) can be carried out between the GFP of OBCAM-Fc-GFP chain and RFP of CEPU-Fc-RFP chain to distinguish between the binding of CO-Fc heterodimeric protein from the contamination that caused by OO-Fc and CC-Fc homodimeric recombinant proteins. However, a problem might be that protein A would no longer bind to the Fc-GFP or RFP and purification from media might have been difficult.

Alternatively, FRET is still a possible option between V5 and myc epitope tags on the CO-Fc complex, which is located at close proximity using anti-V5 Alexa Fluor 488 antibody as a donor, and anti-myc Alexa Fluor 555 as acceptor. Single transient transfection of CEPU-Fc-V5, OBCAM-Fc-myc and a mixture of both were prepared for this experiment. In the case of CO-Fc, an energy transfer between can occur between two fluorphors while no transfer is expected in CC-Fc and OO-Fc, these are important controls as CC-Fc and OO-Fc will bind to IgLONs potentially within a lipid raft and hence will be in reasonably close proximity.

There are several examples for interactions between molecules belong to Ig superfamily that share in formation of receptor complex and guidance molecules. An interaction between Slit axon guidance molecule and its receptor Robo molecule leads to guiding axons across the midline (Long et al., 2004). In addition, Netrin plays a role in attraction of commissural axons toward the floorplate by interacting with its receptors DCC and UNC-5 (Keleman and Dickson, 2001). The neurite outgrowth is stimulated by interaction between netrin and DCC receptor only,

however, when a receptor complex formed due to *cis* interaction between UNC-5 and DCC, netrin becomes inhibitor to the neurite outgrowth (Hong et al., 1999).

As the putative receptors for IgLONs/DigLONs are not yet known, there are different proposed options for the nature of these receptors. The first option is that IgLONs/DigLONs signal to the cytoskeleton without the transmembrane receptor which could be by endocytosis such as T-lymphocyte activation (discussed later). Secondly, IgLONs/DigLONs may bind to a transmembrane receptor alone (with no interaction in cis to IgLONs) which signals through a cytoplasmic domain. The last option is that IgLONs interact with a transmembrane receptor in order to form a receptor complex to initiate signalling pathway. For example, neuroplastin-55 induces the neurite outgrowth through binding to and activation of FGFR1 (Owczarek et al., 2009). In Drosophila, amalgam is a three Ig domain secreted CAM which signals through interaction with neurotactin transmembrane receptor (Liebl et al., 2003). Cripto-1 is GPI- anchored protein that could be associated with a transmembrane receptor to activate signalling pathway for Nodal/ALK4/ALK7/Smad-2 and a Glypican-1/c-Src/MAPK/AKT (Hendrix et al., 2007; Strizzi et al., 2005)

To investigate the role of IgLONs in formation of the receptors, the binding of CO-Fc heterodimeric recombinant protein was tested in the presence of the IgLONs/DigLONs on the surface of the forebrain neurons and after removal of IgLONs by PI-PLC treatment which cleaves the GPI-anchored proteins from the lipid rafts of the cell membrane. The findings of this experiment suggested that IgLONs/DigLONs play a role in formation of the putative receptors. Because the inhibition caused by the CO-Fc heterodimeric recombinant protein was reversed after PI-PLC treatment of the neurons, this supports the hypothesis that IgLONs/DigLONs

act as receptor, although it is still unclear whether a transmembrane receptor is required for signaling or IgLONs initiate the signalling pathway (figure 7.1). As a conclusion, IgLONs/DigLONs may have a role in formation of the putative receptor complex for CO-Fc heterodimeric recombinant protein when acts as ligand. Once the CO-Fc interacts in *trans* with IgLON/DigLON as surface receptor.

ROCK is a part of the Rho kinase signalling pathway; it was inhibited by Y27632 (specific inhibitor) when added to the CO forebrain culture which reversed the inhibitory activity of CO on neurite outgrowth (Christine McNamee PhD thesis, University of Liverpool 2008). This suggests that IgLONs/DigLONs with other guidance molecules may signal to the cytoskeleton of the growth cone during axonal guidance through members of the Rho family. They are considered as GTPases and involve Rho guanine exchange factors (GEFs) and guanine activating protein (GAPs) which are responsible for initiation of the signals through Rho, Cdc 42 and Rac to the cytoskeleton (Huber et al., 2003).

In summary, CO-Fc heterodimeric recombinant protein inhibits the initiation of neurite outgrowth from E8 forebrain neurons as the CO-transfected cell line (Christine McNamee PhD thesis, University of Liverpool 2008). In addition, CO-Fc inhibits the outgrowth from E10 DRG and sympathetic chain neurons compatible with the evidence that GP55 which may contains DigLONs and inhibits the neurite outgrowth from DRG neurons (Moss and Clarke, 1994). In contrast, the CO-transfected cell line and CO-Fc at low concentration fail to inhibit.

IgLONs may be a part of the putative receptor for CO-Fc heterodimeric recombinant protein. This was revealed from PI-PLC treated and untreated forebrain neurite outgrowth assay and immunofluorescence studies. In particularly, CO-Fc

binds to the IgLON-transfected CHO cell lines; CEPU-1, OBCAM, LAMP and interestingly CL and not CO-CHO cell lines which suggests that the putative receptor for CO-Fc could be (CL) DigLONs or single IgLONs. A transmembrane receptor may be required to initiate the signalling pathway but this needs further investigation.

Interestingly, activation of T-cell lymphocyte by crosslinking of different GPI-anchored proteins such as CD48 suggested that signaling transduction through GPI anchored protein might be possible (Ilangumaran et al., 2000; Robinson, 1991). In addition, interleukin-18 (IL-18) binds to CD48 GPI anchored protein beside IL-18 receptor result in stimulation of T-cells and natural killer (NK) cells to produce interferon-gamma (Fukushima et al., 2005). The production of interferon-gamma was inhibited by PI-PLC treatment of these cells which supports the involvement of CD48 in signaling process (Fukushima et al., 2005).

Endocytosis of GPI-anchored proteins are considered to be a possible mechanism of signaling of GPI-anchored proteins, which are distinguished from those signal through transmembrane proteins which thought to be internalised through clathrin-coated vesicles(Bamezai et al., 1992; Bamezai and Rock, 1991; Deckert et al., 1996; Keller et al., 1992). The folate binds to a GPI-anchored folate receptor on the surface of MA104 cells, and then the complex moves into the intracellular compartment in intracellular endosomal compartments. The ligand remains in the intracellular compartment and free receptors move back to the cell surface (Kamen et al., 1988). Folate internalisation by cells that express constructed chimeric folate receptors that have a transmembrane receptor with transmembrane domains instead of GPI-anchors via clathrin-coated vesicles is less efficient than those expressing receptors with GPI-anchored folate receptors (Ritter et al., 1995). There is a contradiction between endocytosis of folate-receptor GPI-anchored

proteins (FR-GPI) and prion proteins, which are cell surface proteins and shows role of clathrin-coated vesicles (Sabharanjak et al., 2002). There is role for sphingolipids and cholesterol in GPI-anchored protein endocytosis. Endocytosis of urokinase-type plasminogen activator receptor (uPAR) required interaction with transmembrane receptor such as LDL-receptor related protein (LRP (Czekay et al., 2001). FRET analysis revealed that uPAR exists in either dimeric or monomeric forms in the basal membrane (Figure 7.2) (Caiolfa et al., 2007).

A large number of GPI-anchored protein are able to activate signaling pathway despite the lack of transmembrane or cytoplasmic domains (Robinson, 1991). Signal transduction due to phosphorylation of tyrosine residue of intracellular substrates by cross linking of GPI-anchored proteins (Brown and Cooper, 1996). CAECAM6 is an example for GPI-anchored protein that may manipulate intracellular signal transduction; however, the mechanism is not clear. Activation of c-Src by cross-linking of CAECAM6 is associated with phosphorylation of FAK (Duxbury et al., 2004). Thy-1 is GPI-anchored protein that inhibits the neurite outgrowth over astrocytes, replacement of its GPI-anchor with a transmembrane domain of CD8 or NCAM reverse the inhibitory action. This suggests the importance of the GPI anchor in locating specific proteins in lipid rafts and in contact with other signaling partners such as SFK (Kasahara and Sanai, 2000; Rege et al., 2006; Tiveron et al., 1994). In addition, Thy-1 is required for fibroblast migration which induced by TSP-1/hep I interaction which lead to FAK phosphorylation (Figure 7.3) (Rege et al., 2006).

So far all the evidence for DigLONs have been obtained by our group until recently, key functional data on the role of IgLONs in synapse formation has been obtained which supports the hypothesis that IgLONs act as heterodimeric complexes (DigLONs) (Hashimoto et al., 2009; Reed et al., 2004). There was a significant

reduction in the number of synapses occurring due to double overexpression of Ntm (CEPU-1) and OBCAM in hippocampal neurons, while single overexpression of OBCAM caused significant increase of synaptic number, whereas no change occurred with overexpression of single Ntm (CEPU-1). In addition, overexpression of kilon-Ntm, kilon-OBCAM or LAMP-Ntm caused reduction in synaptic number. Surprisingly, LAMP-OBCAM had no effect on the number of synapses. This suggests the crucial role of IgLON-IgLON *cis* homophilic and heterophilic interactions at pre and post synaptic sites (Hashimoto et al., 2009).

ELISA assays revealed that CHO stable cell line secreted a mixture of CO-Fc, CC-Fc and OO-Fc. CO-Fc was not fully purified by affinity columns. Therefore, FRET is required to distinguish the CO-Fc heterodimeric recombinant protein from the CC-Fc and OO-Fc homodimeric recombinant protein using anti-V5 Alexa Fluor 488 and anti-myc Alexa Fluor 555 antibodies. Preliminary FRET experiments were carried out to generate a positive control and testing the two fluorphors.

In parallel to preparation of CO-Fc heterodimeric protein, I have generated pBudCE4.1-LAMP-Fc-myc construct which was used alongside pcDNA6-CEPU-Fc-V5 construct in generation of CEPU-LAMP-Fc stable CHO cell line (CL-Fc). However, due to lack of time, I have concentrated on investigation of activity and interactions of CO-Fc heterodimeric recombinant protein.

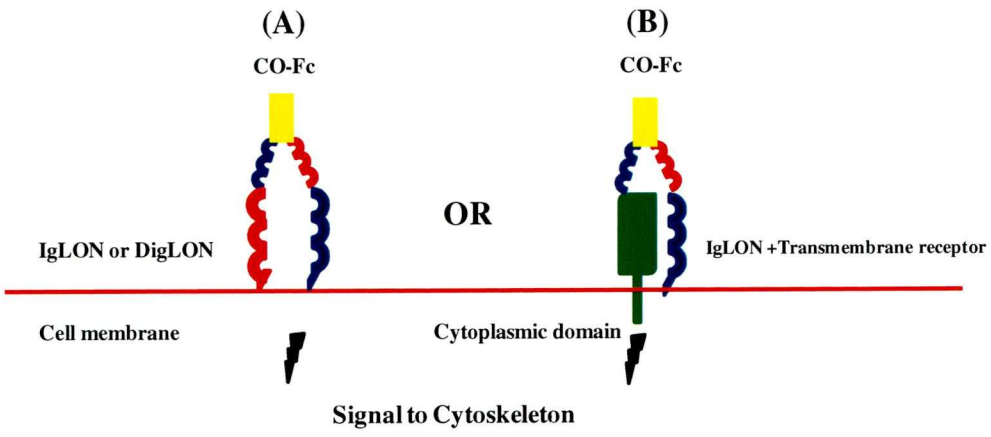

Figure 7.1: the proposed options for the putative receptor for CO-Fc complex and role of IgLONs

There are two proposed options for the putative receptor for CO-Fc heterodimeric recombinant protein that are suggested by the evidences in this thesis

A) CO-Fc binds to IgLONs or DigLONs on the surface of the growth cone and initiate signalling pathway to the cytoskeleton of the growth cone.

B) CO-Fc binds to a receptor complex formed by IgLON and transmembrane receptor with cytoplasmic domain which initiate the signal pathway to the cytoskeleton.

In both options, IgLON has a role in the formation of the putative CO-Fc receptor.

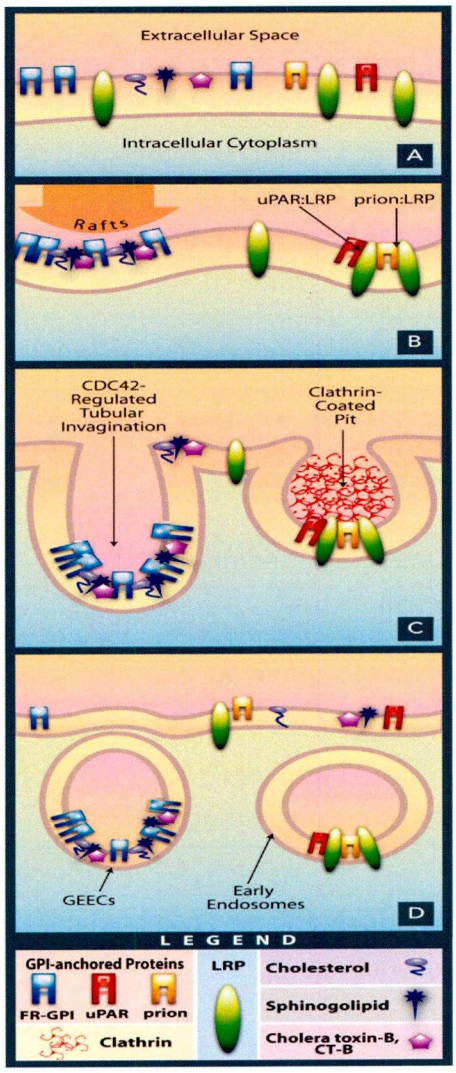

Figure 7.2: Endocytosis of GPI-anchored protein mechanisms:

An illustration describes the mechanism of endocytosis of GPI-anchored proteins. Different GPI-anchored proteins distributed on the cell membrane (A). The interaction GPI anchored proteins (FR-GPI) (blue), uPAR (red) or prion (yellow) with a transmembrane receptor (LRP) (green). The sphingolipids and cholesterol in the lipid are essential for these interactions (B). There are two ways of endocytosis; CD42 endocytosed into tubular invagination to form GPI-AP enriched endosomal compartments (GEECs), or LRP-GPI-anchored protein complex was endocytosis in clathrin-coated pits(C, D) (Lakhan et al., 2009).

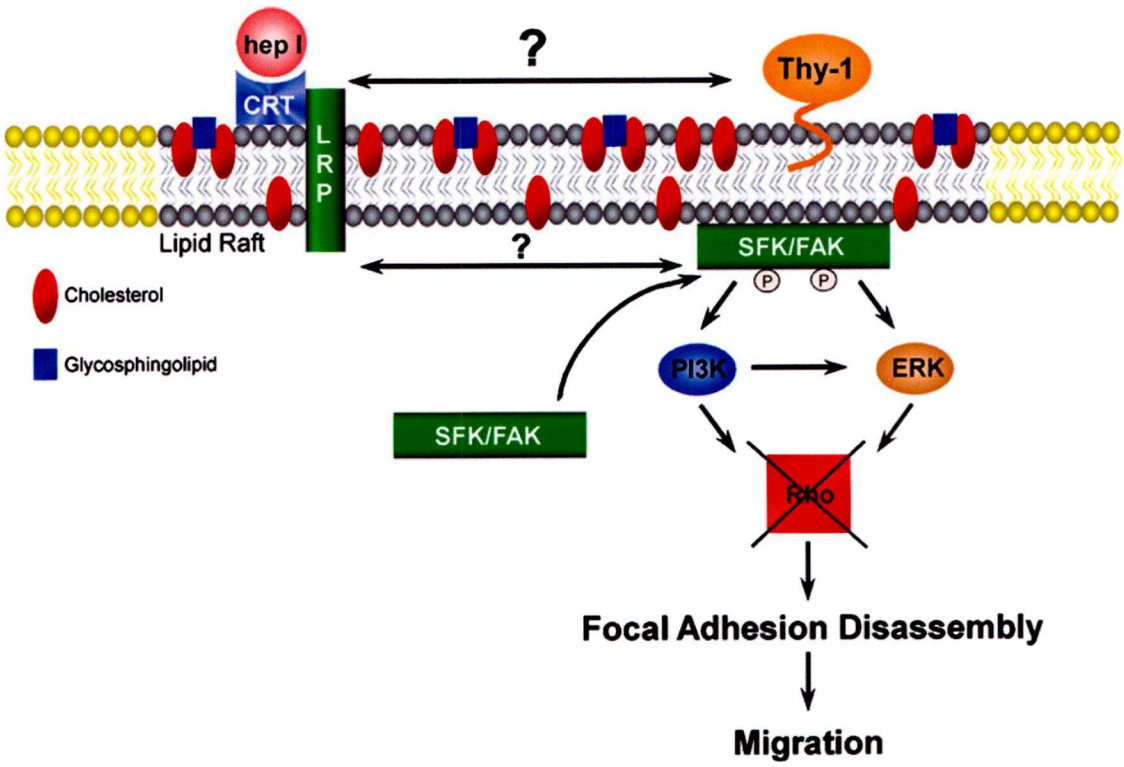

Figure 7.3: Modulation of FAK signaling pathway by GPI-anchored proteins:

A schematic diagram describes the effect of Thy-1 (GPI-anchored protein) on signaling of TSP/hep I. This interaction lead to recruitment of SFK and FAK to the lipid raft, and then initiate the downstream signaling pathway such as PI 3-kinase and ERK which result in focal adhesion assembly and migration of fibroblast (Rege et al., 2006).

References

Anderson, R.G., and Jacobson, K. (2002). A role for lipid shells in targeting proteins to caveolae, rafts, and other lipid domains. Science *296*, 1821-1825.

Bamezai, A., Goldmacher, V.S., and Rock, K.L. (1992). Internalization of glycosyl-phosphatidylinositol (GPI)-anchored lymphocyte proteins. II. GPI-anchored and transmembrane molecules internalize through distinct pathways. Eur J Immunol *22*, 15-21.

Bamezai, A., and Rock, K.L. (1991). Effect of ras-activation on the expression of glycosyl-phosphatidylinositol-anchored proteins on the plasma membrane. Oncogene *6*, 1445-1451.

Bernstein, H.G., Smalla, K.H., Bogerts, B., Gordon-Weeks, P.R., Beesley, P.W., Gundelfinger, E.D., and Kreutz, M.R. (2007). The immunolocalization of the synaptic glycoprotein neuroplastin differs substantially between the human and the rodent brain. Brain Res *1134*, 107-112.

Biederer, T. (2006). Bioinformatic characterization of the SynCAM family of immunoglobulin-like domain-containing adhesion molecules. Genomics *87*, 139-150.

Biederer, T., Sara, Y., Mozhayeva, M., Atasoy, D., Liu, X., Kavalali, E.T., and Sudhof, T.C. (2002). SynCAM, a synaptic adhesion molecule that drives synapse assembly. Science *297*, 1525-1531.

Bonfanti, L. (2006). PSA-NCAM in mammalian structural plasticity and neurogenesis. Prog Neurobiol *80*, 129-164.

Brauer, A.U., Savaskan, N.E., Plaschke, M., Prehn, S., Ninnemann, O., and Nitsch, R. (2000). IG-molecule Kilon shows differential expression pattern from LAMP in the developing and adult rat hippocampus. Hippocampus *10*, 632-644.

Brose, K., Bland, K.S., Wang, K.H., Arnott, D., Henzel, W., Goodman, C.S., Tessier-Lavigne, M., and Kidd, T. (1999). Slit proteins bind Robo receptors and have an evolutionarily conserved role in repulsive axon guidance. Cell *96*, 795-806.

Brown, D.A., and London, E. (2000). Structure and function of sphingolipid- and cholesterol-rich membrane rafts. J Biol Chem *275*, 17221-17224.

Brown, M.T., and Cooper, J.A. (1996). Regulation, substrates and functions of src. Biochim Biophys Acta *1287*, 121-149.

Brummendorf, T., and Lemmon, V. (2001). Immunoglobulin superfamily receptors: cis-interactions, intracellular adapters and alternative splicing regulate adhesion. Curr Opin Cell Biol *13*, 611-618.

Brummendorf, T., and Rathjen, F.G. (1995). Cell adhesion molecules 1: immunoglobulin superfamily. Protein Profile *2*, 963-1108.

Brummendorf, T., and Rathjen, F.G. (1996). Structure/function relationships of axon-associated adhesion receptors of the immunoglobulin superfamily. Curr Opin Neurobiol *6*, 584-593.

Brummendorf, T., Spaltmann, F., and Treubert, U. (1997). Cloning and characterization of a neural cell recognition molecule on axons of the retinotectal system and spinal cord. Eur J Neurosci *9*, 1105-1116.

Brummendorf, T., Wolff, J.M., Frank, R., and Rathjen, F.G. (1989). Neural cell recognition molecule F11: homology with fibronectin type III and immunoglobulin type C domains. Neuron *2*, 1351-1361.

Buckby, L.E., Mummery, R., Crompton, M.R., Beesley, P.W., and Empson, R.M. (2004). Comparison of neuroplastin and synaptic marker protein expression in acute and cultured organotypic hippocampal slices from rat.

Brain Res Dev Brain Res *150*, 1-7.

Butler, S.J., and Dodd, J. (2003). A role for BMP heterodimers in roof plate-mediated repulsion of commissural axons. Neuron *38*, 389-401.

Caiolfa, V.R., Zamai, M., Malengo, G., Andolfo, A., Madsen, C.D., Sutin, J., Digman, M.A., Gratton, E., Blasi, F., and Sidenius, N. (2007). Monomer dimer dynamics and distribution of GPI-anchored uPAR are determined by cell surface protein assemblies. J Cell Biol *179*, 1067-1082.

Castellani, V., Chedotal, A., Schachner, M., Faivre-Sarrailh, C., and Rougon, G. (2000). Analysis of the L1-deficient mouse phenotype reveals cross-talk between Sema3A and L1 signaling pathways in axonal guidance. Neuron *27*, 237-249.

Castranio, T., and Mishina, Y. (2009). Bmp2 is required for cephalic neural tube closure in the mouse. Dev Dyn *238*, 110-122.

Catania, E.H., Pimenta, A., and Levitt, P. (2008). Genetic deletion of Lsamp causes exaggerated behavioral activation in novel environments. Behav Brain Res *188*, 380-390.

Chan, J., Mably, J.D., Serluca, F.C., Chen, J.N., Goldstein, N.B., Thomas, M.C., Cleary, J.A., Brennan, C., Fishman, M.C., and Roberts, T.M. (2001). Morphogenesis of prechordal plate and notochord requires intact Eph/ephrin B signaling. Dev Biol *234*, 470-482.

Charron, F., Stein, E., Jeong, J., McMahon, A.P., and Tessier-Lavigne, M. (2003). The morphogen sonic hedgehog is an axonal chemoattractant that collaborates with netrin-1 in midline axon guidance. Cell *113*, 11-23.

Chen, H., Ye, F., Zhang, J., Lu, W., Cheng, Q., and Xie, X. (2007). Loss of OPCML expression and the correlation with CpG island methylation and LOH

in ovarian serous carcinoma. Eur J Gynaecol Oncol *28*, 464-467.

Chen, S., Gil, O., Ren, Y.Q., Zanazzi, G., Salzer, J.L., and Hillman, D.E. (2001). Neurotrimin expression during cerebellar development suggests roles in axon fasciculation and synaptogenesis. J Neurocytol *30*, 927-937.

Chen, Y.J., Wing, D.R., Guile, G.R., Dwek, R.A., Harvey, D.J., and Zamze, S. (1998). Neutral N-glycans in adult rat brain tissue--complete characterisation reveals fucosylated hybrid and complex structures. Eur J Biochem *251*, 691-703.

Cheng, X., Hsu, C.M., Currle, D.S., Hu, J.S., Barkovich, A.J., and Monuki, E.S. (2006). Central roles of the roof plate in telencephalic development and holoprosencephaly. J Neurosci *26*, 7640-7649.

Chisholm, A., and Tessier-Lavigne, M. (1999). Conservation and divergence of axon guidance mechanisms. Curr Opin Neurobiol *9*, 603-615.

Chizhikov, V.V., and Millen, K.J. (2005). Roof plate-dependent patterning of the vertebrate dorsal central nervous system. Dev Biol *277*, 287-295.

Clarke, G.A., and Moss, D.J. (1994). Identification of a novel protein from adult chicken brain that inhibits neurite outgrowth. J Cell Sci *107 (Pt 12)*, 3393-3402.

Clarke, G.A., and Moss, D.J. (1997). GP55 inhibits both cell adhesion and growth of neurons, but not non-neuronal cells, via a G-protein-coupled receptor. Eur J Neurosci *9*, 334-341.

Cocchi, F., Menotti, L., Mirandola, P., Lopez, M., and Campadelli-Fiume, G. (1998). The ectodomain of a novel member of the immunoglobulin subfamily related to the poliovirus receptor has the attributes of a bona fide receptor for herpes simplex virus types 1 and 2 in human cells. J Virol *72*, 9992-10002.

Connor, R.M., and Key, B. (2002). Expression and role of Roundabout-1 in embryonic Xenopus forebrain. Dev Dyn *225*, 22-34.

Correia, A.C., Costa, M., Moraes, F., Bom, J., Novoa, A., and Mallo, M. (2007). Bmp2 is required for migration but not for induction of neural crest cells in the mouse. Dev Dyn *236*, 2493-2501.

Czekay, R.P., Kuemmel, T.A., Orlando, R.A., and Farquhar, M.G. (2001). Direct binding of occupied urokinase receptor (uPAR) to LDL receptor-related protein is required for endocytosis of uPAR and regulation of cell surface urokinase activity. Mol Biol Cell *12*, 1467-1479.

Deckert, M., Ticchioni, M., and Bernard, A. (1996). Endocytosis of GPI-anchored proteins in human lymphocytes: role of glycolipid-based domains, actin cytoskeleton, and protein kinases. J Cell Biol *133*, 791-799.

Dickson, B.J. (2002). Molecular mechanisms of axon guidance. Science *298*, 1959-1964.

Dickson, B.J., and Gilestro, G.F. (2006). Regulation of commissural axon pathfinding by slit and its Robo receptors. Annu Rev Cell Dev Biol *22*, 651-675.

Doherty, P., Fazeli, M.S., and Walsh, F.S. (1995). The neural cell adhesion molecule and synaptic plasticity. J Neurobiol *26*, 437-446.

Duxbury, M.S., Ito, H., Ashley, S.W., and Whang, E.E. (2004). CEACAM6 cross-linking induces caveolin-1-dependent, Src-mediated focal adhesion kinase phosphorylation in BxPC3 pancreatic adenocarcinoma cells. J Biol Chem *279*, 23176-23182.

Eastwood, S.L., Law, A.J., Everall, I.P., and Harrison, P.J. (2003). The axonal chemorepellant semaphorin 3A is increased in the cerebellum in

schizophrenia and may contribute to its synaptic pathology. Mol Psychiatry *8*, 148-155.

Empson, R.M., Buckby, L.E., Kraus, M., Bates, K.J., Crompton, M.R., Gundelfinger, E.D., and Beesley, P.W. (2006). The cell adhesion molecule neuroplastin-65 inhibits hippocampal long-term potentiation via a mitogen-activated protein kinase p38-dependent reduction in surface expression of GluR1-containing glutamate receptors. J Neurochem *99*, 850-860.

Ericson, J., Briscoe, J., Rashbass, P., van Heyningen, V., and Jessell, T.M. (1997). Graded sonic hedgehog signaling and the specification of cell fate in the ventral neural tube. Cold Spring Harb Symp Quant Biol *62*, 451-466.

Ericson, J., Morton, S., Kawakami, A., Roelink, H., and Jessell, T.M. (1996). Two critical periods of Sonic Hedgehog signaling required for the specification of motor neuron identity. Cell *87*, 661-673.

Erskine, L., and Herrera, E. (2007). The retinal ganglion cell axon's journey: insights into molecular mechanisms of axon guidance. Dev Biol *308*, 1-14.

Fazeli, A., Dickinson, S.L., Hermiston, M.L., Tighe, R.V., Steen, R.G., Small, C.G., Stoeckli, E.T., Keino-Masu, K., Masu, M., Rayburn, H., *et al.* (1997). Phenotype of mice lacking functional Deleted in colorectal cancer (Dcc) gene. Nature *386*, 796-804.

Fogel, A.I., Akins, M.R., Krupp, A.J., Stagi, M., Stein, V., and Biederer, T. (2007). SynCAMs organize synapses through heterophilic adhesion. J Neurosci *27*, 12516-12530.

Friedrichson, T., and Kurzchalia, T.V. (1998). Microdomains of GPI-anchored proteins in living cells revealed by crosslinking. Nature *394*, 802-805.

Fukuda, S., Abematsu, M., Mori, H., Yanagisawa, M., Kagawa, T.,

Nakashima, K., Yoshimura, A., and Taga, T. (2007). Potentiation of astrogliogenesis by STAT3-mediated activation of bone morphogenetic protein-Smad signaling in neural stem cells. Mol Cell Biol *27*, 4931-4937.

Fukushima, K., Ikehara, Y., and Yamashita, K. (2005). Functional role played by the glycosylphosphatidylinositol anchor glycan of CD48 in interleukin-18-induced interferon-gamma production. J Biol Chem *280*, 18056-18062.

Funatsu, N., Miyata, S., Kumanogoh, H., Shigeta, M., Hamada, K., Endo, Y., Sokawa, Y., and Maekawa, S. (1999). Characterization of a novel rat brain glycosylphosphatidylinositol-anchored protein (Kilon), a member of the IgLON cell adhesion molecule family. J Biol Chem *274*, 8224-8230.

Furuta, Y., Piston, D.W., and Hogan, B.L. (1997). Bone morphogenetic proteins (BMPs) as regulators of dorsal forebrain development. Development *124*, 2203-2212.

Gascon, E., Vutskits, L., and Kiss, J.Z. (2007). Polysialic acid-neural cell adhesion molecule in brain plasticity: from synapses to integration of new neurons. Brain Res Rev *56*, 101-118.

Gil, O.D., Zanazzi, G., Struyk, A.F., and Salzer, J.L. (1998). Neurotrimin mediates bifunctional effects on neurite outgrowth via homophilic and heterophilic interactions. J Neurosci *18*, 9312-9325.

Gil, O.D., Zhang, L., Chen, S., Ren, Y.Q., Pimenta, A., Zanazzi, G., Hillman, D., Levitt, P., and Salzer, J.L. (2002). Complementary expression and heterophilic interactions between IgLON family members neurotrimin and LAMP. J Neurobiol *51*, 190-204.

Guirland, C., and Zheng, J.Q. (2007). Membrane lipid rafts and their role in axon guidance. Adv Exp Med Biol *621*, 144-155.

Hancox, K.A., Gooley, A.A., and Jeffrey, P.L. (1997). AvGp50, a predominantly axonally expressed glycoprotein, is a member of the IgLON's subfamily of cell adhesion molecules (CAMs). Brain Res Mol Brain Res *44*, 273-285.

Hashimoto, T., Maekawa, S., and Miyata, S. (2009). IgLON cell adhesion molecules regulate synaptogenesis in hippocampal neurons. Cell Biochem Funct *27*, 496-498.

Hendrix, M.J., Seftor, E.A., Seftor, R.E., Kasemeier-Kulesa, J., Kulesa, P.M., and Postovit, L.M. (2007). Reprogramming metastatic tumour cells with embryonic microenvironments. Nat Rev Cancer *7*, 246-255.

Herincs, Z., Corset, V., Cahuzac, N., Furne, C., Castellani, V., Hueber, A.O., and Mehlen, P. (2005). DCC association with lipid rafts is required for netrin-1-mediated axon guidance. J Cell Sci *118*, 1687-1692.

Hong, K., Hinck, L., Nishiyama, M., Poo, M.M., Tessier-Lavigne, M., and Stein, E. (1999). A ligand-gated association between cytoplasmic domains of UNC5 and DCC family receptors converts netrin-induced growth cone attraction to repulsion. Cell *97*, 927-941.

Horton, H.L., and Levitt, P. (1988). A unique membrane protein is expressed on early developing limbic system axons and cortical targets. J Neurosci *8*, 4653-4661.

Hu, H. (1999). Chemorepulsion of neuronal migration by Slit2 in the developing mammalian forebrain. Neuron *23*, 703-711.

Huber, A.B., Kania, A., Tran, T.S., Gu, C., De Marco Garcia, N., Lieberam, I., Johnson, D., Jessell, T.M., Ginty, D.D., and Kolodkin, A.L. (2005). Distinct roles for secreted semaphorin signaling in spinal motor axon guidance.

Neuron *48*, 949-964.

Huber, A.B., Kolodkin, A.L., Ginty, D.D., and Cloutier, J.F. (2003). Signaling at the growth cone: ligand-receptor complexes and the control of axon growth and guidance. Annu Rev Neurosci *26*, 509-563.

Hubschmann, M.V., Skladchikova, G., Bock, E., and Berezin, V. (2005). Neural cell adhesion molecule function is regulated by metalloproteinase-mediated ectodomain release. J Neurosci Res *80*, 826-837.

Huot, J. (2004). Ephrin signaling in axon guidance. Prog Neuropsychopharmacol Biol Psychiatry *28*, 813-818.

Ilangumaran, S., He, H.T., and Hoessli, D.C. (2000). Microdomains in lymphocyte signalling: beyond GPI-anchored proteins. Immunol Today *21*, 2-7.

Irie, K., Shimizu, K., Sakisaka, T., Ikeda, W., and Takai, Y. (2004). Roles and modes of action of nectins in cell-cell adhesion. Semin Cell Dev Biol *15*, 643-656.

Itoh, S., Hachisuka, A., Kawasaki, N., Hashii, N., Teshima, R., Hayakawa, T., Kawanishi, T., and Yamaguchi, T. (2008). Glycosylation analysis of IgLON family proteins in rat brain by liquid chromatography and multiple-stage mass spectrometry. Biochemistry *47*, 10132-10154.

Jungbluth, S., Phelps, C., and Lumsden, A. (2001). CEPU-1 expression in the early embryonic chick brain. Mech Dev *101*, 195-197.

Kakunaga, S., Ikeda, W., Itoh, S., Deguchi-Tawarada, M., Ohtsuka, T., Mizoguchi, A., and Takai, Y. (2005). Nectin-like molecule-1/TSLL1/SynCAM3: a neural tissue-specific immunoglobulin-like cell-cell adhesion molecule localizing at non-junctional contact sites of presynaptic

nerve terminals, axons and glia cell processes. J Cell Sci *118*, 1267-1277.

Kalus, I., Bormann, U., Mzoughi, M., Schachner, M., and Kleene, R. (2006). Proteolytic cleavage of the neural cell adhesion molecule by ADAM17/TACE is involved in neurite outgrowth. J Neurochem *98*, 78-88.

Kamen, B.A., Wang, M.T., Streckfuss, A.J., Peryea, X., and Anderson, R.G. (1988). Delivery of folates to the cytoplasm of MA104 cells is mediated by a surface membrane receptor that recycles. J Biol Chem *263*, 13602-13609.

Kasahara, K., and Sanai, Y. (2000). Functional roles of glycosphingolipids in signal transduction via lipid rafts. Glycoconj J *17*, 153-162.

Keleman, K., and Dickson, B.J. (2001). Short- and long-range repulsion by the Drosophila Unc5 netrin receptor. Neuron *32*, 605-617.

Keleman, K., Rajagopalan, S., Cleppien, D., Teis, D., Paiha, K., Huber, L.A., Technau, G.M., and Dickson, B.J. (2002). Comm sorts robo to control axon guidance at the Drosophila midline. Cell *110*, 415-427.

Keleman, K., Ribeiro, C., and Dickson, B.J. (2005). Comm function in commissural axon guidance: cell-autonomous sorting of Robo in vivo. Nat Neurosci *8*, 156-163.

Keller, G.A., Siegel, M.W., and Caras, I.W. (1992). Endocytosis of glycophospholipid-anchored and transmembrane forms of CD4 by different endocytic pathways. EMBO J *11*, 863-874.

Kennedy, T.E., Serafini, T., de la Torre, J.R., and Tessier-Lavigne, M. (1994). Netrins are diffusible chemotropic factors for commissural axons in the embryonic spinal cord. Cell *78*, 425-435.

Kim, T.H., Lee, H.K., Seo, I.A., Bae, H.R., Suh, D.J., Wu, J., Rao, Y., Hwang, K.G., and Park, H.T. (2005). Netrin induces down-regulation of its receptor,

Deleted in Colorectal Cancer, through the ubiquitin-proteasome pathway in the embryonic cortical neuron. J Neurochem *95*, 1-8.

Kimura, Y., Katoh, A., Kaneko, T., Takahama, K., and Tanaka, H. (2001). Two members of the IgLON family are expressed in a restricted region of the developing chick brain and neural crest. Dev Growth Differ *43*, 257-263.

Kingsley, D.M. (1994). The TGF-beta superfamily: new members, new receptors, and new genetic tests of function in different organisms. Genes Dev *8*, 133-146.

Kiselyov, V.V., Skladchikova, G., Hinsby, A.M., Jensen, P.H., Kulahin, N., Soroka, V., Pedersen, N., Tsetlin, V., Poulsen, F.M., Berezin, V., *et al.* (2003). Structural basis for a direct interaction between FGFR1 and NCAM and evidence for a regulatory role of ATP. Structure *11*, 691-701.

Kiselyov, V.V., Soroka, V., Berezin, V., and Bock, E. (2005). Structural biology of NCAM homophilic binding and activation of FGFR. J Neurochem *94*, 1169-1179.

Kleene, R., and Schachner, M. (2004). Glycans and neural cell interactions. Nat Rev Neurosci *5*, 195-208.

Klein, R. (2001). Excitatory Eph receptors and adhesive ephrin ligands. Curr Opin Cell Biol *13*, 196-203.

Knoll, B., and Drescher, U. (2002). Ephrin-As as receptors in topographic projections. Trends Neurosci *25*, 145-149.

Kramer, S.G., Kidd, T., Simpson, J.H., and Goodman, C.S. (2001). Switching repulsion to attraction: changing responses to slit during transition in mesoderm migration. Science *292*, 737-740.

Kreutz, M.R., Langnaese, K., Dieterich, D.C., Seidenbecher, C.I.,

Zuschratter, W., Beesley, P.W., and Gundelfinger, E.D. (2001). Distribution of transcript and protein isoforms of the synaptic glycoprotein neuroplastin in rat retina. Invest Ophthalmol Vis Sci *42*, 1907-1914.

Kullander, K., and Klein, R. (2002). Mechanisms and functions of Eph and ephrin signalling. Nat Rev Mol Cell Biol *3*, 475-486.

LaBonne, C., and Bronner-Fraser, M. (1999). Molecular mechanisms of neural crest formation. Annu Rev Cell Dev Biol *15*, 81-112.

Lakhan, S.E., Sabharanjak, S., and De, A. (2009). Endocytosis of glycosylphosphatidylinositol-anchored proteins. J Biomed Sci *16*, 93.

Lee, K.J., Dietrich, P., and Jessell, T.M. (2000). Genetic ablation reveals that the roof plate is essential for dorsal interneuron specification. Nature *403*, 734-740.

Lee, K.J., Mendelsohn, M., and Jessell, T.M. (1998). Neuronal patterning by BMPs: a requirement for GDF7 in the generation of a discrete class of commissural interneurons in the mouse spinal cord. Genes Dev *12*, 3394-3407.

Leptin, M. (2005). Gastrulation movements: the logic and the nuts and bolts. Dev Cell *8*, 305-320.

Levitt, P. (1984). A monoclonal antibody to limbic system neurons. Science *223*, 299-301.

Liebl, E.C., Rowe, R.G., Forsthoefel, D.J., Stammler, A.L., Schmidt, E.R., Turski, M., and Seeger, M.A. (2003). Interactions between the secreted protein Amalgam, its transmembrane receptor Neurotactin and the Abelson tyrosine kinase affect axon pathfinding. Development *130*, 3217-3226.

Liem, K.F., Jr., Jessell, T.M., and Briscoe, J. (2000). Regulation of the neural

patterning activity of sonic hedgehog by secreted BMP inhibitors expressed by notochord and somites. Development *127*, 4855-4866.

Liem, K.F., Jr., Tremml, G., and Jessell, T.M. (1997). A role for the roof plate and its resident TGFbeta-related proteins in neuronal patterning in the dorsal spinal cord. Cell *91*, 127-138.

Linker, C., and Stern, C.D. (2004). Neural induction requires BMP inhibition only as a late step, and involves signals other than FGF and Wnt antagonists. Development *131*, 5671-5681.

Lodge, A.P., Howard, M.R., McNamee, C.J., and Moss, D.J. (2000). Co-localisation, heterophilic interactions and regulated expression of IgLON family proteins in the chick nervous system. Brain Res Mol Brain Res *82*, 84-94.

Lodge, A.P., McNamee, C.J., Howard, M.R., Reed, J.E., and Moss, D.J. (2001). Identification and characterization of CEPU-Se-A secreted isoform of the IgLON family protein, CEPU-1. Mol Cell Neurosci *17*, 746-760.

Long, H., Sabatier, C., Ma, L., Plump, A., Yuan, W., Ornitz, D.M., Tamada, A., Murakami, F., Goodman, C.S., and Tessier-Lavigne, M. (2004). Conserved roles for Slit and Robo proteins in midline commissural axon guidance. Neuron *42*, 213-223.

Lopez, M., Cocchi, F., Avitabile, E., Leclerc, A., Adelaide, J., Campadelli-Fiume, G., and Dubreuil, P. (2001). Novel, soluble isoform of the herpes simplex virus (HSV) receptor nectin1 (or PRR1-HIgR-HveC) modulates positively and negatively susceptibility to HSV infection. J Virol *75*, 5684-5691.

Lu, Q.R., Yuk, D., Alberta, J.A., Zhu, Z., Pawlitzky, I., Chan, J., McMahon,

A.P., Stiles, C.D., and Rowitch, D.H. (2000). Sonic hedgehog--regulated oligodendrocyte lineage genes encoding bHLH proteins in the mammalian central nervous system. Neuron *25*, 317-329.

Lupo, G., Harris, W.A., and Lewis, K.E. (2006). Mechanisms of ventral patterning in the vertebrate nervous system. Nat Rev Neurosci *7*, 103-114.

Lyuksyutova, A.I., Lu, C.C., Milanesio, N., King, L.A., Guo, N., Wang, Y., Nathans, J., Tessier-Lavigne, M., and Zou, Y. (2003). Anterior-posterior guidance of commissural axons by Wnt-frizzled signaling. Science *302*, 1984-1988.

Mann, F., Zhukareva, V., Pimenta, A., Levitt, P., and Bolz, J. (1998). Membrane-associated molecules guide limbic and nonlimbic thalamocortical projections. J Neurosci *18*, 9409-9419.

Marg, A., Sirim, P., Spaltmann, F., Plagge, A., Kauselmann, G., Buck, F., Rathjen, F.G., and Brummendorf, T. (1999). Neurotractin, a novel neurite outgrowth-promoting Ig-like protein that interacts with CEPU-1 and LAMP. J Cell Biol *145*, 865-876.

Marti, E., Takada, R., Bumcrot, D.A., Sasaki, H., and McMahon, A.P. (1995). Distribution of Sonic hedgehog peptides in the developing chick and mouse embryo. Development *121*, 2537-2547.

Martinez-Rico, C., Pincet, F., Perez, E., Thiery, J.P., Shimizu, K., Takai, Y., and Dufour, S. (2005). Separation force measurements reveal different types of modulation of E-cadherin-based adhesion by nectin-1 and -3. J Biol Chem *280*, 4753-4760.

Marzban, H., Khanzada, U., Shabir, S., Hawkes, R., Langnaese, K., Smalla, K.H., Bockers, T.M., Gundelfinger, E.D., Gordon-Weeks, P.R., and Beesley,

P.W. (2003). Expression of the immunoglobulin superfamily neuroplastin adhesion molecules in adult and developing mouse cerebellum and their localisation to parasagittal stripes. J Comp Neurol *462*, 286-301.

Maurel, P., Einheber, S., Galinska, J., Thaker, P., Lam, I., Rubin, M.B., Scherer, S.S., Murakami, Y., Gutmann, D.H., and Salzer, J.L. (2007). Nectin-like proteins mediate axon Schwann cell interactions along the internode and are essential for myelination. J Cell Biol *178*, 861-874.

Mayor, S., and Riezman, H. (2004). Sorting GPI-anchored proteins. Nat Rev Mol Cell Biol *5*, 110-120.

McNamee, C.J., Reed, J.E., Howard, M.R., Lodge, A.P., and Moss, D.J. (2002). Promotion of neuronal cell adhesion by members of the IgLON family occurs in the absence of either support or modification of neurite outgrowth. J Neurochem *80*, 941-948.

Mehlen, P. (2003). Neurobiology: a new way to network. Nature *424*, 381-382.

Mishina, Y. (2003). Function of bone morphogenetic protein signaling during mouse development. Front Biosci *8*, d855-869.

Miyata, S., Matsumoto, N., and Maekawa, S. (2003). Polarized targeting of IgLON cell adhesion molecule OBCAM to dendrites in cultured neurons. Brain Res *979*, 129-136.

Miyata, S., Matsumoto, N., Taguchi, K., Akagi, A., Iino, T., Funatsu, N., and Maekawa, S. (2003). Biochemical and ultrastructural analyses of IgLON cell adhesion molecules, Kilon and OBCAM in the rat brain. Neuroscience *117*, 645-658.

Munoz-Sanjuan, I., and Brivanlou, A.H. (2002). Neural induction, the default

model and embryonic stem cells. Nat Rev Neurosci *3*, 271-280.

Munro, S. (2003). Lipid rafts: elusive or illusive? Cell *115*, 377-388.

Murai, K.K., Nguyen, L.N., Irie, F., Yamaguchi, Y., and Pasquale, E.B. (2003). Control of hippocampal dendritic spine morphology through ephrin-A3/EphA4 signaling. Nat Neurosci *6*, 153-160.

Nakai, Y., and Kamiguchi, H. (2002). Migration of nerve growth cones requires detergent-resistant membranes in a spatially defined and substrate-dependent manner. J Cell Biol *159*, 1097-1108.

Nakakita, S., Natsuka, S., Ikenaka, K., and Hase, S. (1998). Development-dependent expression of complex-type sugar chains specific to mouse brain. J Biochem *123*, 1164-1168.

Nakanishi, H., and Takai, Y. (2004). Roles of nectins in cell adhesion, migration and polarization. Biol Chem *385*, 885-892.

Neiiendam, J.L., Kohler, L.B., Christensen, C., Li, S., Pedersen, M.V., Ditlevsen, D.K., Kornum, M.K., Kiselyov, V.V., Berezin, V., and Bock, E. (2004). An NCAM-derived FGF-receptor agonist, the FGL-peptide, induces neurite outgrowth and neuronal survival in primary rat neurons. J Neurochem *91*, 920-935.

Nelovkov, A., Philips, M.A., Koks, S., and Vasar, E. (2003). Rats with low exploratory activity in the elevated plus-maze have the increased expression of limbic system-associated membrane protein gene in the periaqueductal grey. Neurosci Lett *352*, 179-182.

Niethammer, P., Delling, M., Sytnyk, V., Dityatev, A., Fukami, K., and Schachner, M. (2002). Cosignaling of NCAM via lipid rafts and the FGF receptor is required for neuritogenesis. J Cell Biol *157*, 521-532.

Ntougkos, E., Rush, R., Scott, D., Frankenberg, T., Gabra, H., Smyth, J.F., and Sellar, G.C. (2005). The IgLON family in epithelial ovarian cancer: expression profiles and clinicopathologic correlates. Clin Cancer Res *11*, 5764-5768.

Ogita, H., and Takai, Y. (2006). Nectins and nectin-like molecules: roles in cell adhesion, polarization, movement, and proliferation. IUBMB Life *58*, 334-343.

Otal, R., Burgaya, F., Frisen, J., Soriano, E., and Martinez, A. (2006). Ephrin-A5 modulates the topographic mapping and connectivity of commissural axons in murine hippocampus. Neuroscience *141*, 109-121.

Owczarek, S., Kiryushko, D., Hald Larsen, M., Sandholm Kastrup, J., Gajhede, M., Sandi, C., Berezin, V., Bock, E., and Soroka, V. (2009). Neuroplastin-55 binds to and signals through the fibroblast growth factor receptor. FASEB J.

Pimenta, A.F., Reinoso, B.S., and Levitt, P. (1996). Expression of the mRNAs encoding the limbic system-associated membrane protein (LAMP): II. Fetal rat brain. J Comp Neurol *375*, 289-302.

Pimenta, A.F., Zhukareva, V., Barbe, M.F., Reinoso, B.S., Grimley, C., Henzel, W., Fischer, I., and Levitt, P. (1995). The limbic system-associated membrane protein is an Ig superfamily member that mediates selective neuronal growth and axon targeting. Neuron *15*, 287-297.

Placzek, M., Tessier-Lavigne, M., Yamada, T., Jessell, T., and Dodd, J. (1990). Mesodermal control of neural cell identity: floor plate induction by the notochord. Science *250*, 985-988.

Raper, J.A. (2000). Semaphorins and their receptors in vertebrates and

invertebrates. Curr Opin Neurobiol *10*, 88-94.

Reed, J., McNamee, C., Rackstraw, S., Jenkins, J., and Moss, D. (2004). Diglons are heterodimeric proteins composed of IgLON subunits, and Diglon-CO inhibits neurite outgrowth from cerebellar granule cells. J Cell Sci *117*, 3961-3973.

Reed, J.E., Dunn, J.R., du Plessis, D.G., Shaw, E.J., Reeves, P., Gee, A.L., Warnke, P.C., Sellar, G.C., Moss, D.J., and Walker, C. (2007). Expression of cellular adhesion molecule 'OPCML' is down-regulated in gliomas and other brain tumours. Neuropathol Appl Neurobiol *33*, 77-85.

Rege, T.A., Pallero, M.A., Gomez, C., Grenett, H.E., Murphy-Ullrich, J.E., and Hagood, J.S. (2006). Thy-1, via its GPI anchor, modulates Src family kinase and focal adhesion kinase phosphorylation and subcellular localization, and fibroblast migration, in response to thrombospondin-1/hep I. Exp Cell Res *312*, 3752-3767.

Reinoso, B.S., Pimenta, A.F., and Levitt, P. (1996). Expression of the mRNAs encoding the limbic system-associated membrane protein (LAMP): I. Adult rat brain. J Comp Neurol *375*, 274-288.

Reymond, N., Fabre, S., Lecocq, E., Adelaide, J., Dubreuil, P., and Lopez, M. (2001). Nectin4/PRR4, a new afadin-associated member of the nectin family that trans-interacts with nectin1/PRR1 through V domain interaction. J Biol Chem *276*, 43205-43215.

Rice, D.S., Huang, W., Jones, H.A., Hansen, G., Ye, G.L., Xu, N., Wilson, E.A., Troughton, K., Vaddi, K., Newton, R.C., *et al.* (2004). Severe retinal degeneration associated with disruption of semaphorin 4A. Invest Ophthalmol Vis Sci *45*, 2767-2777.

Rikitake, Y., and Takai, Y. (2008). Interactions of the cell adhesion molecule nectin with transmembrane and peripheral membrane proteins for pleiotropic functions. Cell Mol Life Sci *65*, 253-263.

Ritter, T.E., Fajardo, O., Matsue, H., Anderson, R.G., and Lacey, S.W. (1995). Folate receptors targeted to clathrin-coated pits cannot regulate vitamin uptake. Proc Natl Acad Sci U S A *92*, 3824-3828.

Robinson, P.J. (1991). Signal transduction by GPI-anchored membrane proteins. Cell Biol Int Rep *15*, 761-767.

Roelink, H., Porter, J.A., Chiang, C., Tanabe, Y., Chang, D.T., Beachy, P.A., and Jessell, T.M. (1995). Floor plate and motor neuron induction by different concentrations of the amino-terminal cleavage product of sonic hedgehog autoproteolysis. Cell *81*, 445-455.

Ronn, L.C., Doherty, P., Holm, A., Berezin, V., and Bock, E. (2000). Neurite outgrowth induced by a synthetic peptide ligand of neural cell adhesion molecule requires fibroblast growth factor receptor activation. J Neurochem *75*, 665-671.

Rutishauser, U. (2008). Polysialic acid in the plasticity of the developing and adult vertebrate nervous system. Nat Rev Neurosci *9*, 26-35.

Sabharanjak, S., Sharma, P., Parton, R.G., and Mayor, S. (2002). GPI-anchored proteins are delivered to recycling endosomes via a distinct cdc42-regulated, clathrin-independent pinocytic pathway. Dev Cell *2*, 411-423.

Saffell, J.L., Williams, E.J., Mason, I.J., Walsh, F.S., and Doherty, P. (1997). Expression of a dominant negative FGF receptor inhibits axonal growth and FGF receptor phosphorylation stimulated by CAMs. Neuron *18*, 231-242.

Saito, A., Fujikura-Ouchi, Y., Kuramasu, A., Shimoda, K., Akiyama, K.,

Matsuoka, H., and Ito, C. (2007). Association study of putative promoter polymorphisms in the neuroplastin gene and schizophrenia. Neurosci Lett *411*, 168-173.

Sakisaka, T., and Takai, Y. (2004). Biology and pathology of nectins and nectin-like molecules. Curr Opin Cell Biol *16*, 513-521.

Salinas, P.C. (2003). The morphogen sonic hedgehog collaborates with netrin-1 to guide axons in the spinal cord. Trends Neurosci *26*, 641-643.

Sara, Y., Biederer, T., Atasoy, D., Chubykin, A., Mozhayeva, M.G., Sudhof, T.C., and Kavalali, E.T. (2005). Selective capability of SynCAM and neuroligin for functional synapse assembly. J Neurosci *25*, 260-270.

Satoh-Horikawa, K., Nakanishi, H., Takahashi, K., Miyahara, M., Nishimura, M., Tachibana, K., Mizoguchi, A., and Takai, Y. (2000). Nectin-3, a new member of immunoglobulin-like cell adhesion molecules that shows homophilic and heterophilic cell-cell adhesion activities. J Biol Chem *275*, 10291-10299.

Schafer, M., Brauer, A.U., Savaskan, N.E., Rathjen, F.G., and Brummendorf, T. (2005). Neurotractin/kilon promotes neurite outgrowth and is expressed on reactive astrocytes after entorhinal cortex lesion. Mol Cell Neurosci *29*, 580-590.

Schofield, P.R., McFarland, K.C., Hayflick, J.S., Wilcox, J.N., Cho, T.M., Roy, S., Lee, N.M., Loh, H.H., and Seeburg, P.H. (1989). Molecular characterization of a new immunoglobulin superfamily protein with potential roles in opioid binding and cell contact. EMBO J *8*, 489-495.

Sellar, G.C., Watt, K.P., Rabiasz, G.J., Stronach, E.A., Li, L., Miller, E.P., Massie, C.E., Miller, J., Contreras-Moreira, B., Scott, D., *et al.* (2003).

OPCML at 11q25 is epigenetically inactivated and has tumor-suppressor function in epithelial ovarian cancer. Nat Genet *34*, 337-343.

Serafini, T., Colamarino, S.A., Leonardo, E.D., Wang, H., Beddington, R., Skarnes, W.C., and Tessier-Lavigne, M. (1996). Netrin-1 is required for commissural axon guidance in the developing vertebrate nervous system. Cell *87*, 1001-1014.

Serafini, T., Kennedy, T.E., Galko, M.J., Mirzayan, C., Jessell, T.M., and Tessier-Lavigne, M. (1994). The netrins define a family of axon outgrowth-promoting proteins homologous to C. elegans UNC-6. Cell *78*, 409-424.

Sharma, P., Varma, R., Sarasij, R.C., Ira, Gousset, K., Krishnamoorthy, G., Rao, M., and Mayor, S. (2004). Nanoscale organization of multiple GPI-anchored proteins in living cell membranes. Cell *116*, 577-589.

Shimizu, K., and Takai, Y. (2003). Roles of the intercellular adhesion molecule nectin in intracellular signaling. J Biochem *134*, 631-636.

Shingai, T., Ikeda, W., Kakunaga, S., Morimoto, K., Takekuni, K., Itoh, S., Satoh, K., Takeuchi, M., Imai, T., Monden, M., *et al.* (2003). Implications of nectin-like molecule-2/IGSF4/RA175/SgIGSF/TSLC1/SynCAM1 in cell-cell adhesion and transmembrane protein localization in epithelial cells. J Biol Chem *278*, 35421-35427.

Simons, K., and Ikonen, E. (1997). Functional rafts in cell membranes. Nature *387*, 569-572.

Simons, K., and Toomre, D. (2000). Lipid rafts and signal transduction. Nat Rev Mol Cell Biol *1*, 31-39.

Smalla, K.H., Matthies, H., Langnase, K., Shabir, S., Bockers, T.M., Wyneken, U., Staak, S., Krug, M., Beesley, P.W., and Gundelfinger, E.D.

(2000). The synaptic glycoprotein neuroplastin is involved in long-term potentiation at hippocampal CA1 synapses. Proc Natl Acad Sci U S A *97*, 4327-4332.

Solnica-Krezel, L. (2005). Conserved patterns of cell movements during vertebrate gastrulation. Curr Biol *15*, R213-228.

Stein, E., and Tessier-Lavigne, M. (2001). Hierarchical organization of guidance receptors: silencing of netrin attraction by slit through a Robo/DCC receptor complex. Science *291*, 1928-1938.

Stemple, D.L. (2005). Structure and function of the notochord: an essential organ for chordate development. Development *132*, 2503-2512.

Stoeckli, E.T., and Landmesser, L.T. (1998). Axon guidance at choice points. Curr Opin Neurobiol *8*, 73-79.

Strizzi, L., Bianco, C., Normanno, N., and Salomon, D. (2005). Cripto-1: a multifunctional modulator during embryogenesis and oncogenesis. Oncogene *24*, 5731-5741.

Struyk, A.F., Canoll, P.D., Wolfgang, M.J., Rosen, C.L., D'Eustachio, P., and Salzer, J.L. (1995). Cloning of neurotrimin defines a new subfamily of differentially expressed neural cell adhesion molecules. J Neurosci *15*, 2141-2156.

Takahashi, K., Nakanishi, H., Miyahara, M., Mandai, K., Satoh, K., Satoh, A., Nishioka, H., Aoki, J., Nomoto, A., Mizoguchi, A., *et al.* (1999). Nectin/PRR: an immunoglobulin-like cell adhesion molecule recruited to cadherin-based adherens junctions through interaction with Afadin, a PDZ domain-containing protein. J Cell Biol *145*, 539-549.

Takai, Y., Irie, K., Shimizu, K., Sakisaka, T., and Ikeda, W. (2003). Nectins

and nectin-like molecules: roles in cell adhesion, migration, and polarization. Cancer Sci *94*, 655-667.

Tamagnone, L., and Comoglio, P.M. (2000). Signalling by semaphorin receptors: cell guidance and beyond. Trends Cell Biol *10*, 377-383.

Tamagnone, L., and Comoglio, P.M. (2004). To move or not to move? Semaphorin signalling in cell migration. EMBO Rep *5*, 356-361.

Thomas, L.A., Akins, M.R., and Biederer, T. (2008). Expression and adhesion profiles of SynCAM molecules indicate distinct neuronal functions. J Comp Neurol *510*, 47-67.

Tiveron, M.C., Nosten-Bertrand, M., Jani, H., Garnett, D., Hirst, E.M., Grosveld, F., and Morris, R.J. (1994). The mode of anchorage to the cell surface determines both the function and the membrane location of Thy-1 glycoprotein. J Cell Sci *107 (Pt 7)*, 1783-1796.

Togashi, H., Miyoshi, J., Honda, T., Sakisaka, T., Takai, Y., and Takeichi, M. (2006). Interneurite affinity is regulated by heterophilic nectin interactions in concert with the cadherin machinery. J Cell Biol *174*, 141-151.

Wilson, D.J., Kim, D.S., Clarke, G.A., Marshall-Clarke, S., and Moss, D.J. (1996). A family of glycoproteins (GP55), which inhibit neurite outgrowth, are members of the Ig superfamily and are related to OBCAM, neurotrimin, LAMP and CEPU-1. J Cell Sci *109 (Pt 13)*, 3129-3138.

Wilson, L., and Maden, M. (2005). The mechanisms of dorsoventral patterning in the vertebrate neural tube. Dev Biol *282*, 1-13.

Wong, J.T., Wong, S.T., and O'Connor, T.P. (1999). Ectopic semaphorin-1a functions as an attractive guidance cue for developing peripheral neurons. Nat Neurosci *2*, 798-803.

Yamada, M., Hashimoto, T., Hayashi, N., Higuchi, M., Murakami, A., Nakashima, T., Maekawa, S., and Miyata, S. (2007). Synaptic adhesion molecule OBCAM; synaptogenesis and dynamic internalization. Brain Res *1165*, 5-14.

Yamada, T., Placzek, M., Tanaka, H., Dodd, J., and Jessell, T.M. (1991). Control of cell pattern in the developing nervous system: polarizing activity of the floor plate and notochord. Cell *64*, 635-647.

Yazdani, U., and Terman, J.R. (2006). The semaphorins. Genome Biol *7*, 211.

Zacco, A., Cooper, V., Chantler, P.D., Fisher-Hyland, S., Horton, H.L., and Levitt, P. (1990). Isolation, biochemical characterization and ultrastructural analysis of the limbic system-associated membrane protein (LAMP), a protein expressed by neurons comprising functional neural circuits. J Neurosci *10*, 73-90.

Zakin, L., and De Robertis, E.M. (2004). Inactivation of mouse Twisted gastrulation reveals its role in promoting Bmp4 activity during forebrain development. Development *131*, 413-424.

Zakin, L., Reversade, B., Kuroda, H., Lyons, K.M., and De Robertis, E.M. (2005). Sirenomelia in Bmp7 and Tsg compound mutant mice: requirement for Bmp signaling in the development of ventral posterior mesoderm. Development *132*, 2489-2499.

Zhao, G.Q. (2003). Consequences of knocking out BMP signaling in the mouse. Genesis *35*, 43-56.

Zhukareva, V., and Levitt, P. (1995). The limbic system-associated membrane protein (LAMP) selectively mediates interactions with specific

central neuron populations. Development *121*, 1161-1172.

Zou, Y. (2004). Wnt signaling in axon guidance. Trends Neurosci *27*, 528-532.